ASSESSING THE EPIGENETIC MODIFIERS OF DRUG RESPONSE IN HUMAN ASTROCYTE AND GLIOBLASTOMA CO-CULTURES

by

Ali Cenk AKSU

A Dissertation Submitted to the

Graduate School of Health Sciences

in Partial Fulfillment of the Requirements for

the Degree of

Doctor of Philosophy

in

Cellular and Molecular Medicine

KOÇ
UNIVERSITY

June 30, 2022

Assessing the epigenetic modifiers of drug response in human astrocyte and glioblastoma co-cultures

Koç University

Graduate School of Health Sciences

This is to certify that I have examined this copy of a doctoral dissertation by

Ali Cenk AKSU

and have found that it is complete and satisfactory in all respects,

and that any and all revisions required by the final

examining committee have been made.

Committee Members:

_____

Prof. Tuğba Bağcı-Önder (Advisor)

_____

Assoc. Prof. Ceyda Ayhan Acilan

_____

Prof. Mehmet Kaya

_____

Assoc. Prof. Mehmet Ozansoy

_____

Assoc. Prof. Adam P. Cribbs

Date: _____

To all my friends,
some who still walk with me,
some others who follow their own paths,
and some who will never be forgotten,
to strive, to seek, and not to yield…

ABSTRACT

Assessing the epigenetic modifiers of drug resistance in human astrocyte and glioblastoma co-cultures.
Ali Cenk Aksu
Doctor of Philosophy in Cellular and Molecular Medicine
30th of June 2022

Glioblastoma (GBM) is the most common and malignant of all primary CNS tumours. Unfortunately, GBM has very low survival. The standard treatment regimen consists of surgery, ionizing radiation, and chemotherapy. The most common chemotherapeutic used for the treatment of GBM is temozolomide, followed by carmustine, which could not change the overall survival rates in the last 25 years. Unfortunately, most drug trials fail at the initial phases. For this failure in progress, tumour-microenvironment interactions play an important role, beside others causes. Therefore, understanding the nature of therapy resistance in relation to tumour-microenvironment interactions is essential.

In this thesis, a new co-culture model was established to examine temozolomide response of tumour cells in the context of astrocyte microenvironment. Contact-dependent and contact-independent co-culture models were examined with cell viability and imaging methods. Contact-dependent astrocyte-U87MG co-cultures presented temozolomide resistance. Transcriptomic differences between U87MG cells alone and in co-cultures with astrocytes were examined by cell sorting, followed by RNA sequencing. As a testament to increased cell-to-cell interaction, co-culture models were found to express high levels of several cell-extracellular matrix interaction pathway components. Specifically, increased levels of collagen (*COL*), matrix-metalloproteins (*MMP*), and tubulin (*TUB*) families were observed. These adaptive changes were most likely vital elements of drug resistance in co-cultures.

As contact-dependent temozolomide resistance may involve genetic and epigenetic changes, epigenetic vulnerabilities of tumour cells in co-cultures were examined. Cancers show altered epigenetic regulation; global changes in DNA and histone methylation. Yet, the epigenetic regulation of temozolomide response in co-cultures is not established. We performed a small molecule epigenetic inhibitor probe library screen to examine and identify epigenetic regulators of temozolomide response in co-cultures. We identified several histone demethylase inhibitors, in combination with temozolomide, as potent agents to target U87MG cells cultured with astrocytes. We then focused on GSK-J4, a histone demethylase inhibitor, as a potent agent that could affect GBM cells that are grown in co-cultures. GSK-J4 is a known agent that inhibits KDM6A and KDM6B, whose roles have not been studied in the context of temozolomide response in GBM. To understand the mechanisms of GSK-J4 in co-cultures, cell viability assays with chemical inhibition and CRISPR/Cas9-targeted gene silencing of KDM6A or KDM6B were applied. Further CITE-single cell sequencing was performed in U87MG-astrocyte co-cultures in the presence and absence of GSK-J4. We showed that both cell compartments were differentially represented at their transcriptome levels. Hypoxia and glycolysis-related genes *MT-CYB*, *MT-CO2*, *MT-ND2*, and *MTRNR2L10* were upregulated and apoptosis-related genes were down-regulated in both tumour cells and astrocytes in response to GSK-J4.

In conclusion, by generating and characterising co-culture models of GBM, we were able to find epigenetic regulators of temozolomide response and present transcriptomic differences that may serve as potential therapeutic intervention points for GBM in the future.

ÖZETÇE

Astrosit ve glioblastom birlikte kültürüne bağlı ilaç direncinde rol alan epigenetik faktörlerin incelenmesi.
Ali Cenk Aksu
Hücresel ve Moleküler Tıp, Doktora
30 Haziran 2022

Glioblastom (GBM), merkezi sinir sistemi tümörleri arasında en yaygın ve en habis tümör tipidir. Ne yazık ki, düşük hayatta kalma oranı ve hastalığın nüks etmesi GBM'de sıklıkla görülmektedir. Standart tedavi yöntemleri genellikle cerrahi müdahale, radyoterapi ve kemoterapiden oluşmaktadır. Son yirmi beş yıldır temozolomid kemoterapide en çok kullanılan ilaç olmakla beraber, onu karmustin türevi ilaçlar takip etmektedir. Yeni ilaç bulma çalışmaları sırasında maalesef çoğu ilaç araştırma safhalarının başında başarısız olmaktadır. Bunun bir sebebi de tümörün mikro çevresi ile olan etkileşimlerinin çalışmalarda sınırlayıcı bir etken olmasıdır. Bu nedenle, terapi direncinin doğasını ve mikro çevre etkileşimlerini anlamak esastır.

Bu çalışmada, temozolomid direncinin sağlıklı hücreler ile etkileşimleri incelemek için yeni ko-kültür modellemeleri yapılmıştır. Temasa-bağlı ve bağımsız ko-kültür modelleri hücre canlılığı ve görüntüleme yöntemleri ile çalışılmıştır. Astrosit ve U87MG ko-kültür deneylerinin sonucunda temozolomid direncinin temasa-bağlı olduğu bulunmuştur. U87MG tümörlerinde astrosit ile birlikte kültür sonucu oluşan arasındaki transkriptomik farklılıklar, akım sitometre bazlı hücre seleksiyonu ardından RNA dizilimi ile incelendi. Sekanslama sonucunda ko-kültür modellerinde çeşitli yolakların ifadelerinin yükseldiği bulundu. Spesifik olarak, hücre-hücre etkileşimleri ile doğrudan ilişkili olan kolajen (*COL*), matris-metalloprotein (*MMP*) ve tübülin (TUB) ailelerinin artan seviyeleri bulundu.

Bilindiği üzere kanserler DNA metilasyonu ve histon metilasyon ve asetilasyon profillerinde oluşan global değişiklikler gibi çokça epigenetik düzen değişimleri gösterir. Ancak, astrosit kaynaklı temozolomid direncindeki epigenetik düzenleme iyi bilinmemektedir. Bu sebeple, birlikte kültürlenen bu hücrelerin epigenetik değişimlerini de incelemek için epigenetik hedefleyen inhibitör kütüphanesi kullanılarak tarama yapılmıştır. Tekli inhibitör ya da temozolomid ile kombinasyon olarak yapılan kütüphane taraması sonucunda çeşitli histon demetilaz inhibitörleri tanımlanmıştır. Bu inhibitörlerin arasından GBM'de daha önce iyi çalışılmamış olan GSK-J4'a odaklanılmıştır.GSK-J4'ün ko-kültürlerdeki rolünü anlamak için, kimyasal inhibisyon, CRISPR/Cas9 yöntemi ile KDM6A veya KDM6B susuturulmuş ve canlılık deneyleri yapılmıştır. Ayrıca, CITE-tek hücre dizilimi ile tümör ve astrosit hücre ko-kültürlerinde GSK-J4 yanıtı incelenmiştir. Sonuç olarak Hipoksi ve glikoliz ile ilgili *MT-CYB*, *MT-CO2, MT-ND2* ve *MTRNR2L10* genlerinin her iki hücre tipinde de farklı şekilde ifade edildiği görülmüştür. Buna ek olarakm programlı hücre ölümü ile alakalı genlerin ifadelerinde ise azalma görülmüştür.

Sonuç olarak, GBM'nin ko-kültür modellerini başarılı bir şekilde oluşturarak ve karakterize ederek, temozolomide direncinde etkili olabilecek epigenetik düzenleyiciler tanımlanmış, ve ileride potansiyel tedavi yöntemleri için önemli olabilecek hücrelerdeki transkriptomik değişiklikler aydınlatılmıştır.

ACKNOWLEDGMENTS

I want to thank everybody who touched my life and made me the person I am today. There are more than I count, and some deserve special thanks.

Dr. Tugba Bagci-Onder. I know that I am not the easiest person to handle. However, she managed and focused me perfectly, when I was at the edge of a breakdown, both scientifically and personally. Therefore, thank you for being a supportive and helpful advisor.

I want to thank *Dr. Ceyda Acilan-Ayhan* and *Dr. Mehmet Ozansoy* for their endless support and guidance throughout my thesis.

I would like to thank Koç University Research Centre for Translational Medicine (KUTTAM), The Scientific and Technological Research Council of Turkey (TÜBİTAK) and the Newton Royal Fellowship for the financial support.

I thank *Dr. Adam P. Cribbs,* he taught and supported me so much, but the most important lesson I learned was: 'how to be an individual researcher'. Also, I thank *Dr. James Dunford, Dr. Martin Philphott,* and *Dr. Udo Opperman* for giving me the best scientific and friendly environment during my visit to Botnar Research Centre, University of Oxford.

My fondest memories had shaped while I was a TBO lab member. All TBO lab members and my other friends in the KUTTAM family are valuable to me. Therefore, I want to thank *Dr. Ahmet Cingoz, Dr. Alisan Kayabolen, Dr. Buse Cevatemre, Dr. Dogancan Ozturan, Dr. Ezgi Ozyerli, Dr. Fatma Ozgun, Dr. Fidan Seker-Polat, Dr. Gizem Nur Sahin-Kayabolen, Dr. Ilknur Sur-Erdem, Dr. Merve Ozgur-Erat, Dr. Ugur Akcan, Arda Odabas, Beril Esin, Canan Bayraktar, Ebru Yilmaz, Ezgi Kurt, Mina Fulya Kucuktas, Nareg Pinarbasi-Degirmenci, Vuslat Akcay,* and all my other friends. Thank you for being the most enormous, supportive, helpful, and open-minded family I will never forget.

I would like to thank *Dr. Deniz Ata* and *Dr. Ozen Leylek. They* were the best flatmates that I could have. We shared everything we got, and we shared without hesitation. My friends from my undergraduate *Selda Coban* and *M.Sc. Ozge Barim* deserves all my best; thank you for being the safest place where I could express myself freely. *Dr. Burcu Ozcimen* and *Dr. Deniz Ugurlu-Cimen* we shared late-night waffles, mutual work times in cafés, supper and meals. We had enjoyed each other's company always; thank you for everything. My undergraduate trainee *Mami Burgac* deserves special thanks; he worked

tirelessly and taught me how to be an advisor and student simultaneously. I want to thank *Ezgi Yagmur Kala* and *Batuhan Mert Kalkan* for opening their home and their friendship. *Goktug Karabiyik,* we shared a mutual interest in Lord of the Rings and many more mutual interests. May the stars shine upon the end of your road. *Ozlem Yedier-Bayram* has helped me a lot throughout my journey. She, her husband, *Sefa Bayram* and her newborn son *Mert Bayram,* are such a delight to have around.

I wish to thank my mother, *Ayse Aksu,* my father, *Sabri Sadettin Aksu* and my sister *Damla Aksu.* They were always supportive and sympathetic.

Last in the text, but always the first in my thoughts, my best friend, fellow traveller, long-lost company, and biggest fan, my dear *Dr. Filiz Senbabaoglu-Aksu*, thank you just for being yourself.

TABLE OF CONTENTS

TABLE OF FIGURES

Nomenclature

αKG	Isocitrate to αKetoglutarate
AML	Acute myeloid leukaemia
ARID1A	AT-rich interaction domain 1A
ATCC	American Tissue Type Culture Collection
ATF4	Transcription activating factor 4
BER	Base excision repair
BGI	Beijing Genomics Institute
BTPC	Brain tumour propagating cell
CAF	Carcinoma-associated fibroblast
CITE	Cellular Indexing of Transcriptomes and Epitopes
CM	Condition medium
CNS	Central Nervous System
CNX43	Connexin 43
COL	Collagen
CTG	Cell Titer Glo
dCas9	dead-Cas9
DE	Differential expression
DNMT	DNA methyltransferase
DNMT3A	DNA methyltransferase 3 alpha
DR	Death receptor
ECM	Extracellular matrix
EPD	Eukaryotic promoter database
ER	Endoplasmic reticulum
EZH2	Zeste 2 polycomb repressive complex 2 subunit
FACS	Fluorescence-Activated Cell Sorting
FasL	Fas ligand
FLUC	Firefly luciferin
GBM	Glioblastoma multiforme
GDNF	Glial cell line-derived neurotrophic factor
GEMs	Gel Beads in Emulsion
GFP	Green fluorescent protein
GLUT	Glucose transporters
gRNA	Guide RNA
GSC	Glioblastoma stem-like cell
GSEA	Gene Set Enrichment Analysis
GTME	Glioblastoma microenvironment
HAT	Histone acetyltransferase
HDAC	Histone deacetylase
HMT	Histone methyltransferase
HRI	Heme-regulated eIF2α kinase

IDH	Isocitrate Dehydrogenase
INHA	Immortal normal human astrocyte
KDM6A	lysine demethylase 6A
KDM6B	lysine demethylase 6B
LFC	Log fold change
MDS	Myelodysplastic syndrome
MGMT	O6-Methylguanin-DNA Methyltransferase
MMP	Matrix-metalloprotein
MSKCC	Memorial Sloan Kettering Cancer Center
MTIC	5-(3-methyltriaze-1-yl) imidazole-4-carboxamide
NBLs	Neuroblastoma cells
NCCSC	National Cancer Chemotherapy Service Centre
NHA	Primary human astrocytes
NK	Natural killer
NSD2	Nuclear receptor binding SET domain protein 2
NT	Non-targeting
PBS	Phosphate-buffered saline
PcG	Polycomb group
PEG	Polyethylene glycol
PI3K	Phosphate Inositol 3 Kinase
PMT	Post Translational Modification
PKMT	Protein lysine methyltransferase
PRC	Polycomb repressive complexes
PRMT	Protein arginine methyltransferase
PS	Protamine sulphate
qRT-PCR	Quantitative Real-Time Polymerase Chain Reaction
RAS	Rat Sarcoma
RLU	Relative luminescence units
ROS	Reactive oxygen species
RTK	Receptor Tyrosine Kinase
SEM	Scanning-electron microscopy
t-SNE	t-stochastic neighbour embedding
TAMs	Tumour-associated macrophages
TERT	Telomerase reverse transcriptase
TM	Tumour microtube
TNT	Tunnelling nanotube
TPR	Tetratricopeptide repeat
TSS	Transcription start site
TUB	Tubulin
UMAP	Uniform manifold approximation
UMI	Unique molecular identifier
UTR	Lysine demethylase 6B
UTX	Lysine demethylase 6A

VEGF	Vascular endothelial growth factor

SIGNIFICANCE

In this thesis, we pursued the question: "Does tumour microenvironment have an epigenetic regulatory effect on drug response in glioblastoma, and can we identify new targets to overcome this environment-induced drug resistance?". We suggested that while cancer cells are exposed to therapeutic agents, healthy cells in the microenvironment are also exposed. The healthy cells in the microenvironment could adapt to the exposed drug and affect the response of tumour cells via cell-to-cell interaction. To uncover this, we established a glioblastoma-astrocyte co-culture system and tested our hypothesis with 3 significant aims:

Aim 1: Establishment of glioblastoma-astrocyte co-cultures.

To model and study the cell-to-cell interactions, we established a U87MG – astrocyte co-culture. While investigating the temozolomide (TMZ) response, we used contact-independent and contact-dependent cell-to-cell interaction methods. We observed TMZ resistance in contact-dependent co-cultures. In addition, with RNA sequencing of tumour cells and astrocytes upon isolation, we showed that co-cultured tumour cells present increased cell-to-cell interaction transcriptional landscape.

Aim 2: Identifying the epigenetic drug resistance regulators in co-cultures

The epigenetic factors regulating TMZ response in our co-culture models were examined with an unbiased epigenetic small molecule inhibitor screen in our co-culture model. Histone lysine demethylase inhibitor, GSK-J4 suspended tumour proliferation in co-cultures. Additionally, we observed that the inhibitory effects of GSK-J4 in co-cultures were contact-dependent.

Aim 3: Addressing candidate genes as targets

The transcriptomic landscape changes upon GSK-J4 treatment in our co-culture models were studied with a novel, combined, single-cell – cellular indexing of transcriptomes and epitopes (CITE) sequencing. *MT-CO2*, *MT-ND2*, and *MT-CYB*, closely related to mitochondrial regulation, were differentially expressed in tumour and healthy cells. Additionally, several pathways were specifically regulated in each cell compartment, which indicates a more complex and intervened regulation in co-cultures.

1 Introduction

1.1 Central Nervous System (CNS) Tumours

Central nervous system tumours are formed in the brain or spinal cord. In 2021, CNS tumours were found to be the 10th leading cause of death for all genders. Even though the likelihood of developing a CNS tumour is less than 1%, approximately 300,000 people are diagnosed with this cancer type each year and unfortunately their mortality rate is very high. 30% of all CNS tumours are malignant and 55% of CNS tumours are gliomas (Miller et al., 2021). The tumours can be focal or spread across the different regions of the brain (Lapointe et al., 2018).

1.1.1 The components of the brain

The most complex organ of the body is the brain, which could be divided into three parts: 1) brain stem, 2) cerebellum, and 3) cerebrum. Each component of the brain serves an individual function for CNS. The mosaic of the brain consists of two main groups of cells, namely, neuronal and glial cells. The neuronal cells are post-mitotic; thus, their possibility of forming tumours is very low. Whereas the glial cells, responsible for brain homeostasis, undergo cell replication frequently, increasing the chance of tumour formation (Herbet & Duffau, 2020; Wardlaw et al., 2020).

Oligodendrocytes, microglial cells, and astrocytes are the three main groups of glial cells. Oligodendrocytes are insulator sheaths of CNS cells for higher electrical transfer speed. These cells increase the electrical conductance by myelinating the CNS cells. Even though their primary responsibility is myelination, oligodendrocytes also function to provide metabolic support to other cells (Bradl & Lassmann, 2010). 10 -15% of the brain cells are microglial cells. Microglial cells present similar traits like macrophages, so they act as the first line of defense in the CNS. Among their immune role in CNS, microglial cells are responsible for scavenging and phagocytosis, and they have a role in extracellular signalling (Bachiller et al., 2018). Astrocytes or astroglia are the most abundant cells in CNS; they make up 55 – 60% of all CNS. Biochemical control, nutrient provision, ion balance, cerebral blood flow regulation, and repair of injured or

infected cells in the CNS are the most well-known functions of the astrocytes. The importance of healthy human astrocytes in the microenvironment has been proved over time. Recent studies have shown that astrocytes have the ability to make 10 times more contact compared to the other CNS cells. Especially, Ca^{+2} propagation over a long distance in response to stimulation and communication with neurons by Ca^{+2} release made astrocyte research extremely important in neuroscience (Allen, 2014; Fiacco et al., 2009; Freeman & Rowitch, 2013; Khakh & Deneen, 2019; Siracusa et al., 2019).

1.1.2 Tumour development in the brain

The tumours of CNS are named after their tissue-of-origin. Glial tissue develops glioma, oligodendrocytes produce oligodendroglioma, and astrocytes give rise to astrocytoma. Even though the early diagnosis, initial diagnosis and treatment options advance over time, the main reason why tumours develop in the brain remains unanswered. While the mechanisms behind tumour development are yet not fully discovered, the development and progression could be tracked with driver mutations and several cancer hallmarks (Hanahan, 2022; *The Development and Causes of Cancer - The Cell - NCBI Bookshelf*, n.d.).

The latest cancer hallmarks contain ten different commonalities among the majority of cancers. Even though there are 10 hallmarks, we can simplify the grouping as 1) (epi)genomic alterations, 2) proliferative support, and 3) escaping from dangers. Genomic or epigenomic alterations support the cancer cells in various ways, such as enabling replicative immortality, increasing favourable mutations and much more. Genomic alterations are more prominent of the hallmarks, because they aid all other hallmarks by epigenetic regulation. Proliferative support is based on the cell proliferation either by increasing growth signal or promoting the cells' accessibility to nutrients via neo-vascularisation. Evasion from dangers consists of escaping immune control checkpoints, resisting cell death signals, and evading growth suppressions of the environment (Hanahan, 2022).

Every time a cell replicates, there is a chance of mutation due to several reasons. From the cancer point of view, two types of mutations occur 1) driver and 2) passenger. Passenger mutations are less dangerous, but congregated passenger mutations could give cancer cells advantages. Deep sequencing of tumour and tumour-free samples from

surrounding tissue presented some commonly mutated genes such as *TP53, TERT, EGFR*, and *PTEN*. The morphological and quantitative data demonstrated signs of *de novo* tumour development in tumour-free tissues. Especially *TERT* mutation was observed even in selected subclones without any tumour indication. These results prove that *TERT* mutation starts as a passenger mutation, but with the accumulation of other mutations, *TERT* becomes one of the driver mutations (J. H. Lee et al., 2018b).

Meanwhile, driver mutations are very dangerous, and this type of mutation alone could cause extreme changes in the cells. The well-known driver genes are *MYC, EGFR, RB1, PTEN,* among many others. Similar to passenger mutations, the accumulation of driver mutations speeds up the progression of the tumour. Several years prior to the initial tumour diagnosis, single-gene driver mutations could be observed. However, most of the time, single-gene drivers are neglectable and do not have extreme cellular outcomes. The progression timeline shows that the first driver mutation could take long years to develop, but the second mutation could only take 6 months to 8.3 years. The third mutation only takes 3 months to 4.5 years, and the accumulation of subsequent driver mutations becomes faster with each new driver mutation. In comparison, the mutation count increases logarithmically, and the time for a new mutation decreases in the opposite way. This progress continues until the patient's loss, or the driver mutation count reaches a plateau (Bozic et al., 2010; Wijewardhane et al., 2021; Wodarz et al., 2018).

The typical hallmarks of tumours and mutations of the genes play an essential role in tumour development and progression. However, the tumour cells need all the advantages to overcome any possible danger to survive. Therefore, instead of mutating the genes, regulating gene expression would be more advantageous for tumour cells (Jiang et al., 2020).

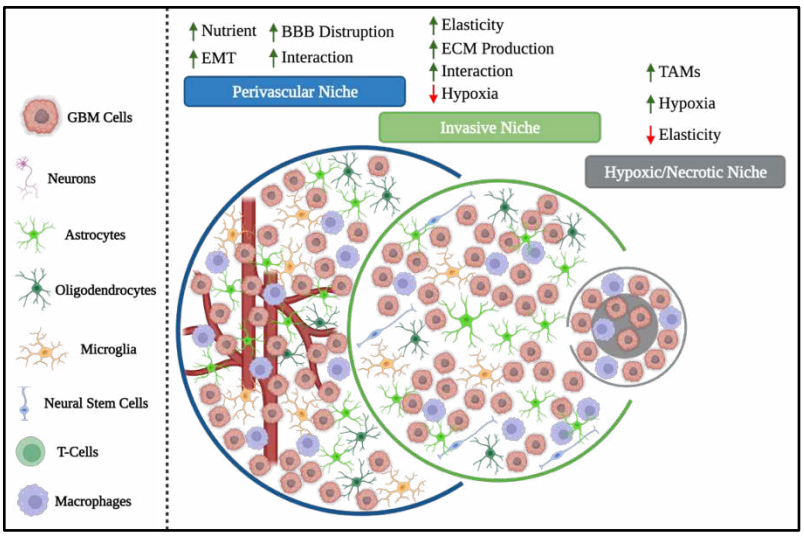

Figure 1.1 Illustration of GBM microenvironment.

1.2 Epigenetic Regulation of Cells

Chromatin is the macromolecular structure of tightly condensed DNA wrapped around histone proteins. Every 147 bp of DNA is found wrapped around histone octamers, which provides the compactness of the genome. Histones are 'DNA packaging' proteins and, like all other proteins, they can be altered with posttranslational modifications. These modifications change the histone charges to loosen or tighten the DNA around histones. This is one of the fundamental mechanisms allowing cells to express genes whenever needed. The field that studies these alterations and control mechanisms is called epigenetics. Epigenetics could also be defined as phenotypic alterations without somatic mutations in the human genome (Dupont et al., 2009).

Histones are classified as linker and core histones. The DNA is wrapped around H2A-H2B dimers and H3-H4 tetramers. The DNA is negatively charged, and histones are positively charged. So, DNA wrapping occurs around histones. The histones contain long N-terminal tails, rich in amino-acid residues, which could be modified chemically (Mariño-Ramírez et al., 2005; Nelson & Cox, 2011).

The development and function of the mammalian CNS depend on proper epigenetic regulation. Global DNA methylation levels can vary and are dynamic among different brain regions (Ladd-Acosta et al., 2007; Lein et al., 2006; Tawa et al., 1990). A particular cytosine-guanine-rich site within Glial Fibrillary Acidic Protein *(GFAP)* promoter is methylated during astrogliogenesis in neural precursors and post-mitotic neurons. However, mature astrocytes have unmethylated *GFAP* promoter (Condorelli et al., 1994,

1997; Takizawa et al., 2001). Another important gene is DNA methyltransferase 1 (*DNMT1),* which is highly expressed in the mammalian brain, including post-mitotic neurons. *DNMT1's* primary role is methylation during DNA replication, whereas its role after neuron development is still elusive (Goto et al., 1994). *DNMT1* deletion in murine post-mitotic neurons did not affect DNA methylation; however, in neuroblasts, the DNA was hypomethylated and lethal after birth. This indicates that *DNMT1* significantly affects CNS development (Fan et al., 2001; Nguyen et al., 2007).

1.2.1 Mechanisms of epigenetic modifications

To date, there are 8 well-known chemical modification mechanisms with different outcomes. Well-known modifications are acetylation, methylation, phosphorylation and ubiquitylation, and less well-known modifications are GlcNAcylation, citrullination, krotonilation, and isomerisation. The modifications are named by the name of histone, amino acid abbreviation, type of modification, and the number of modifications. Most studied modifications are H3K4, H3K9, H3K27, and H3K36 methylation or acetylation (Handy et al., 2011; Zhao et al., 2020). Epigenetic mechanisms change the access of DNA sequences by tightening or loosening the DNA wrap around the histones leading to 2 main structural alterations: 1) Loosening (Histone Acetylation) and 2) Tightening (Histone Methylation, DNA Methylation). Loosening results with heterochromatin (tightly packed) to euchromatin (loosened) transition, which opens genes for expression, and tightening is vice versa (Ellis et al., 2009; Rodríguez-Paredes & Esteller, 2011). The loosening (euchromatin) or tightening (heterochromatin) mechanisms are post-translational mechanisms of core histone proteins. These post-translational mechanisms are tightly regulated by the epigenetic writer, eraser, and readers. As the name implies, the writers add epigenetic marks or write on histones, while erasers remove the pre-existing or written histone marks (Gillette & Hill, 2015a). Even though the action and reaction of tightening and loosening occur with writers and erasers, the mediators are readers. The PTMs occur in several steps: recognition, complex formation, transferring or removing the mark, and release. The writer and erasers are not a single protein; instead, they consist of several proteins with different purposes. For example, HAT complex CREB binding protein consists of CBP/p300, P/CAF, p160, activator bridge and mediator. Each protein of complex is needed to complete a specific task during PTM.

Mediator protein (reader) recognize the binding site, activator protein recruit CBP/p300 to the active site, and P/CAF – p160 act as cofactors during PTM (Vo & Goodman, 2001). The mediator proteins recognize specific sites on DNA. The DNA contains particular sites with a high affinity for methylation or acetylation. Chromatin organization modifier (chromo), Tudor, and Plant Homeodomain (PhD) sites present higher affinity to methylation; meanwhile, Bromo and PhD Finger domains are associated with acetylation (Gillette & Hill, 2015b, 2015a; Marmorstein & Zhou, 2014; Vo & Goodman, 2001).

Histone acetylation and methylation were first reported in 1964(ALLFREY et al., 1964). Histone acetylation was associated with gene activation. Since then, two enzymes with opposite functions, histone acetyltransferases (HATs) and histone deacetylases (HDACs), have been identified and studied for their effect on RNA transcription. HATs catalyse an acetyl group transfer to a lysine residue of histone; HDACs remove the acetyl group from lysine. The acetylation and de-acetylation have a considerable impact on RNA transcription. The positive charge of acetylation loosens the DNA wrapped around the histones and allows transcription factors and RNA polymerases to bind to DNA. Therefore, it is predicted that acetylation commonly initiates and increases RNA transcription, while de-acetylation acts opposite and decreases the RNA transcription (Verdone et al., 2006).

Histone methylation is dynamically controlled with histone methyltransferase and demethylases. Studies have shown that the methyltransferases or demethylases are recruited to the site of action by specific DNA sequences. Among others, polycomb group (PcG) response elements are closely associated with recruitment in *Drosophila melanogaster* (Benedí et al., 1986; Chan et al., 1994). PcG in humans present conserved sequences and possibly recruits the methyltransferases and demethylases. Unlike histone acetylation, methyl group transfer or removal does not change the charge of histone protein, could be mono-, di- or tri-methyl group change, and does not directly activate or repress the genes. H3K4me3 and H3K79me3 were associated with activation. Meanwhile, H3K9me3 and H3K27me3 show transcriptional repression characteristics (Chan et al., 1994; Fritsch et al., 1999; Kooistra & Helin, 2012; Rice et al., 2003; Tillib et al., 1999).

1.2.2 Epigenetic changes in tumour development

Cancer cells have altered epigenetic regulations, which could be grouped as 1) deactivated tumour suppressor genes and 2) activated oncogenes. The transcriptional silencing of tumour-suppressor genes by methylation is essential regulation of tumour suppression, where these genes cannot prevent the cells tumour progression. Activation of oncogenes by acetylation promotes cancer development in different ways, contributing to the typical hallmarks of cancer (Allis & Jenuwein, 2016; Dawson & Kouzarides, 2012).

In general, both deactivations of tumour suppressor genes and activation of oncogenes support tumour progression. One crucial difference between these groups is that deactivation primarily targets the tight regulative genes critical for cell maintenance, whereas activation of any gene could act as an oncogene (Ellis et al., 2009; Rodríguez-Paredes & Esteller, 2011).

One of the most established activations in glioblastoma is telomerase reverse transcriptase (*TERT)*. The *TERT* promoter is mutated and has aberrant activation, which causes cells to bypass replicative senescence and overcome apoptosis for cancer cells' extended (immortalised) lifespan. Another example is *SMC4* in glioblastoma. Upon activation, *SMC4* up-regulates TGFβ/Smad signalling and promotes an aggressive phenotype (Cai & Sughrue, 2018; Romani et al., 2018; Tang et al., 2018).

Glioblastomas have many methylated genes, but Isocitrate Dehydrogenase (*IDH)* and O^6-Methylguanin-DNA Methyltransferase (*MGMT)* are the most known ones. IDH enzymes normally convert Isocitrate to αKetoglutarate (αKG, also known as, 2-OG), which is essential for the proper functioning of 2-OG dependent dioxygenases, JHDM1, KDM4 and TET1. *IDH1/2* mutations are among the most recently described, which leads to the production of 2-Hydroxyglutarate (2-HG) from αKG. Therefore, if *IDH* is mutated, 2-HG accumulates acting as an inhibitor of these demethylases, leading to increased histone and DNA methylation in different target genes (Cai & Sughrue, 2018; Romani et al., 2018; Tang et al., 2018).

MGMT is very well known because of its inhibitory effect against temozolomide, the only drug used for the treatment of glioblastoma. MGMT corrects the alkylating effect of temozolomide, and the treatment success is dependent on *MGMT* promoter CpG island methylation. If the *MGMT* promoter is not methylated, gene expression occurs and MGMT protein is produced. MGMT can then repair the damage inflicted by the

alkylating effect of temozolomide and decrease treatment efficacy. Whereas, if *MGMT* promoter is methylated, temozolomide will have higher efficacy because *MGMT* cannot repair the damage and protect the cells (Cai & Sughrue, 2018; Romani et al., 2018; Tang et al., 2018).

1.2.3 Targeting epigenetic regulators for cancer therapy

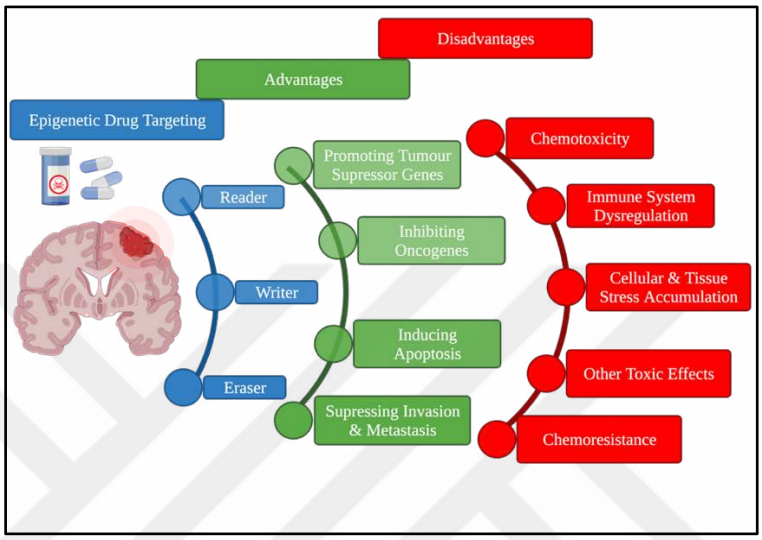

Figure 1.2 Illustration of epigenetic drug targeting advantages and disadvantages.

Mutations, chromosomal translocations or deletions are well studied in the context of cancer progression. However, the role of epigenetics is less well-defined. Epigenetic changes could induce pre-tumour characteristics even in healthy cells. The essential hallmarks guide was recently improved by the addition of "non-mutational epigenetic reprogramming" among other hallmarks (Hanahan, 2022). The non-mutational epigenetic reprogramming in the tumour cells provides an opportunity for therapeutic targeting.

DNMT and HDAC inhibitors were first-generation epigenetic modulators approved for clinical use for myelodysplastic syndrome (MDS) and cutaneous T cell lymphoma. However, they have shown toxicity and limited activity in solid tumours (Chitambar et al., 1991; Constantinides et al., 1978; Gallicchio, 1985; Vidali et al., 1978; Whittaker et al., 2010). Studies of somatic alterations in epigenetic factors in tumours reveal that most of these alterations lead to a loss of function. Chromatin re-modeler AT-rich interaction domain 1A (ARID1A) (S. Jones et al., 2010), lysine demethylase 6A (KDM6A or UTX) (van Haaften et al., 2009), and enhancer of zeste 2 polycomb repressive complex 2 subunit (EZH2) (Nikoloski et al., 2010) are the most known down-regulated genes in cancer. However, because there is a loss of function in these genes,

they are not ideal drug targets because restoring the lost function is more complicated. Instead, DNA methyltransferase 3 alpha (DNMT3A) (Russler-Germain et al., 2014) or nuclear receptor binding SET domain protein 2 (NSD2) (Kuo et al., 2011) genes with a gain of function are potential targets for inhibitory drugs.

The potential of epigenetic drugs is still a hot topic in cancer research. Pharmaco-biologists and chemists modify existing drugs or discover new epigenetic drugs for testing. New generation HDAC inhibitors such as vorinostat, panobinostat, and belinostat are approved as mono- or combination therapy in glioblastoma (Falkenberg & Johnstone, 2014).

1.3 Glioblastoma

The term *Brain Tumour* arises from different types of cancers in the CNS, as explained above(Butowski, 2015). The most common form of CNS neoplasms is gliomas, which are classified on their phenotypic cell characteristics. The gliomas that originated from astrocytes are called *Astrocytomas* (Louis et al., 2016; Perkins,A. Liu, 2016; van den Bent et al., 2017).

1.3.1 Glioblastoma development and progression

The most common malignant CNS tumour is Glioblastoma (Astrocytoma, WHO Grade IV), with an incidence of 3.19% per 100000 people annually. After diagnosis, the median survival rate is 15 to 17 months (Louis et al., 2016; Perkins, A. Liu, 2016; van den Bent et al., 2017).

To understand the complex nature of cancer, integral components of most cancer and some acquired capabilities (the hallmarks of cancer) are proposed. The cancer cells need to create genomic instability and mutations, resist cell death, deregulate cellular energetics, evade growth suppression, enable replicative immortality, activate invasion and metastasis, sustain proliferative signalling, avoid immune destruction, and induce angiogenesis (Hanahan & Weinberg, 2011).

Evaluating glioblastoma from the hallmarks of cancer perspective can give insight into several interconnected aspects. Escaping from apoptosis, autophagy or necrosis after genomic instability is vital for glioblastoma's developmental continuity. Tumours

develop over time with driver and passenger mutations, which create aberrant forms of genes. These mutations are needed to develop cancer cells and tumour environments (Brennan et al., 2014; Ceccarelli et al., 2016; J. H. Lee et al., 2018a; McLendon et al., 2008). Even though cells have DNA damage repair mechanisms, these mutations escape from repair mechanisms. Glioblastoma cells are less prone to cell death because mutant *TP53* and *RB,* which are two genes that take part in cellular and genomic damage control pathways, are mutated. Mutations in these genes decrease the cell death mechanisms' effectivity, creating a cell death escape and cell death resistance opportunity for glioblastoma (Biasoli et al., 2013; Jiang et al., 2009; Lefranc & Kiss, 2006; Stegh et al., 2010).

Mortality of the cells is closely related to telomere sequences, which are non-coding, repetitive nucleotides at the end of a chromosome. These sequences protect the chromosome from deterioration or fusion with neighbouring chromosomes, and during each replication, the telomeres are shortened because the DNA could not synthesize up to the end. If telomerase is erased after lots of duplication, each duplication would have a chance of mutations (frameshift, partial deletion of the gene). The cells have TERT to protect genomic integrity, which can add telomere sequences at the end of the chromosomes. Most cancer cells duplicate faster than non-cancerous cells, which could lead to essential gene interruptions with telomerase shortening. Therefore, cancerous cells have altered *TERT* activity, preventing unwanted deletions and protecting genomic integrity. Glioblastoma has mutated *TERT* (51% mutated) and *ATRX* (84% mutated). Therefore, these cells can avoid telomere shortening and create an immortality illusion (Bamford et al., 2004; Brennan et al., 2014; Ceccarelli et al., 2016).

Non-cancerous cells grow with autocrine and paracrine signalling and regulate proliferation in a sensitive equilibrium with growth suppressors. Once the cells are no longer needed or have any type of deficit, these cells would undergo growth suppression, followed by careful clearance. On the other hand, cancer cells are immortal and need to grow continuously, so sustaining proliferative signalling and evading growth suppression are necessary. Glioblastoma has three significant and proliferation promoting mutations: 1) Receptor Tyrosine Kinase (*RTK)*/ Rat Sarcoma (*RAS)*/ Phosphate Inositol 3 Kinase (*PI3K)*; 2) *TP53;* 3) *RB* with mutations rates of 88%, 78%, 87%, respectively (Brennan et al., 2014; McLendon et al., 2008; Zandi et al., 2007).

Basal metabolism of non-cancerous cells is tightly controlled with interconnected physiological levels of environmental and intracellular metabolite levels. In contrast, the tumour cells have limited access to blood vessels and metabolites. To overcome this problem, firstly, cancer cells secrete vascular endothelial growth factor (*VEGF)* for angiogenesis stimulation and connect tumours with blood vessels. Thus, essential metabolites could be carried to the tumour microenvironment. Secondly, cells adapt their metabolism to favour anaerobic glycolysis, reducing ATP production but allowing intermediate metabolites in other metabolic activities. The reduced ATP production is compiled with increased glucose intake so that the energy could be replaced. Glioblastoma has mutated glucose uptake receptor *GLUT1* for increased glucose intake and IDH isoforms to mediate transitional metabolites (Das & Marsden, 2013; Liberti & Locasale, 2016; Yan et al., 2009).

The immune system continuously investigates homeostasis and eradicates the old, dangerous, or foreign cells from the system. Research showed that a decrease of the effectiveness of the immune system is closely related to increased cancer development (Candeias & Gaipl, 2016; Fuertes et al., 2011; Gonzalez et al., 2018). Glioblastoma cells avoid immune response by presenting a limited number of antigens and recruiting immune suppressor cells (Keep et al., 2014).

The ability to invade other tissues is a common trait of cancer cells. However, it is infrequent in glioblastoma. Instead of distant metastasis, glioblastoma invades and migrates by spreading locally (Johansen et al., 2016). One of the proposed mechanisms is downregulating 'Connexin 43 (CNX43)' to decrease adherence and to increase invasion of nearby tissue (Sin et al., 2012). Another way is by degrading the extracellular matrix. Also, hypoxia increases cancer stem cell and myeloid cell recruitment (Tafani et al., 2011). The recruitment of myeloid cells causes upregulation of several growth factors, promoting epithelial to mesenchymal transition. Finally, epithelial to mesenchymal transition can occur because E-cadherin is lacking in glioblastoma (Guarino et al., 2007; Iwadate, 2016).

1.3.2 Current treatment options for glioblastoma

Current therapy for glioblastoma is surgery, irradiation therapy and chemotherapeutic agent temozolomide. Temozolomide is applied at a daily dose of 75 mg/m^{2}body surface

area, in parallel to radiotherapy, and six cycles of temozolomide alone at the dose of 175 mg/m^2 for five days every 28 days. This combination therapy increases the survival rate to 15 months compared with 12 months median survival of only radiotherapy-acquired patients (Messaoudi et al., 2015; Stupp et al., 2009).

1.3.2.1 Mechanism of action of temozolomide

Temozolomide is a small (194 Da) lipophilic midazotetrazine derivative, an oral alkylating agent used to treat glioblastoma and other astrocytomas. Brain tumours possess a more alkaline pH compared to surrounding healthy tissue, a favour for temozolomide, which is stable at acidic pH after passing the blood-brain barrier (S. Y. Lee, 2016).

Temozolomide induces cell cycle arrest at G_2/M and eventually leads to apoptosis. After being administrated orally and passing the blood-brain barrier, temozolomide at physiologic pH is hydrolysed to 5-(3-methyltriaze-1-yl) imidazole-4-carboxamide (MTIC). This is followed by MTIC hydrolysation to 5-amino-imidazole-4-carboxamide (AIC) and methylhydrazine. The Methylhydrazine group is an unstable, methyl donating group to O^6 sites of guanines in genomic DNA. Alkylation of the O^6-guanine leads to mismatch thymine addition instead of cytosine, resulting in cell cycle arrest and apoptosis (S. Y. Lee, 2016; Stupp et al., 2009).

However, 50% of the patients do not respond to temozolomide. The guanine mismatch-based cell cycle arrest could be repaired with base excision (BER) or DNA mismatch repair and reverse the effect of temozolomide. Also, MGMT acts to reverse the effect. However, it has been shown that MGMT status is not the only determinant of temozolomide resistance. Different groups showed that 1) Cells expressing MGMT, 2) MGMT promoter methylation status, 3) p53 mutation status, and 4) increased BER expression are several determinants for temozolomide resistance. All these indicate that temozolomide resistance results from a complex cellular response rather than one gene or pathway mutation (S. Y. Lee, 2016; Mallick et al., 2016).

1.3.2.2 Therapy resistance and recurrence of glioblastoma

The treatment regimen of surgery, radiation and chemotherapy prolongs the life of glioblastoma patients. Nevertheless, recurrence is inevitable for 25% of the patients, and 90% have been shown to recur at the primary site. Recurrence happens because of four main reasons: 1) Highly infiltrative nature, 2) Almost impossible resection because of unclear margins, 3) Decreased efficacy of radiation due to hypoxia, and 4) Blood-brain barrier's drug selectivity (Hudson et al., 2018).

The heterogeneous nature of the tumours presents variations and somatic genetic differences in cells. Even though therapy becomes more aggressive, acquired resistance is almost inevitable. Therapy resistance can be correlated with several factors, such as transporters, which can detect and efflux the chemotherapeutic agents from cells. Other drug resistance reasons include altered gene regulation, increased activation of oncogenes, inactivation of tumour suppressor genes, and amplified DNA repair capacity (Hudson et al., 2018; S. Y. Lee, 2016).

The resistant nature of some cells in heterogeneous tumour populations, and cancer stem cells that survive therapy, can be one of the explanations for cancer recurrence. Mostly these cells will have exhibit acquired resistance to survive the intense treatment, which leads to recurrent tumour formation (Hudson et al., 2018; Mallick et al., 2016).

In the case of glioblastoma, resistance to therapy is a critical issue due to limited therapeutic options. If the temozolomide chemotherapy fails, there is no other option. Therefore, understanding and evaluating the resistant nature of glioblastoma is vital. Since temozolomide is the golden standard chemotherapeutic of glioblastoma treatment, the actions to prevent temozolomide's working mechanisms are discussed above. (Hudson et al., 2018; S. Y. Lee, 2016; Mallick et al., 2016; Stupp et al., 2009).

1.3.3 Epigenetic regulation of glioblastoma

The most common metabolism alterations in GBM are increased Warburg effect(Poteet et al., 2013), disordered lipid metabolism (Lewis et al., 2015), and dysfunctional oxidative phosphorylation(Park et al., 2018). Aerobic glycolysis (Warburg effect) is controlled by *GLUT1-4 (*glucose transporters), *HK1-3, GAPDH, GLAM, and PKM2* (glycolytic enzymes). Even though the first studies suggested that factors such as *PI3K/AKT, TP53,* and *c-MYC* are solely responsible for the Warburg effect, recent studies have revealed that epigenetic regulators also contribute to the regulation of cell

metabolism (Clarke et al., 2013; Heiden et al., 2009; Lewis et al., 2015; Park et al., 2018; Poteet et al., 2013).

DNMT1, DNMT2 and *DNMT3* are the three families of active DNA methyltransferases in mammals (Berger, 2007). They regulate the genes by transferring the methyl group to promotoers or regulatory sites of active genes. Since a series of enzymes mediate cell metabolisms, regulation of these enzymes is essential for tumour metabolism and progression (Berger, 2007). Research has shown the hypomethylation of *PKM* intron 1 in GBM, and high gene expression of *PKM2* is correlated with glycolysis. However, the promoter regions of other glycolytic genes are hypermethylated. For example, *HK2* isoforms are hypermethylated; therefore, *HK2* is less presented in GBM cell lines. Moreover, GBM cells with low *HK2* treated with decitabine presented promising elevation in *HK2* expression levels and partial recovery in glycolysis (Berger, 2007; A. Wolf et al., 2011). All this research indicates that DNA methylation plays a vital role in the Warburg effect regulation and cell metabolism.

Histone methylation, demethylation and the importance in tumour initiation and progression are described above. HMTs and HDMs play opposite roles. It has been shown that arginine residues could be mono- or di-methylated; meanwhile, lysine residues could be mono-, di-, and tri-methylated(Wood & Shilatifard, 2004). So, HMTs are divided according to their active methylation residue, protein lysine methyltransferase (PKMTs) or protein arginine methyltransferase (PRMTs) (Tiedeken & Chang, 2015). EZH2 up-regulates H3K27me3 levels of *EAF2*, which promotes HIF1α signalling. This mechanism downregulates mitochondrial respiration and up-regulates glycolysis in GBM. In opposite, LSD1, one of the HDMs, decreases H3K4me3 at the *MYC* promoter and increases its production in the cells. *MYC* regulates several transcription factors associated with the stemness of GBM. It has also been shown that LSD1 suppresses the *p53* gene by demethylation of the promotor site and intron 2. Suppressed p53 pathway inhibits apoptosis of the cells and promotes tumorigenesis of GBM (Kozono et al., 2015; Yi et al., 2016). Another HDM, JMJD3 (KDM6B), inhibits the p53 pathway and blocks terminal differentiation in GBM (Ene et al., 2012). It has been known that both MYC and p53 are fundamental regulators of glucose metabolism. Since LSD1 and JMJD3 are regulators of *MYC* and *p53*, they also participate in glucose metabolism regulation of GBM (Hu et al., 2016).

HATs and HDACs are responsible for gene activation or repression by adding or removing the acetyl group to promoter sites. Recent studies positively correlated histone acetylation and GBM progression. H3K9 hyperacetylation was observed in Glial cell line-derived neurotrophic factor (*GDNF)* promoter in high-grade glioblastoma. Specifically, PCAF (KAT2B) acetylates *AKT1*, promoting GBM proliferation (Roth et al., 2003). Another HAT, KAT6A, acetylates H3K23 and recruits TRIM24, which initially up-regulates *PIK3CA* and activates AKT-promoted GBM tumorigenesis (Lv et al., 2017). These pieces of evidence prove that the HATs are potential cell regulators. In contrast, HDACs are also potential cell regulators. *FOXO1 and FOXO3* are hyperacetylated in GBM, whereas inhibition of class 2 HDACs leads to an inability to remove the acetyl group. FOXOs suppress *miR-34c* transcription, and *miR-34c* could not inhibit *c-MYC*. Thereby, *c-MYC* overactivation leads to GBM stemness (Masui et al., 2013). All this evidence proves that histone modulation is an essential regulator of cell metabolism and tumour progression.

1.3.4 Targeting epigenetic modification of glioblastoma as a treatment option

Even though current therapeutics increase the survival rate of glioblastoma patients slightly, they do not eradicate the tumours. Epigenetic therapies provide new avenues for the treatment of GBM; however, monotherapies with epigenetic drugs did not show significant improvements in GBM (Uddin et al., 2020). Therefore, the combination of different epigenetic therapeutics or the combination of an epigenetic drug with existing drugs is currently in clinical trials (*Vorinostat, Temozolomide, and Radiation Therapy in Treating Patients With Newly Diagnosed Glioblastoma Multiforme - Full Text View - ClinicalTrials.Gov*, n.d.; *Vorinostat, Temozolomide, or Bevacizumab in Combination With Radiation Therapy Followed by Bevacizumab and Temozolomide in Young Patients With Newly Diagnosed High-Grade Glioma - Full Text View - ClinicalTrials.Gov*, n.d.).

HDAC inhibitors were found to suspend glioma oncogene transcription and degrade heat shock proteins, resulting in cell cycle arrest, eventually inducing apoptosis in GBM. Another favourable drug group in GBM clinical trials is DNMT inhibitors. Currently, the most promising drug combinations are vorinostat/temozolomide and panobinostat/bevacizumab (*Vorinostat, Temozolomide, and Radiation Therapy in*

Treating Patients With Newly Diagnosed Glioblastoma Multiforme - Full Text View - ClinicalTrials.Gov, n.d.; *Vorinostat, Temozolomide, or Bevacizumab in Combination With Radiation Therapy Followed by Bevacizumab and Temozolomide in Young Patients With Newly Diagnosed High-Grade Glioma - Full Text View - ClinicalTrials.Gov*, n.d.).

Vorinostat is an HDAC inhibitor with a broad epigenetic spectrum. A phase I study concluded that vorinostat combined with temozolomide increased H3 acetylation and temozolomide efficacy. Another research, a phase II study, has proven H2B, H3, and H4 acetylation accumulation, increased temozolomide effect, and up-regulation in vorinostat regulated genes (*Vorinostat, Temozolomide, and Radiation Therapy in Treating Patients With Newly Diagnosed Glioblastoma Multiforme - Full Text View - ClinicalTrials.Gov*, n.d.; *Vorinostat, Temozolomide, or Bevacizumab in Combination With Radiation Therapy Followed by Bevacizumab and Temozolomide in Young Patients With Newly Diagnosed High-Grade Glioma - Full Text View - ClinicalTrials.Gov*, n.d.).

Panobinostat is a non-selective HDAC inhibitor, and bevacizumab is a VEGF inhibitor. Phase II monotherapy studies of panobinostat or bevacizumab did not lead to any remarkable improvement, whereas the earlier cohort studies had shown that the combination of panobinostat and bevacizumab gave promising results (E. Q. Lee et al., 2015). The phase I study of combination therapy enhanced the rate of 6-month progression-free survival (PFS6) by 30.4%; meanwhile, panobinostat/radiation therapy showed 83% PFS6 (Shi et al., 2016).

Individually conducted phase I, phase II, and phase III studies with epigenetic drugs have shown limited success. One reason for this observation could be redundant or compensatory mechanisms regulating histone modifications. The histone code hypothesis states that multiple histone modifications could act in a combinatorial or sequential fashion on one or multiple histone tails (Strahl & Allis, 2000). Therefore, targeting one histone modifier enzyme may not be sufficient in achieving the combinatorial effect. Another explanation for the low success rate could be the limitation of pre-clinical studies. While the drugs are tested *in vitro*, the drug discovery, validation and optimisations are conducted on established cell lines (Kaitin, 2010). This limits the studies to cells in isolation, but it is well known that microenvironments have a significant role in regulating pharmacokinetics (Lucas et al., 2017; Salvadori et al., 2019; Ziemys et al., 2016).

1.3.5 Glioblastoma microenvironment and interactions

The endothelial cells, pericytes, astrocytes, neuronal precursor cells, fibroblasts and immune cells coexist with GBM cells and glioblastoma stem-like cells (GSCs) within the extracellular matrix and define the glioblastoma tumor microenvironment (GTME) (Schiffer et al., 2019). The TME interactions create specialised niches, which are associated with tumour progression and resistance to treatment. It has been shown that hypoxic and immune niches promote metabolic adaptation, multiple drug resistance and immune resistance (Hambardzumyan & Bergers, 2015). GSCs have the same self-renewal and differentiation properties as other stem cells. However, GSCs present enhanced adaptability, tumorigenesis and resistance to treatments. The heterogeneity is not limited by the niches; the GBM cells and GSCs present heterogeneity within (Bao et al., 2006; Beier et al., 2007; Hambardzumyan & Bergers, 2015; Salvadori et al., 2019). The heterogeneity should be carefully considered before designing treatment strategies. Defining the heterogeneity at the phenotypic level and finding repetitive phenotypes across patients would open the path for more generalisable treatments.

Recently single-cell transcriptional profiling presented 4 distinct states of GBM cells (Venteicher et al., 2017). The transcriptional patterns were astrocyte cell-like, oligodendrocyte progenitor cell-like, neural progenitor cell-like, and mesenchymal-like, and the distinct states named after these patterns. Even though the states presented stable profiles, the transcriptional patterns presented plasticity (Neftel et al., 2019; Suvà et al., 2014). Complementary transcriptional profiles and histological profiles have resolved unique regional GTMEs.

Hypoxic/necrotic, invasive and perivascular niches have been described for GTMEs. The transcriptional and phenotypic profiles highlight consistent niche-specific molecular dependencies. Hypoxic niches present higher expression of hypoxia-inducible factor-related pathways. Differentiation/proliferation pathways are highly conserved in perivascular niches. Regional studies suggest that microenvironment enforces GBM cells to adopt phenotypic profiles, which could be advantageous for therapy design (Brennan et al., 2013).

Understanding and targeting the GBM profiles in niches could be practical, whereas integration of these levels could discover better synergistic targets. One hypothetical model claimed that the 4 GBM profiles could be nonrandomly distributed among the

niches. This model partially explains the heterogeneity of tumours and, therefore, explains the progression, plasticity, and resistance. However, targeting each subclone is not practical currently due to the additive multiple-level variations. Because 4 transcriptional profiles in 3 distinct niches result in 12 coexisting states, and even with the best approximation needs at least 5 different synergistic drugs for treatment (Lam et al., 2020; Suvà et al., 2014). The regional distributions of transcriptional profiles in each niche suggest a hybrid model. The hybrid model shows mesenchymal-like and astrocyte cell-like patterns align with the hypoxic niche, whereas the neural progenitor cell-like and oligodendrocyte progenitor cell-like patterns appear less. The heterogeneous profile differs in each niche. Therefore, additional single-cell studies complementary to proteomic and histological studies are needed (Bar, 2011; Bar et al., 2010; Brat et al., 2015; Djuric et al., 2019; Eberhart & Bar, 2020; Puchalski et al., 2018).

Astrocytes are the most abundant cells in the central nervous system, which mainly regulate the environmental changes such as angiogenic factors; glutamate, ion and water homeostasis; permeability of the blood-brain barrier (Perrin et al., 2019; C. Yang et al., 2013). These stromal changes promote tumour proliferation directly or indirectly. Still, one emerging question is *whether astrocytes change the cancer cells' behaviour and adapt them to the microenvironment or do the cancer cells alter the behaviour of the astrocytes and create a suitable environment for proliferation*. Recent studies provide evidence that neither of these statements could be accepted as directly valid. Instead of only astrocyte cells or cancer cells changing the microenvironment and behaviour of these cells, both cell types support each other (Perrin et al., 2019; C. Yang et al., 2013). Malignant cancers acquire more metastasis than benign tumours due to the down-regulated cell adhesion receptors necessary for tissue-specific cell-to-cell attachment and up-regulated cell motility. Also, membrane metalloproteases provide a pathway for metastatic cancer cells to spread(ALLFREY et al., 1964; Sarkar et al., 2013; Verdone et al., 2006; Zhao et al., 2020). However, compared to other tumour types, glioblastoma presents less metastatic tendency, which could be due to a more protective environment of the brain, which was discussed above.

The chemoresistance of glioblastoma is discussed above, and recent research has increasing evidence that chemoresistance of glioblastoma is also associated with tumour microenvironment (Chen et al., 2015; Perrin et al., 2019; Schiffer et al., 2019; N. Yang et al., 2014). Especially astrocytes have protective abilities against chemotherapeutics.

The protective effect elicited by astrocytes requires direct contact with tumour cells, which is provided by gap junctions between astrocytes and glioblastoma cells. Some researchers discussed that gap junction formation mainly occurs around the tumour cells and acts as a protective layer against drugs (Perrin et al., 2019; X. Zhang et al., 2019). Gap junctions between astrocytes and tumours also provide intracellular metabolite transfer. In a recent study, intracellular transfer of microRNA from astrocyte to tumour cell induced therapy resistance (X. Zhang et al., 2019).

These pieces of evidence suggest that the tumour cells are under the effect of the tumour microenvironment more than evaluated before. This notion could change the basics of drug development in GBM. Therefore, assessing the tumour cells' response to drugs in the context of a microenvironment would provide more applicable solutions for successful therapies.

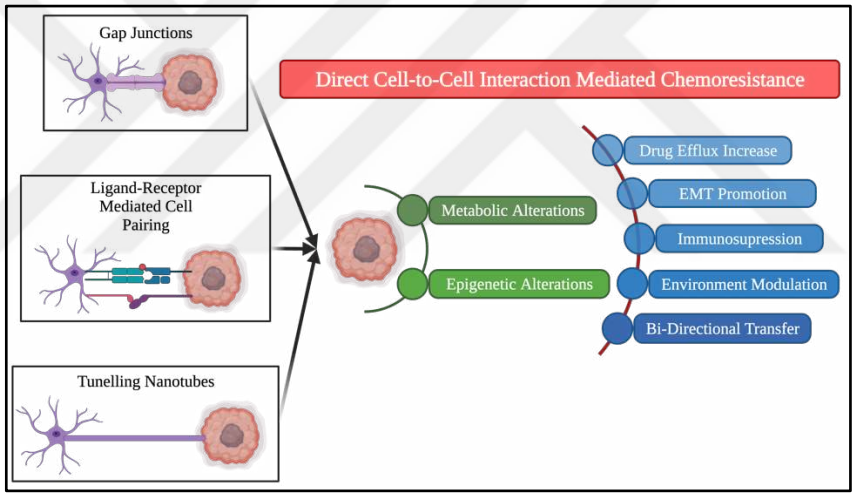

Figure 1.3 Illustration of cell-to-cell interactions and their effect on chemoresistance.

1.3.6 Mitochondrial regulation of glioblastoma and glioblastoma microenvironment

The energy source of the cell, mitochondria, is an emerging player in cancer research. As explained above, the Warburg effect is an essential identifier of GBM. DNA methylation down-regulates glycolysis as well as mitochondria function and oxidative phosphorylation (Dong & Cui, 2019; Kitange et al., 2012). 5-azacytidine and vitamin C induce global DNA methylation and synergistically impair the mitochondrial DNA (mtDNA) copy number in GBM cells, thus promoting the Warburg effect (Semenza,

2003). In parallel, lysine methyltransferases G9A and GLP catalyse H3K9, which suppresses *HIF1* and its downstream targets. Also, MLL1 inhibits the *HIF2* and targets, creating an additive inhibitory effect on glycolysis (Heddleston et al., 2011; Pang et al., 2016; Semenza, 2003).

Cytoplasmic bridges are standard for gene sharing in prokaryotic cells. This communication type could be observed even among more complex eukaryotic cells. Cytoplasmic bridges seem like a conserved formation during oogenesis and spermatogenesis for several reasons. In oogenesis, the bridges are formed to feed and maintain the most stable oocyte until mature ovum formation. Meanwhile, the bridges are formed to distribute equal cytoplasm among the spermatids in meiotic division II during spermatogenesis (*Cytoplasmic Bridges, Intercellular Junctions, and Individualization of Germ Cells during Spermatogenesis in Dermatobia Hominis (Diptera: Cuterebridae)*, n.d.; Ventelä et al., 2003a). DNA containing cytoplasmic bridges in tumour–tumour interactions is the forebearers of the more advanced studies (K. W. Wolf et al., 1996). These studies are closely associated with chromosomal instability (Bakhoum et al., 2014) and chemoresistance (McClelland et al., 2009).

The most interesting cytoplasmic bridge process could be intracellular organelle transfer between cells, which was first studied at spermatids (Ventelä et al., 2003b). Especially, mitochondria transfer between cells and TME has been associated with metabolic and phenotypic consequences, such as restoration of mitochondrial functions in tumour cells, tumour survival and proliferation, tumorigenesis and tumour progression, and chemoresistance (Qin et al., 2021; Zampieri et al., 2021). Tumour survival, especially escaping from immune destruction, was associated with alternative tumour antigen-presenting mechanisms. In contrast, recent studies of TME-tumour interactions presented evidence of another mechanism, mitochondria hijacking. The breast cancer cells, MDA-MB-231, form more than one nanotubule with natural killer (NK) immune cells and hijack mitochondria of immune cells. After 16 hours, the NK cells lose more than 60% of the mitochondria, which decreases the respiration of these cells by 90% and suspend NK cell metabolism and activity (Baldwin & Gattinoni, 2021; Saha et al., 2021). This evidence suggests an alternative immune escape mechanism as well as the importance of mitochondrial regulation in TME.

Another study claimed that the GBM cells could transfer mitochondria from TME. A mitochondria localised transgene was tracked between glial or astrocytic cells and

GBM cells in orthotopically transplanted tumours. The transcriptional landscape of mitochondria-received GBM cells presented up-regulated mitochondrial pathways compared to GBM cells which did not receive mitochondria. Furthermore, the study associated mitochondria transfer with GBM tumourigenesis (Lathia et al., 2021; Watson et al., 2021). However, there is still a lack of understanding about the donor-recipient interactions and downstream effects on both tumour and healthy cells.

2 Material and Methods

2.1 Culturing the Cells

Human GBM cell lines U87MG and 293T cells were purchased from the American Tissue Type Culture Collection (ATCC). Normal human astrocyte was purchased from ScienCell (Catalog #1800). Immortal normal human astrocyte (INHA) was a kind gift from Tim Chan from Memorial Sloan Kettering Cancer Center (MSKCC). All cells were cultured in DMEM medium (Invitrogen #4196029) with 10% fetal bovine serum (Gibco #10500064) and 1% Penicillin/Streptomycin (Invitrogen #15070-063). Cells were grown in a 37 °C humidified incubator with 5% CO_2. Mycoplasma contamination status was checked weekly with Mycoplasma Detection Kit (Lonza). The cells were either mono-cultured or co-cultured.

2.1.1 Mono-Culturing and Co-Culturing the Cells

The U87MG-Untagged, U87MG-FMC$^+$ and INHA-GFP$^+$ cells were individually cultured as described above. The U87MG-Untagged and U87MG-FMC$^+$ cells were separately seeded in a 1:1 portion to create the mono-culture environment. The U87MG-FMC$^+$ and INHA-GFP$^+$ cells were individually seeded in 1:1 proportions to generate a co-culture environment. The cells were co-mixed by pipetting the medium 5 times after individual cell seeding.

2.2 Stable Cell Line Generation

Stable cell lines were produced by lentiviral transduction, which consists of two steps, lentivirus preparation and lentivirus transduction.

2.2.1 Lentivirus Preparation

The lentiviruses were prepared in 293T cells. The 293T cells were seeded $2.5x10^6$ to 10 cm plates one day before transfection. 20 μL Fugene in 180 μL DMEM (without FBS and Pen/Strep) and 250 ng VSVG, 2250 ng pspax2 and 2500 ng desired plasmid in

optiMEM with the total volume of 200 µL prepared individually. Both solutions were mixed and pipetted 5 times for homogenisation and incubated at RT for 30 minutes. After incubation, the whole mix was added to 293T medium. The following day, the DMEM with transfection mix was replenished with fresh medium. 48 hours post-transfection, the supernatant was collected from the plate, and a new medium was added to the plate. 72 hours post-transfection, the supernatant was collected from the plate, and the plate was discarded. The collected supernatant was filtered with a 45 µm filter, and the filtered supernatant was mixed with Polyethylene glycol (PEG) 1:5. Supernatant – PEG mix homogenised thoroughly and incubated at 4 °C 48 hours. After incubation, the mix was centrifuged at 800 x g for 25 minutes. The supernatant was discarded, and the pellet was resuspended in 160 µL. The concentrated virus was aliquoted 20 µL per Eppendorf and stored at -80 °C prior to use.

2.2.2 Lentiviral Transduction of Cells

The cell of interest was seeded to 6 well plate $0.15x10^6$ cell/well and distributed evenly. 24 hours later, the medium was discarded, and a fresh medium containing 5 µg/mL protamine sulphate (PS) was added to the plate. Concentrated virus, thawed on ice, was added to medium and distributed evenly, and the plate was incubated overnight. The following day, the medium was replenished with fresh medium. 48 hours after transduction, the selection was performed according to plasmid selection criteria (Appendix - Table 1).

2.3 Cell Viability Assay

Two different cell viability assays were used throughout the experiments depending on the experiment, Cell Titer Glo (CTG) for individual cell viability detection or D-luciferin Assay for mono-cultured and co-cultured cell viability detection.

2.3.1 Cell Titer Glo (CTG) Assay

Cell Titer Glo® (CTG) Luminescent Cell Viability Assay (Promega, Cat# G7570, USA) reagent was used to determine cell viability. CTG reagent contains luciferase,

luciferin, cell lysis reagents and other reagents for bioluminescent reaction. CTG reagent lyses the cells for ATP release. ATP released from metabolically active cells is necessary for the processing of luciferin by luciferase. Therefore, intensity of the bioluminescence changes with the ATP content, which is used to determine the relative cell viability. The manufacturer's instructions for CTG assay was slightly modified.

Each plate was incubated for 10 minutes at room temperature before CTG reagent addition. For 96 well plates, the medium was removed, and 5 µL CTG reagent + 45 µL DMEM pre-prepared mix was added to 50 µL/per well. Immediately after mix addition, the plate was put in the Synergy H1 Plate Reader (Biotek, USA) for 2 minutes of bi-directional shaking and 8 minutes of incubation and luminometric read. Cell viability was calculated as a percentage by normalising treated samples to untreated control samples.

2.3.2 D-Luciferin Assay for subpopulation tracking

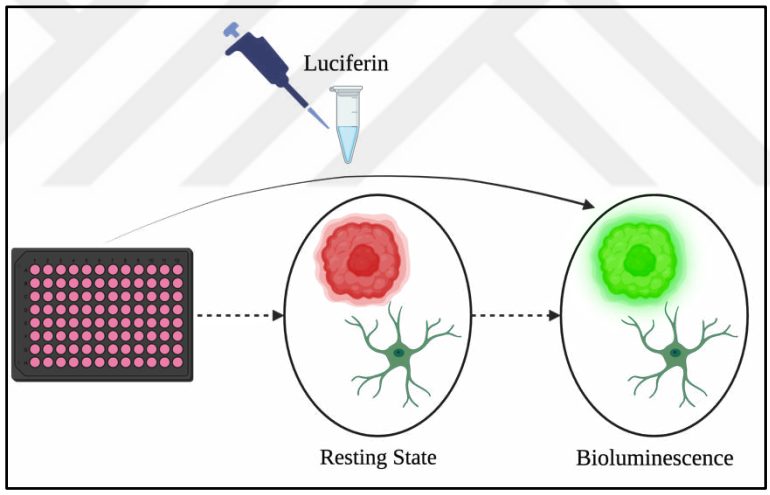

Figure 2.1 Illustration of D-Luciferin assay for subpopulation tracking.

The D-luciferin assay is a similar method to CTG assay with slight differences (Figure 2.1). Both methods depend on luciferin cleavage by cellular ATP-dependent luciferase. Bioluminescence signals of cleaved luciferin were collected for relative cell viability. Therefore, we generated stable firefly luciferin (FLuc) – mCherry expressing U87MG cell lines for constitutive luciferase expression. This cell line presented bioluminescence when treated with D-luciferin.

Cells were seeded, treated and incubated according to the protocol as described. The D-luciferin (10 mg/mL) was thawed at room temperature before use. For 96 well

plates, the medium was removed, and 5 µL D-luciferin + 95 µL medium pre-prepared mix was added 100 µL to each well. Immediately after mix addition, the plate was put in the Synergy H1 Plate Reader (Biotek, USA) for 2 minutes of bi-directional shaking and 8 minutes of incubation and luminometric read. Cell viability was calculated as a percentage by normalising treated samples to untreated control samples.

2.4 Contact Independent Drug Assays

Contact independent drug assays were divided into 1) drug response of cell lines, 2) condition medium assay, and 3) Trans-well assay (Figure 2.2).

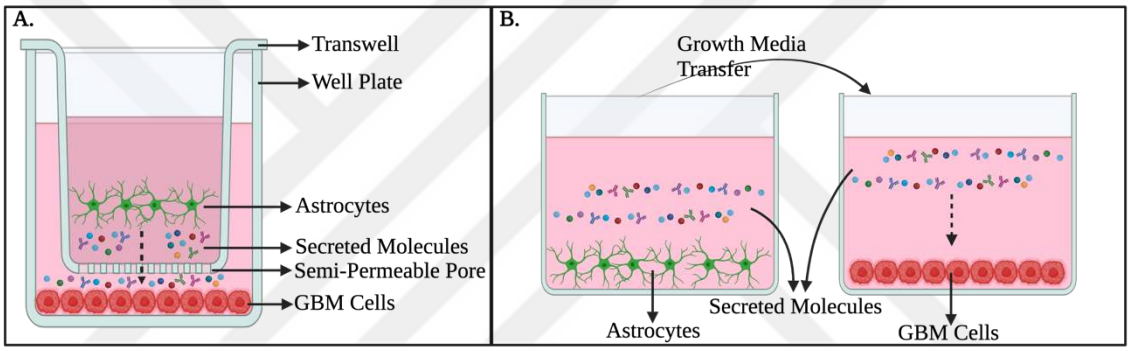

Figure 2.2 Graphical illustration of transwell (A) method and condition medium (B) assay.

2.4.1 Drug dose-response of cell lines

The cells were seeded to black 96 well plate 2000 cell/well and distributed evenly. After 24 hours of incubation, the cells were treated with increasing drug doses. After drug treatment, the plate was incubated for 5 days, and CTG cell viability assay was applied. The TMZ treatment of U87MG cells consisted of increasing, serially diluted, 5 doses between 62,5 µM – 1000 µM. Meanwhile, astrocytes were treated with increasing 5 amounts between 1875 µM – 15'000 µM. GSK-J4 treatment of U87MG cells was between 0,625 µM – 10 µM. The bioluminescence values normalised to untreated control samples, and the cell viability was calculated as % values and standard deviations. The % inputs were fitted to a non-linear normalised inhibitor curve to calculate the IC_{50} values of the drug.

2.4.2 Condition Medium Assay

Two astrocyte plates were seeded to 12 well plates as 50,000 cells/well, three days prior to the initial experiment. Following day, one of the plates was treated with 400 μM TMZ. Both plates were prepared as condition medium (CM). One plate was untreated-CM, while the other was treated-CM.

One day before the initial experiment, U87MG cells were seeded to 12 well plates as 50,000 cells/well. After 24 hours of incubation, the medium was removed from the plates, and the plates were washed twice with phosphate-buffered saline (PBS). Untreated-CM and treated-CM were transferred to the plates and incubated for 24 hours. The following day, both plates were treated with 400 μM TMZ. After 5 days of incubation, the cells were detached from the plate, centrifuged, and the supernatant removed without disturbing the pellet. The pellet was solved in 90 μL fresh medium and seeded to a black 96 well plate, and 10 μL CTG was added to each well. Immediately after CTG addition, the plate was put in the Synergy H1 Plate Reader (Biotek, USA) for 2 minutes of bi-directional shaking and 8 minutes of incubation and luminometric read. Cell viability was calculated as a percentage by normalising treated samples to untreated control samples.

2.4.3 Trans-well Assay

In this assay, astrocytes were seeded to the upper layer of a semi-permeable cell culture insert as 50,000 cells/insert, and U87MG cells were seeded to a well plate as 50,000 cells/well. Two separate plates were prepared, and the following day the plates were treated with TMZ (400 μM). TMZ was applied to insert or directly in the plate's well. After 5 days of incubation, the cells were detached from the plate, centrifuged, and the supernatant removed without disturbing the pellet. The pellet was solved in 90 μL fresh medium and seeded to a black 96 well plate, and 10 μL CTG was added to each well. Immediately after CTG addition, the plate was put in the Synergy H1 Plate Reader (Biotek, USA) for 2 minutes of bi-directional shaking and 8 minutes of incubation and luminometric read. Cell viability was calculated as a percentage by normalising treated samples to untreated control samples.

2.5 Contact-Dependent Drug Treatment

The contact-dependent drug treatment protocol was nearly the same as the drug dose-response protocol. The slight change was at the cell seeding, where instead of seeding individual cell lines, the co-culturing protocol was followed. After 24 hours of incubation, the cells were treated with TMZ (400 µM), GSK-J4 (7.5 µM) or a combination of TMZ and GSK-J4, and cell viability was measured with D-luciferin assay as explained.

2.6 Co-culture cell sorting and bulk RNA sequencing

To identify the differences between mono-cultured and co-cultured U87MG cells, we first incubated mono- and co-cultured cells for 72 hours (3 days). Cell sorting, RNA isolation, and RNA sequencing were applied to the cells in this order (Figure 2.3).

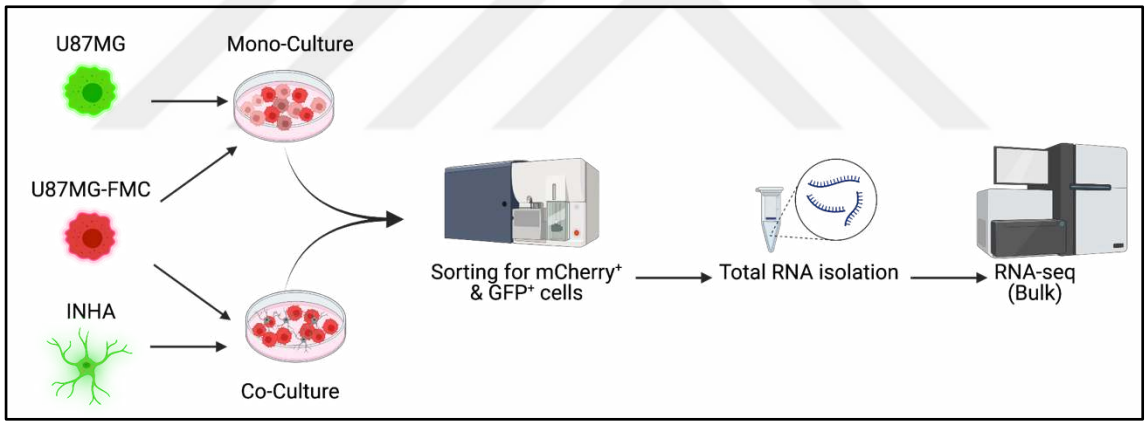

Figure 2.3 Graphical abstract of bulk RNA sequencing after cell sorting.

2.6.1 Cell sorting

Treated cells were detached from the plate. Detached cells were counted and suspended in phosphate-buffered saline (PBS). 1 mL PBS was used for suspending 1 million cells. Suspended U87MG cells presented mCherry fluorescent protein; meanwhile, astrocytes presented green fluorescent protein (GFP).

The whole-cell suspension was loaded to BD Fluorescence-Activated Cell Sorting (FACS) Aria II. The filters were set excitation: 488, emission: 507 for GFP, while

excitation: 587, emission: 610 for mCherry. The electrical field was set to 28 – 45 KHz for single-cell flow, with a 100 μm nozzle diameter. 100'000 droplets per second, 10K threshold, and 90% recovery were used for maximum efficiency. Sorted cells were collected in nuclease-free flow cytometry tubes containing 2 mL PBS.

2.6.2 RNA Isolation and RNA sequencing

Sorted cells were transferred to 2 mL PBS Eppendorf's and centrifuged at 1500 rpm for 5 minutes. The supernatant was removed without disrupting the pellet. The RNA was isolated with MN RNA Isolation Kit following the manufacturer's instructions. The quantity of the RNA samples was verified with NanoDrop Spectrophotometer, and Agilent Tapestation confirmed the quality of the RNA samples. Beijing Genomics Institute (BGI) performed the RNAseq library preparation and sequencing on a NextSeq 500 platform using a paired-end run 2 x 80 bp to an average depth of 40 x 10^6 reads per sample.

2.6.3 Analysis of RNA sequencing

The raw sequencing files were verified with quality control and then analysed with DESeq2 Bulk RNA-seq R markdown pipeline (*GitHub - Cribbslab/Deseq2_report: Deseq2 Automatic Report Generation*, n.d.). Briefly, the reads were pseudo-aligned with Kallisto, and a counts matrix was obtained. The counts matrix was normalised and quantified. Differential expression (DE) analysis was performed with DESeq 2, and all the results were written into an HTML file with an R markdown for further processing.

The differential expression log fold change (LFC) and HGNC symbols were used to perform Gene Set Enrichment Analysis (GSEA). The pre-ranked files were loaded into the GSEA desktop application, and the differentially expressed genes were compared against "Hallmark", "Reactome", and "KEGG" databases to identify the positively and negatively enriched pathways.

2.7 Targeting epigenetic modifying enzymes with a small molecule chemical library

The epigenetic inhibitor small molecule library was a kind gift from Prof. Udo Opperman (University of Oxford). The library is targeting various histone-modifying enzymes.

The mono-culture and co-cultures were seeded as 2000 cells/well to black 96 well plates. The following day, the cells were treated either with a chemical library or chemical library and TMZ (400 μM) combination. Cell viability was detected with D-luciferin assay 5 days after drug treatment, and the reads were normalised to untreated controls. The standard deviation and median values for mono- and combination treatments were used as a reference. The drugs that presented sensitising effects in co-culture conditions were selected as the 'hit' probes.

The hits were validated both in mono-culture and co-culture conditions as explained in contact-dependent drug treatment. The individual drug responses and literature were used to narrow the hits to 1 probe, histone demethylase, GSK-J4.

GSK-J4 IC_{50} value for U87MG cells was determined with a dose-response assay.

2.8 Clustered Regularly Interspaced Short Palindromic Repeats (CRISPR) knockdown of KDM6A/6B

Histone demethylase GSK-J4 targets are *KDM6A* (*UTR*) and *KDM6B* (*UTX*). Therefore, the effect of inhibition of these genes in drug resistance were tested, complementing the chemical approach. We specifically designed CRISPR-inhibition (CRISPRi) guide RNAs (gRNAs) for *KDM6A* and *KDM6B* knockdown and tested the drug response with stable knockdown cell lines.

2.8.1 Guide RNA design and cloning of KDM6A/6B

The promoter regions of *KDM6A* and *KDM6B* were obtained from the eukaryotic promoter database (EPD) (*EPD The Eukaryotic Promoter Database*, n.d.). Guide RNAs (gRNAs) were designed around -200 bp upstream of the transcription start site (TSS), as suggested, with CHOPCHOP gRNA design tool (*CHOPCHOP*, n.d.). The gRNAs designed were plotted and tested with benchling (*Cloud-Based Platform for Biotech R&D | Benchling*, n.d.) and BLAST (*BLAST: Basic Local Alignment Search Tool*, n.d.) tools to validate the binding site and off-target binding scores. Three gRNA

sequences/promoter-site with the highest activity score and minimum off-target binding were selected and ordered for cloning (Table 1).

Table 1: Single Guide RNAs for KDM6A/B Knockdown.

Target	Direction	Sequence
KDM6A_1	Forward	CACCGACAACTTTGTGCTGGTGCCG
	Reverse	AAACCGGCACCAGCACAAAGTTGTC
KDM6A_2	Forward	CACCGGGCGACGAAAAATCCCAACG
	Reverse	AAACCGTTGGGATTTTTCGTCGCCC
KDM6A_3	Forward	CACCGTGCGTTTCCATGAAATCCTG
	Reverse	AAACCAGGATTTCATGGAAACGCAC
KDM6B_1	Forward	CACCGGAGAGGGGGACTAGAGCGCG
	Reverse	AAACCGCGCTCTAGTCCCCCTCTCC
KDM6B_2	Forward	CACCGGCGCGGCGGTCCTTACTGAA
	Reverse	AAACTTCAGTAAGGACCGCCGCGCC
KDM6B_3	Forward	CACCGCTGGTGGGGGTTAGAGACAG
	Reverse	AAACCTGTCTCTAACCCCCACCAGC

gRNAs were cloned in plentiGuide backbone according to Zhang Lab's protocol (Shalem et al., 2014). In sum, plentiGuide was digested with BsmBI and gel purified with MN PCR-Clean Up Kit. Extracted plasmids were treated with Antarctic Phosphatase (AP) for 5' and 3' phosphate removal. 1 µL of each oligo (100 µM) was annealed with T4 Polynucleotide Kinase and T4 DNA Ligase Buffer in 10 µL reaction volume at a thermal cycler with the following settings: 37°C for 30 min, 95°C for 4 min and then ramp down to 25°C at 5°C/min. Oligos were diluted to 1:200 to use as inserts for cloning. 20 µL ligation reactions were prepared with 50 ng BsmBI-digested, AP-treated vectors, 1 µL of inserts and T4 DNA Ligase (NEB) in 10X T4 DNA Ligase buffer (NEB), respectively. The mix was incubated at 25 °C 2 hours and heat-inactivated at 65 °C for 10 minutes. According to the manufacturer's protocol, ligation products were transformed and inoculated with Stbl3 bacterial cells. The plasmids were isolated from bacteria with MN Nucleospin Plasmid Kit. To confirm the inserts, samples were sent to sequencing with U6 promoter sequencing (Forward sequencing primer for U6 promoter: ACTATCATATGCTTACCGTAAC). Verified plasmids were packed into lentiviruses

and transduced as explained. The knockdown was verified with quantitative real time polymerase chain reaction (qRT-PCR). U87MG-WT, U87-KDM6A knockdown (d6A), U87MG-KDM6B knockdown (d6B), non-targeting (NT1, NT2), and dCas9-Only cells were proliferated and collected for RNA purification. The purified RNAs were used for cDNA synthesis (explained below). Synthesized cDNAs were used for qRT-PCR comparison with specific KDM6A, KDM6B, and GAPDH primers (Table 2). Cell lines were compared for RNA levels, and the efficiencies were determined by comparing with WT and NT cells.

2.8.2 Drug response of stable knockdown cell lines

U87MG-WT, U87MG-KDM6A knockdown (d6A), U87MG-KDM6B knockdown (d6B), and U87MG-NT1 cells were grown to 80% confluency. The cells from each group were seeded to a black 96 well plate, 2000 cells/well as triplicates. After 24 hours of incubation, the plate was treated with TMZ (400μM) and incubated for 5 more days. The cell viability was measured with CTG assay, and the results were normalised to control-U87MG-WT to calculate the % cell viability.

2.9 Multimodal Cellular Indexing of Transcriptomes and Epitopes (CITE) – Single Cell Sequencing (Multimodal CITE-Single-Seq)

CITE-seq is a modified single-cell sequencing method which uses barcoded-oligo antibodies to convert the detection of proteins in sequence-able readouts. Oligo sequences act as synthetic barcodes and are captured during most scRNA-seq library preparation protocols (Figure 2.4).

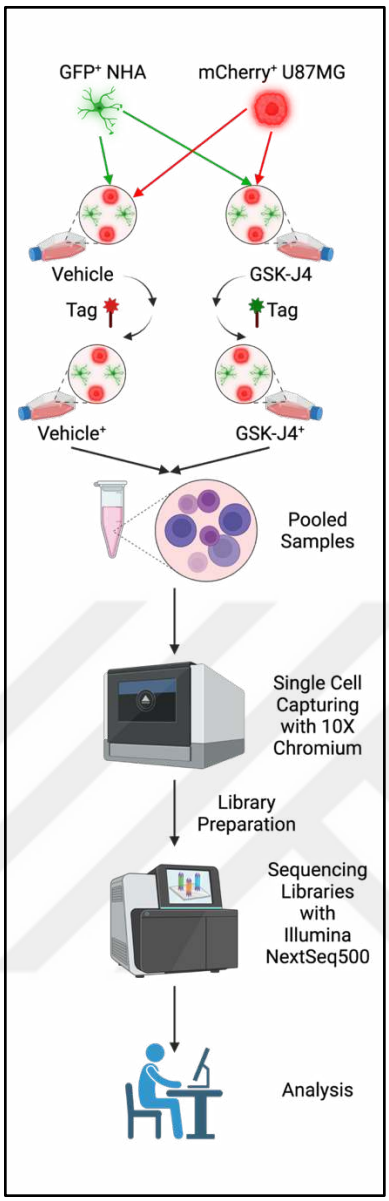

Figure 2.4 Graphical abstract of combined single-cell sequencing experiment.

2.9.1 Sample preparation

Two separate plates were used to co-culture astrocytes and U87MG cells as 500,000:50,000 cells in T75 plates. The following day, both plates' medium was replenished, and one plate was treated with 7.5 µM GSK-J4. After 96 hours of incubation, the cells were detached and counted. Separate condition pellets were tagged according to the manufacturer's protocol, and scRNA libraries were prepared with 10X Chromium single-cell kit according to the manufacturer's protocol.

Briefly, the detached cells were suspended in cell labelling buffer and treated with hashtag antibodies (TotalSeq A0251 – A0252 antibody, BioLegend). Stained samples were blocked, and staining was finished by washing three times with PBS.

Stained samples were used for library preparation following the 10X Chromium Next GEM Single Cell 3' library protocol. Gel Beads in Emulsion (GEMs), stained samples, and partitioning oil loaded on the 10X microfluidic chip. The chip was loaded on the 10X single-cell capture device for single-cell capturing. Captured single-cell partitions were used for barcoding. Barcoded samples are used for cDNA amplification, and then the gene expression library and hashtag library are separated by size selection. Gene expression library and hashtag library were constructed individually and verified with Tapestation.

Separately constructed hashtag and gene expression libraries were pooled 1:4 for full coverage. The pooled libraries were sequenced on a NextSeq 500 (Illumina) platform using a paired-end 2 x 150 bp to an average depth of 25'000 reads per cell. Specifically, Read 1: 28, Index 1 (i7): 8, Index 2 (i5): 0, and Read 2: 91 number of cycles were used for sequencing. The sequencing was performed with the help of Dr. Martin Philpott at the University of Oxford.

2.9.2 Analysis of Multimodal CITE-seq

The raw sequencing files were assembled with Python, and the files were verified with quality control. A Python pipeline was compiled to identify and match the hashtag barcodes with reads, and hashtag–read pairs were exported as FASTQ files. Hashtag pair files were analysed with the scflow repository (*GitHub - Cribbslab/Scflow: Single Cell Pipelines*, n.d.). Scflow is a collection of single-cell analysis pipelines. Briefly, an alignment-free based single-cell quantification was performed on hashtag files to obtain the count matrix. The count matrix was undergone Seurat quality controlling, filtering, clustering, doublet eliminating, integrating and manual annotating. Differential expression analysis was performed with Seurat pipeline, and 1) untreated astrocytes – treated astrocytes, 2) untreated U87MG – treated U87MG, 3) Substitution of 1st list from 2nd steps used to obtain differentially expressed genes.

The differential expression log fold change (LFC) and HGNC symbols were used to perform Gene Set Enrichment Analysis (GSEA). The pre-ranked files were loaded into the GSEA desktop application, and the differentially expressed genes were compared

against "Hallmark", "Reactome", and "KEGG" databases to identify the positively and negatively enriched pathways.

2.9.3 Validation of target genes

Validation of target genes was performed with quantitative Real-Time Polymerase Chain Reaction (qRT-PCR). RNA isolated from sorted GSK-J4 treated co-culture samples, or GSK-J4 treated cell lines with RNA isolation kit. cDNAs were prepared from the RNAs by melting RNA with dNTP and Random Hexamer mix. Then, cDNAs were synthesised by mixing melted RNA with first-strand buffer, DTT, RNAsin, and MMLV RT enzyme. Relative mRNA expression levels were detected by using LightCycler 480 SYBR Green I Master at qRT-PCR machine. Gene specific primers (Table 2) were used to determine the relative gene expression levels.

Table 2: Gene specific primers used in qRT-PCR.

Gene	Direction	Sequence
GAPDH	Forward	AGCCACATCGCTCAGACAC
	Reverse	GCCCAATACGACCAAATC
KDM6A	Forward	TTCCTCGGAAGGTGCTATTCA
	Reverse	GAGGCTGGTTGCAGGATTCA
KDM6B	Forward	CTACCCCCTTCACATGGCAG
	Reverse	CTCTGACTCGTACAGTTGCCC
MT-CYB	Forward	ATCACTCGAGACGTAAATTATGGCT
	Reverse	TGAACTAGGTCTGTCCCAATGTATG
MTND4L	Forward	AGCTCCATACCAATCCCCATCAC
	Reverse	GGACGTAATCTGTTCCGTACGTGT
C-MTRNR2L10	Forward	CGTTCAATGGCCGCAGTATC
	Reverse	CATCATCTGTGGAGCGAGGG
BNIP-3	Forward	CAGGGCTCCTGGGTAGAACT
	Reverse	CTACTCCGTCCAGACTCATGC
C-ENO1	Forward	GAGCTCCGGGACAATGATAA
	Reverse	CTGTTCCATCCATCTCGATC

P4HA1	Forward	GGCAGCCAAAGCTCTGTTAC
	Reverse	AAAGCAGTCCTCAGCCGTTA
HIF1A	Forward	TGCTCATCAGTTGCCACTTC
	Reverse	TCCTCACACGCAAATAGCTG
TPI1	Forward	CCCAGGAAGTACACGAGAAG
	Reverse	CAGTCACAGAGCCTCCATAAA
MT-CO2	Forward	ACAGATGCAATTCCCGGACGTCTA
	Reverse	GGCATGAAACTGTGGTTTGCTCCA
MTND2	Forward	CTAGCCCCCATCTCAATCATA
	Reverse	GAATGCGGTAGTAGTTAGGAT

2.10 Statistical Analysis

All the statistical analyses were performed as students t-test or two-way ANOVA, unless otherwise stated, using the GraphPad Prism version 9.3.1 for MAC (GraphPad Software, San Diego, USA). The statistical significances were presented with asterisks, classified as single $p<0.05$, double $p<0.01$, triple $p<0.001$, and four asterisks as $p<0.0001$.

3 Results

3.1 Establishment of Co-Cultures

To establish glioblastoma-astrocyte co-cultures, we first examined contact-independent and contact-dependent cell-to-cell interactions. Contact-dependent co-cultures presented slightly increased TMZ response. Therefore, we focused on and studied cell-to-cell interactions.

3.1.1 Non-malignant astrocyte cells are resistant to temozolomide

The TMZ response of the healthy astrocytes and glioblastoma cells were identified with drug dose-response curves (Figure 3.1). The U87MG cells presented 406 µM IC_{50}. Meanwhile, the healthy astrocytes, both primary (NHA) and immortalised (INHA) cells, demonstrated an approximate IC_{50} value of 7450 µM.

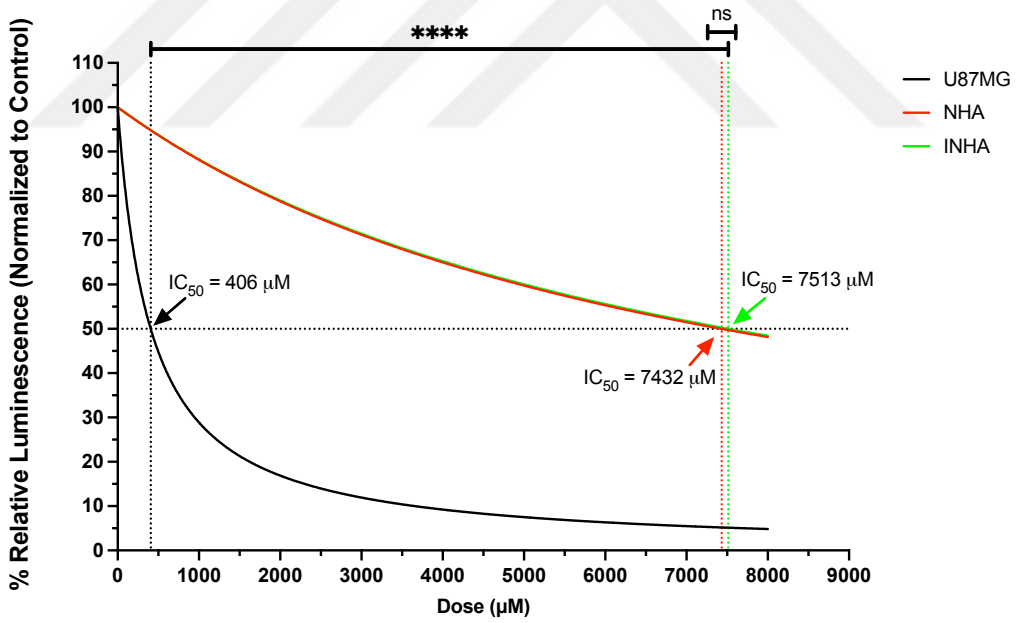

Figure 3.1 Temozolomide dose-response fitting of U87MG tumour cells, primary astrocytes, and immortalised primary astrocytes. The IC_{50} values were 406 µM for U87MG, 7432 µM for primary human astrocytes (NHA), and 7513 µM for immortal primary human astrocytes (INHA), respectively. IC50 was determined via non-linear regression analysis.

3.1.2 Contact-independent co-culturing does not lead to altered drug response

Cell-to-cell interactions and the implications on tumour cells were first studied with contact-independent co-culturing. Two different methods were used to study contact-independent co-culturing. Transwell assay and condition medium (CM) assay; and both methods were used with different setups.

The transwell (insert) assay was separated into two setups, initial drug treatment of astrocytes or U87MG cells. The initial drug treatment of astrocytes or U87MG cells was to observe how both cell types would respond to the drug. U87MG cells in both conditions presented the same 50% cell viability (Figure 3.2).

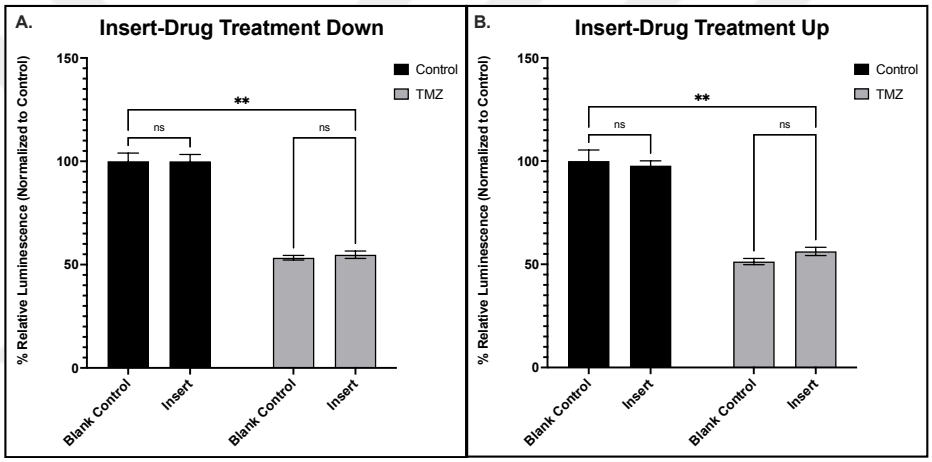

Figure 3.2 Transwell (insert) interaction experiment. Transwell (insert) cell-to-cell interaction of astrocytes and U87MG cells did not lead to an altered temozolomide response. A. Temozolomide was applied to astrocytes to observe the temozolomide response changes of U87MG cells. B. Temozolomide treatment was applied to U87MG.

The second method utilised a condition medium to observe if the astrocytes secrete any protective factors into the growth medium. Similar to the transwell assay, two setups were used. The first setup was a non-treated condition medium to observe whether the astrocytes secrete protective elements to the environment. The second setup was to observe if the astrocytes needed treatment-related changes to secrete protective factors to the growth medium. Both condition media were transferred to U87MG cells, and temozolomide treatment was applied to both setups. None of these contact-independent conditions led to an altered temozolomide response of U87MG cells (Figure 3.3).

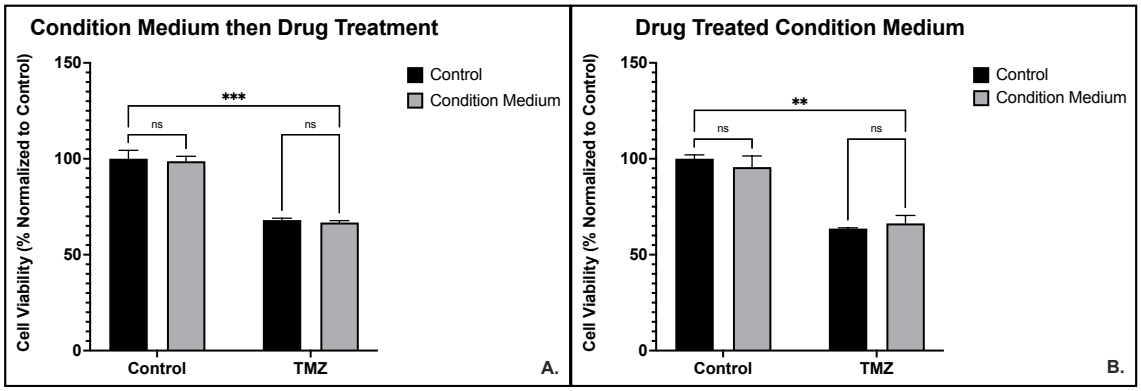

Figure 3.3 Condition medium assay for altered drug response. A. The condition medium was prepared without drug treatment, which did not lead to an altered temozolomide response. B. The condition medium was composed with temozolomide treatment to observe if healthy astrocytes need treatment-induced changes to secrete protective elements.

3.1.3 Establishment of Firefly Luciferin-mCherry (FLuc) expressing U87MG cells and Green Fluorescent Protein expressing Astrocytes for co-cultures

We needed to modify an existing method to track specific sub-population in co-cultured cells. Instead of using commercial cell viability methods, we aimed to use a luciferase-based tracking assay. The stable cell lines, which express luciferase, would create a bioluminescent signal when treated with luciferin. Therefore, when co-cultured, if the plate is treated with luciferin, the bioluminescent signal will only be produced by the specific subpopulation expressing the luciferase.

The U87MG cells were transduced with FLuc-mCherry plasmid (Figure 3.4) for stable mCherry fluorescent protein and luciferase expression. Meanwhile, the astrocytes were transduced with green fluorescent protein (GFP). The transduced cells were observed under a fluorescent microscope to confirm the fluorescent protein expression (Figure 3.5 and Figure 3.6).

Figure 3.4 The FLuc-mCherry plasmid. The FLuc-mCherry plasmid to produce a stable U87MG cell line. The luciferase and mCherry mRNAs are expressed from the same promoter region and separated by F2A-T2A alternative splicing sites.

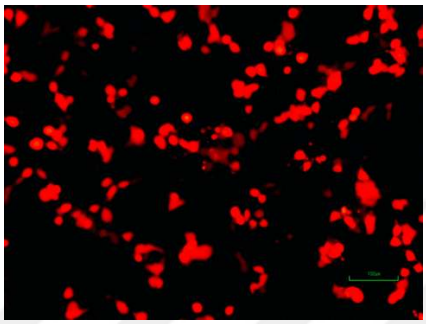

Figure 3.5 Fluorescent image of U87MG cells. Fluorescent image of U87MG cells which express mCherry fluorescent protein under the fluorescence microscope.

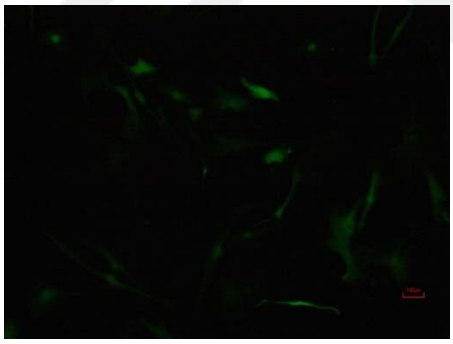

Figure 3.6 Fluorescent image of astrocytes. Fluorescent image of astrocytes transduced with a green fluorescent protein (GFP).

The U87MG-FLuc^{+}-mCherry^{+} cell line was treated with luciferin to observe the bioluminescence of the cells. The transduced cells exhibited 150 relative luminescence units (RLU). Meanwhile, the control (untransduced) cells did not exhibit bioluminescence (Figure 3.7).

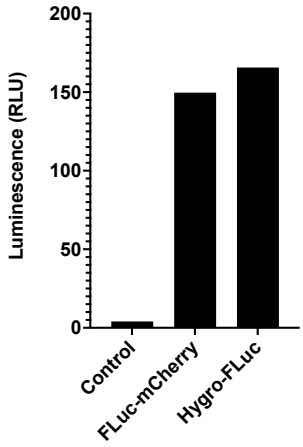

Figure 3.7 The bioluminescent response of stable U87MG-Fluc+ cells. The transduced cells presented 150 RLU bioluminescence, while the control untransduced cells did not exhibit any bioluminescence.

3.1.4 U87MG cells acquire temozolomide resistance in contact-dependent co-culturing

The second approach to co-culture establishment was contact-dependent co-culturing. While establishing co-cultures, understanding the proliferation limits of the cells in various plate set-ups was important . Therefore, we conducted 3 day long longitudinal cell proliferation experiments with cells seeded individually or as co-cultures.

When the cells were seeded individually in 96 well plates, we observed that 2000 cells did not present contact inhibition, whereas seeding more cells resulted in contact inhibition. Similarly, we observed that co-cultured cells started to show contact inhibited proliferation when the cells were seeded more than 1000:1000 cells in the environment (Figure 3.8).

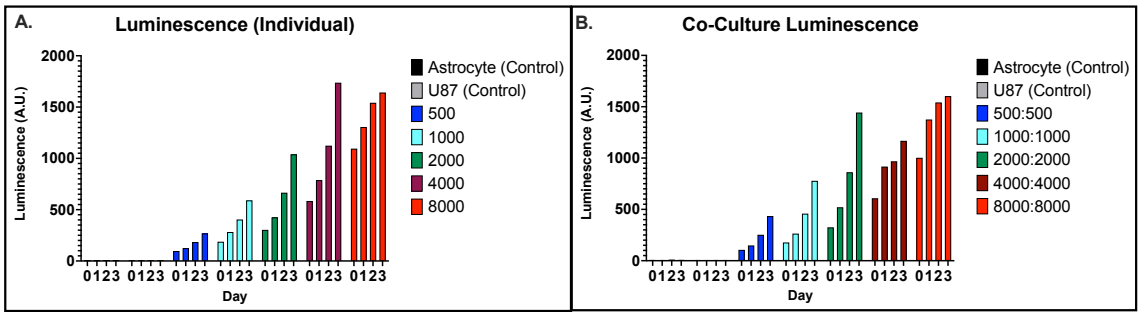

Figure 3.8 Individual and co-cultured cell proliferation. A. Individual cells presented a 2^n doubling when seeded as 500, 1000 or 2000 cell/well. The same effect was not observed when the cells/well count was increased. **B.** Subpopulation of co-cultured cells presented expected doubling when seeded 500:500 or 1000:1000 cells only. The further counts did not show the expected doubling of the cells.

After the cell counts were determined, we implemented a TMZ response experiment with co-cultured 2000 GFP^+-astrocytes and 2000 FMC^+-U87MG cells. At the same time, the control group consisted of 2000 GFP^+-U87MG cells and 2000 FMC^+-U87MG cells. This allowed us to properly track FMC^+ cells, while the total cell count was the same in both conditions. The co-cultured U87MG cells presented a slight resistance to TMZ compared to the control group (Figure 3.9).

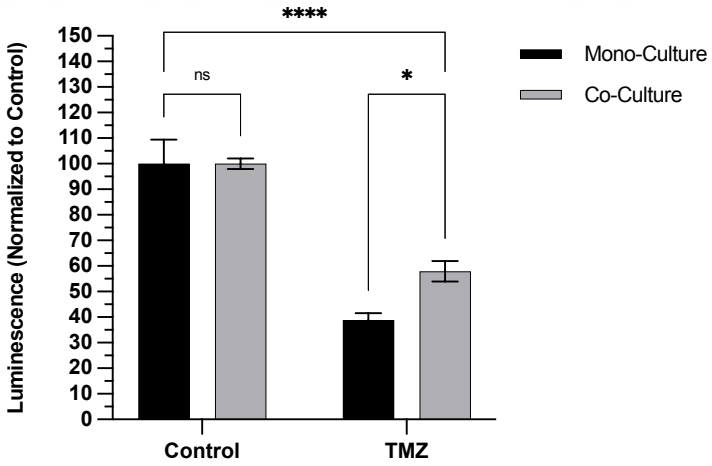

Figure 3.9 Relative luminescence of temozolomide treated FMC+-U87MG cells in mono-culture or co-culture conditions. The co-cultured cells presented statistically significant resistance to temozolomide treatment.

3.1.5 Dual colour fluorescent imaging and temozolomide response

Utilizing the advantage of stable cell lines with fluorescent proteins. we tracked the cell proliferation and temozolomide response of the cells with dual colour fluorescent imaging (Figure 3.10). Day initial and day final imaging from several independent regions on the plates were used to determine the proliferation of both cell types in the co-culture conditions, as well as TMZ response. Quantified images of both conditions were compared. The co-cultured U87MG-FMC^{+} cells presented elevated drug resistance compared to mono-cultured cells. In parallel, the GFP^{+}-astrocytes did not show altered proliferation (Figure 3.11).

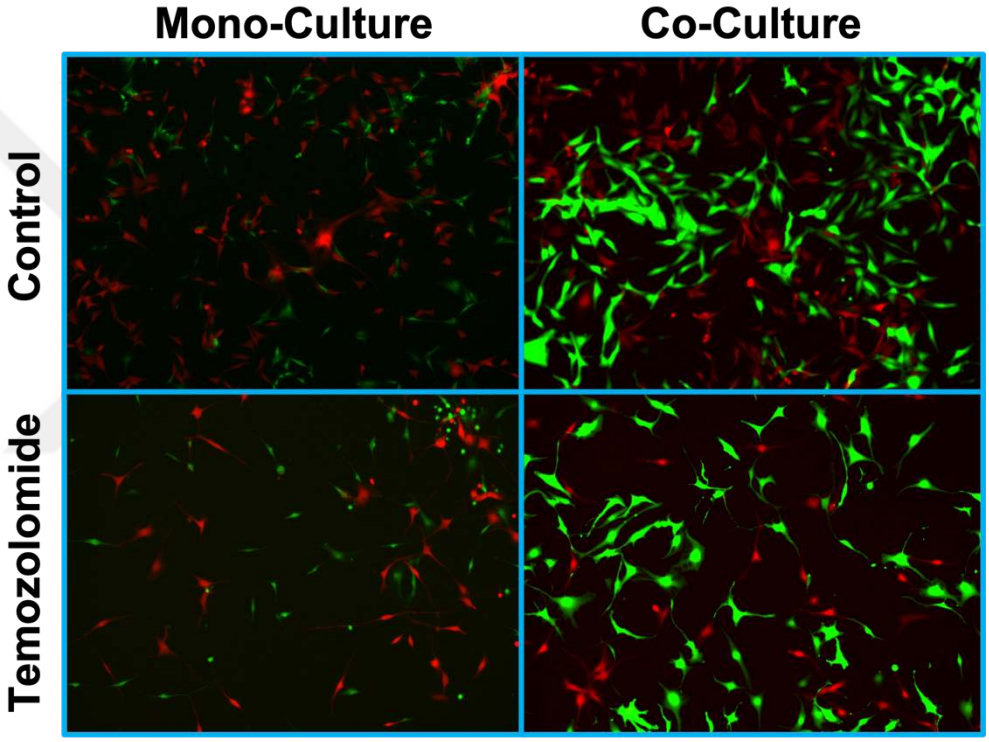

Figure 3.10 Day final fluorescent images of mono-cultured cells and co-cultured cells. Mono-culture consists of FMC^{+}-U87MG and GFP^{+}-U87MG cells. Co-culture consists of FMC^{+}-U87MG and GFP^{+}-astrocyte cells.

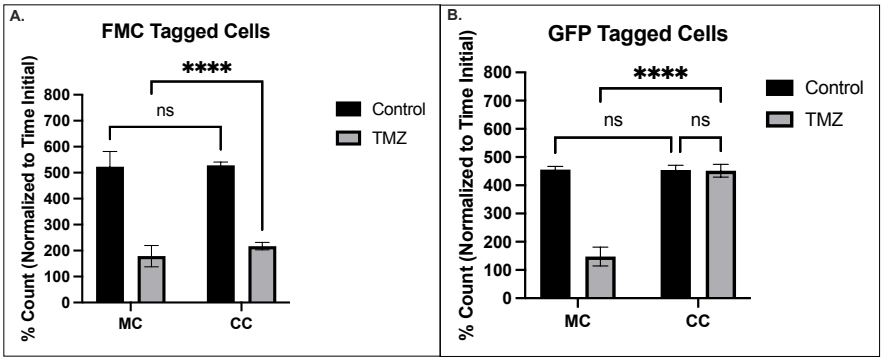

Figure 3.11 Quantified and normalized counts of FMC+ and GFP+ cells in mono-culture and co-culture. A. FMC^{+} cell quantification shows temozolomide resistance in co-cultured U87MG cells. **B.** GFP^{+} quantification shows 50% cell viability in U87MG cells, while astrocytes were not affected by temozolomide.

3.1.6 Co-cultures present close-contact interactions

The fluorescence images showed direct cell-to-cell contact between glioblastoma cells and astrocytes. Therefore, we wanted to take a closer look at the co-cultured cells with scanning-electron microscopy (SEM). The co-cultured cells were observed at 500X, 200K X, and 600K X resolution. The magnified images presented close cell-to-cell contact structure development (Figure 3.12).

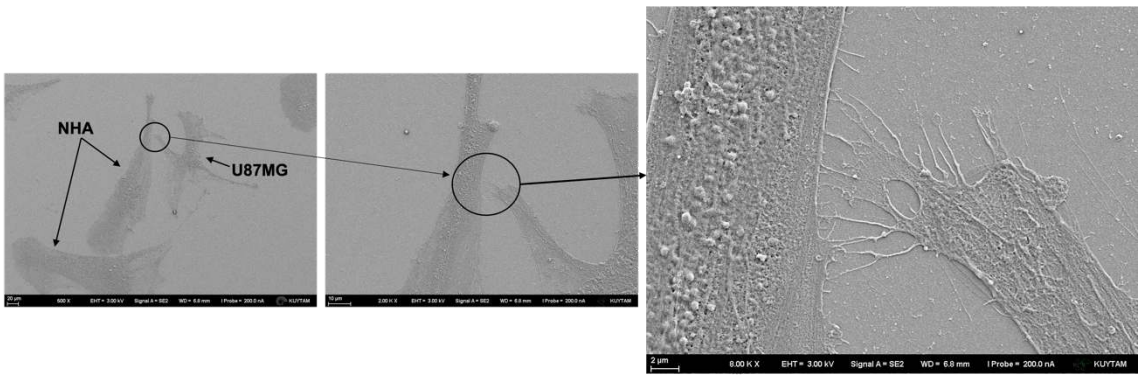

Figure 3.12 SEM images of co-cultured cells. The cells were identified at 500X magnification. The close contact structures were observed at 200K X and 600K X, respectively.

3.1.7 Transcriptomic analysis of co-cultures and mono-cultures reveals elevated cell-cell interaction related alterations.

The U87MG transcriptomic landscapes of mono-cultured and co-cultured conditions were compared. To conduct the experiment, the mono-cultured or co-cultured FMC^+ cells were sorted with FACS according to their $mCherry^+$ signal. Sorted cells were used for RNA isolation, library preparation and sequencing. The sequencing results were pseudo-aligned and compared.

The mono-culture and co-cultured samples were clustered together during the quality control (Figure 3.15). The dispersion–count graphs perfectly fit and selectively dispersed transcriptomic landscape (Figure 3.16).

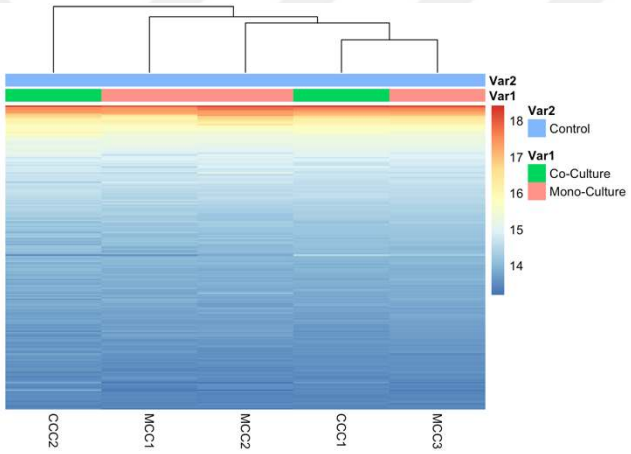

Figure 3.13 Heatmap of the sample quality control. The variance and the similarity of all the samples were compared. The mono-culture and co-culture samples were clustered together with slight variances.

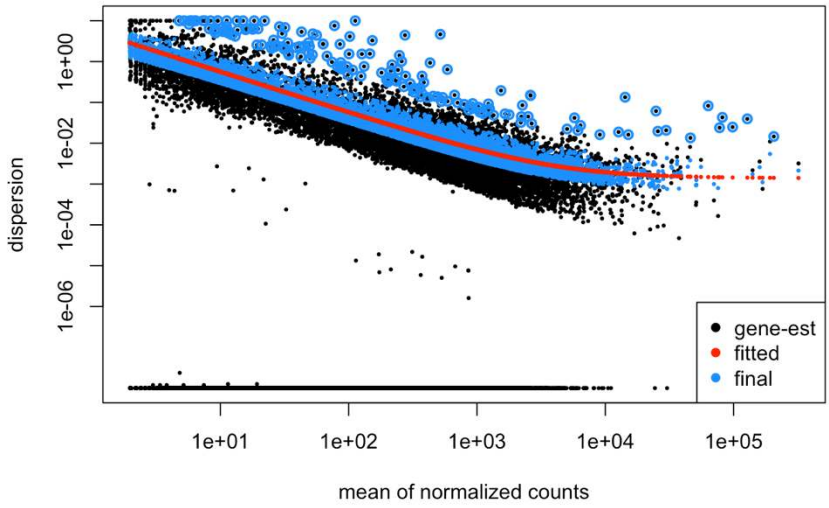

Figure 3.14 Dispersion-count graphs of the samples. All combined samples were fitted to non-linear regression. 90% of the genes were aligned with the regression model.

In DESeq2, the attributable changes to a given variable over the mean of normalized counts for all the samples and log2 fold change (LFC) of all samples could be observed with MA plots. The mono-culture and co-culture samples presented an excellent distribution (Figure 3.17), indicating that the samples did not need further transformation.

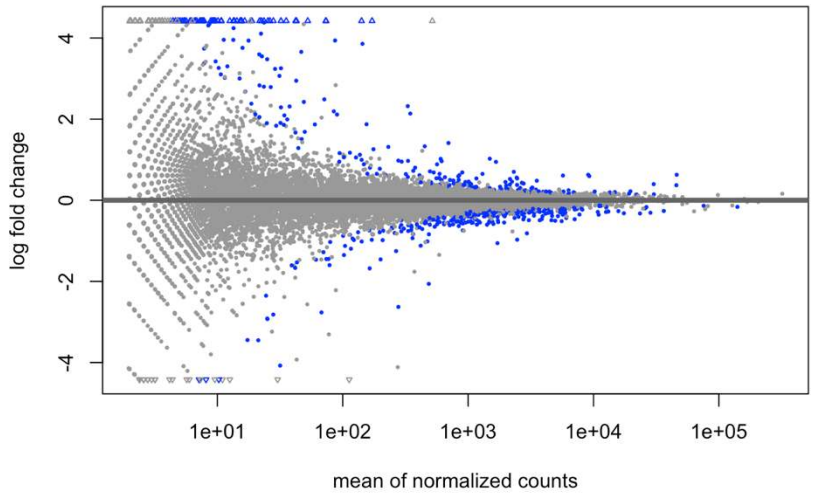

Figure 3.15 The MA plot of all the samples. The rotated scatter plot did present a good distribution of the samples, and the difference in expression against the mean expression levels was as expected.

A volcano plot in DESeq2 is a scatter plot which visualizes and explains the statistical significance (P-value) against the magnitude of change. The U87MG cells isolated from co-cultures exhibited 140 differentially expressed genes (Figure 3.18).

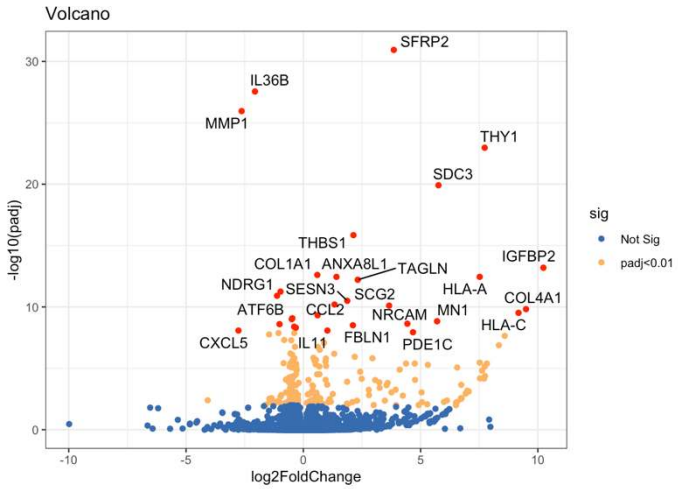

Figure 3.16 The volcano plot of the samples. Co-culture derived U87MG cells present approximately 140 differentially expressed genes. Non-significant genes are blue, while significant ones are yellow, and the top DE genes are red.

The differentially expressed genes were used for the gene set enrichment analysis (GSEA) to identify significantly altered pathways. The co-cultured cells did present elevated cell-to-cell interaction pathways, such as adherent junction interactions, apical surface, and gap junction, among the others (Figure 3.19).

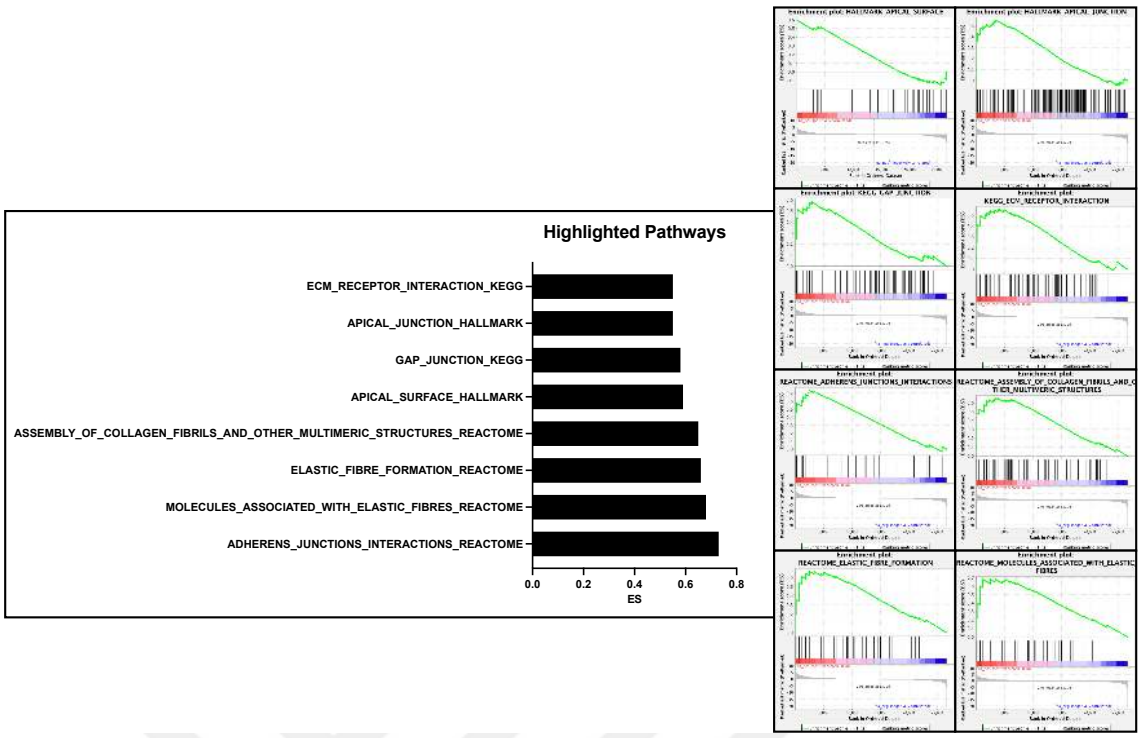

Figure 3.17 GSEA analysis of differentially expressed genes. The co-cultured cells present a 0.5 to 0.8 positive enrichment score of contact-dependent cell interactions.

3.2 Targeting epigenetic modifiers to overcome co-culture temozolomide resistance

The co-culture model we established presented slight temozolomide resistance compared to the mono-culture model. To understand the limitations and vulnerabilities of the acquired drug resistance by co-culture, we conducted a small molecule epigenetic inhibitor screen, among other experiments.

3.2.1 Established co-culture presented Topotecan sensitisation

Since the co-culture system we developed was only tested with TMZ treatment, we wanted to expand our observations with well-known combination therapies. Therefore, we conducted an experiment with topotecan, a validated TMZ sensitizer in GBM. The mono-cultured and co-cultured cells were treated with TMZ only, topotecan only, or TMZ and topotecan combination (Figure 3.20). The TMZ-only treatment presented statistically significant resistance compared to mono-culture as well as compared to control. Meanwhile, the topotecan-only treatment showed a similar effect

compared to the control, whereas it did not show a statistical difference between mono-culture and co-culture. The combination therapy showed a sensitizing effect compared to TMZ only or topotecan only treatment, while the sensitizing effect on co-culture was significantly elevated.

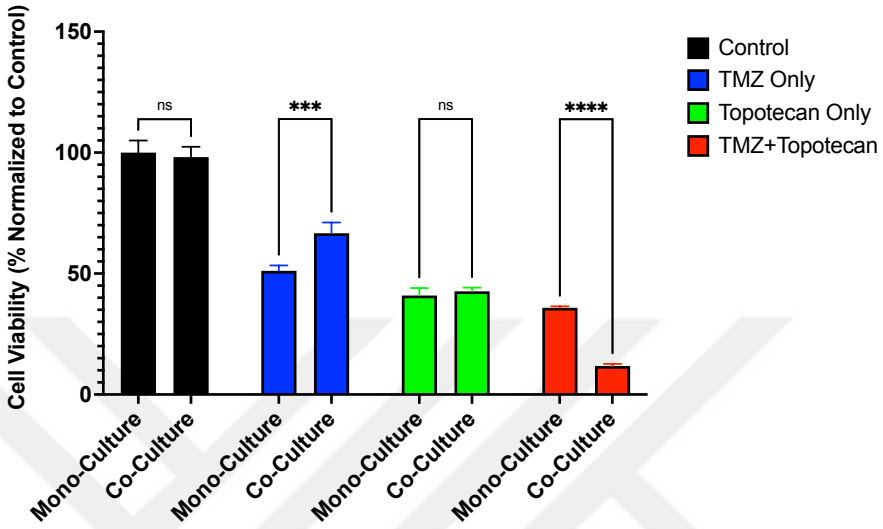

Figure 3.18 The temozolomide and topotecan combination therapy in co-cultures. The combination therapy of U87MG cells with TMZ and topotecan presented a sensitizing effect. The effects of TMZ only, topotecan only, and combination therapy on cell viability were statistically significant compared to control. Meanwhile, topotecan only effect was not substantially different between mono-culture and co-culture, but the TMZ only or combination therapy was significantly different.

3.2.2 Epigenetic small molecule inhibitor screen identified GSK-J4 as a temozolomide sensitiser

Our co-culture models were used to identify epigenetic drugs that could overcome TMZ resistance in co-culture. The experimental conditions consisted of 1) mono-culture drug only, 2) mono-culture drug and TMZ treatment, 3) co-culture drug only, and 4) co-culture drug and TMZ treatment. Drug-only conditions were used to identify and eliminate the epigenetic probes which causes the loss of cell viability when applied individually. Meanwhile, the drug and TMZ were used to determine the sensitizing probes.

First, we calculated the overall response of all the epigenetic probes in all conditions (Figure 3.21). The temozolomide resistance of co-cultures compared to mono-culture was observed, in accordance with our previous results. Also, in the drug-only (control) conditions, the co-cultures presented less response to epigenetic probes than the mono-cultures. Yet, the probe and TMZ combination showed more agents compared to mono-culture. When the results were further analysed, we observed that only 20% of the overall drugs were eligible as TMZ sensitizers in mono-culture condition (Figure 3.22). In contrast, in the co-culture conditions, the sensitizers were 40% of the entire drug library (Figure 3.23).

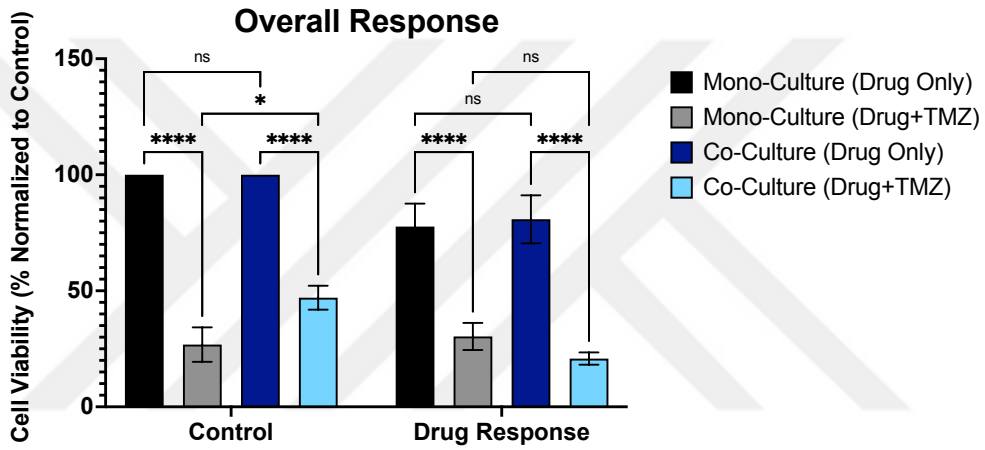

Figure 3.19 The overall response of all combined drugs. Temozolomide reduced the viability by 60% in mono-culture as expected; however, in co-culture, the population was less affected. Similarly, the individual drug treatments presented an overall reduced effect in co-cultures compared to mono-cultures. However, when combined with temozolomide, the mono-culture only presented a 60% overall effect, while the co-culture presented 70%.

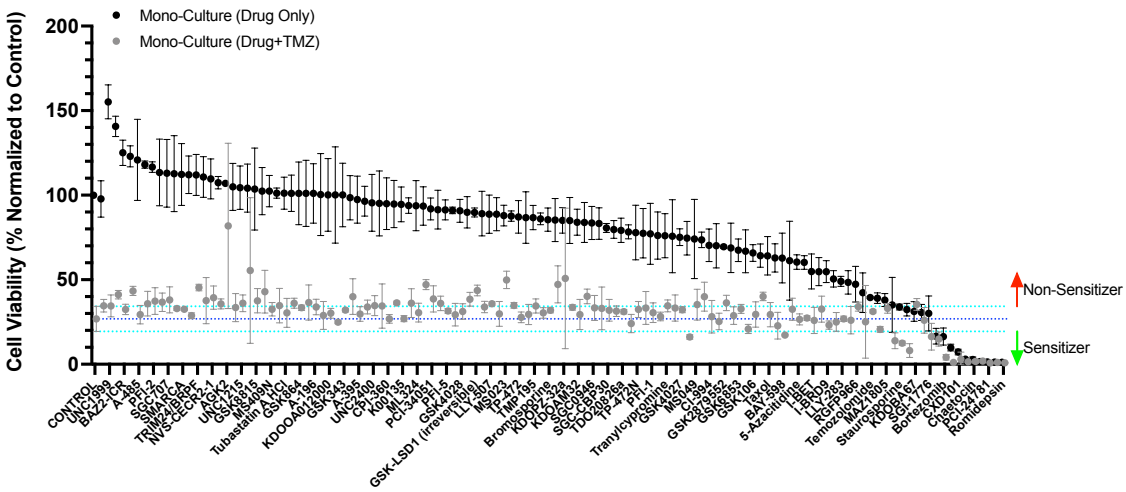

Figure 3.20 The comparison of the mono-culture drug only versus drug and temozolomide. The TMZ only and DMSO were used as controls, the probes which affected the cells on their own were eliminated, while the probes which reduced viability below threshold were selected as sensitizers.

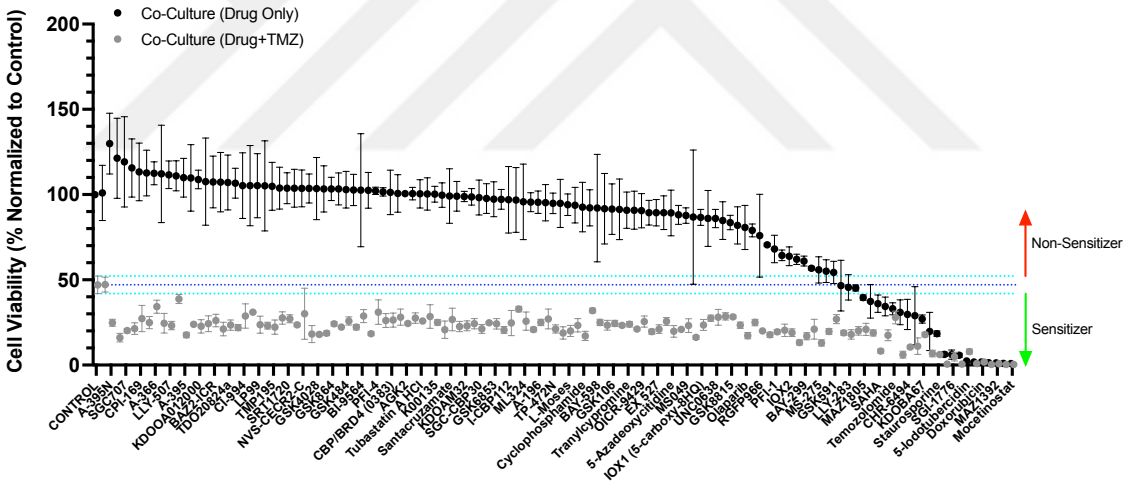

Figure 3.21 The comparison of the co-culture drug only versus drug and temozolomide. The TMZ only and DMSO were used as controls, the probes which affected the cells on their own were eliminated, while the probes which reduced viability below threshold were selected as sensitizers.

The sensitizers from mono-culture and co-culture were compared to identify the probes which majorly affected co-culture (Figure 3.24). 24 of the probes were selected and were compared for all the screen groups. MS049, GSK-J4, MS023 and SGC707 presented a better sensitizing effect in co-culture conditions. Therefore, the selected

sensitizers were tested against astrocytes to understand how they affect the astrocytes. The astrocytes were not affected by GSK-J4, MS023, and MS049, while the U87MG cells viability decreased by 50% (Figure 3.25).

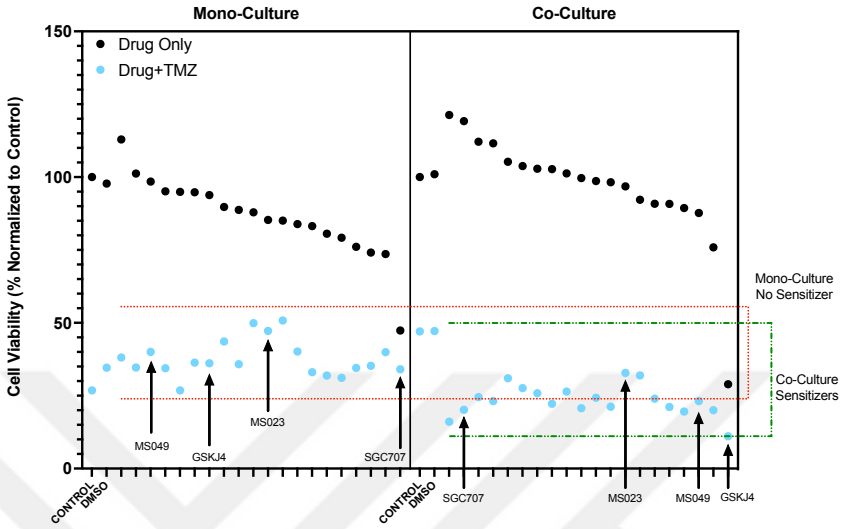

Figure 3.22 Comparison of selected drugs in mono- and co-culture conditions. The drugs MS049, GSK-J4, MS023, and SGC707, presented sensitizing effects in co-cultures.

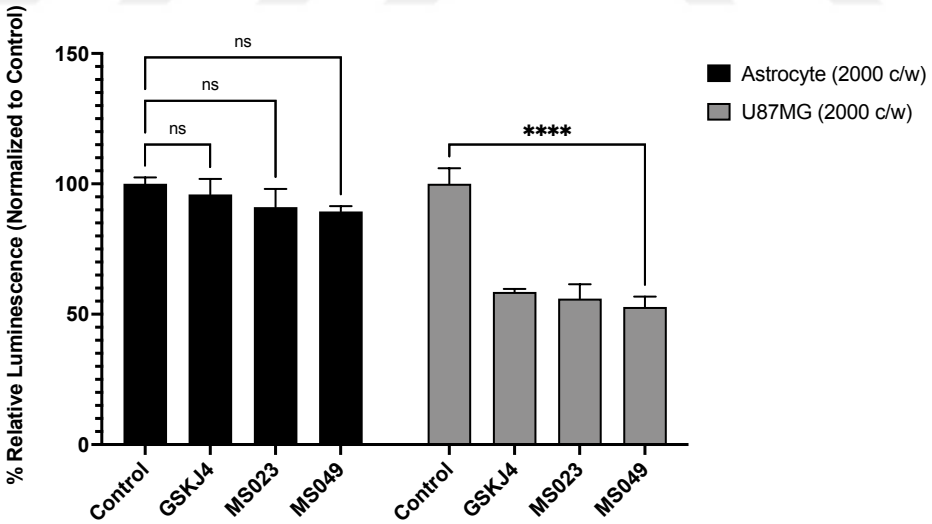

Figure 3.23 Single drug effects on individual cell lines. GSK-J4, MS023, and MS049 did not present any significant inhibitory effect on astrocytes. In parallel, U87MG cells were affected by the probes, and the RLU of U87MG cells decreased by approximately 40%.

Further investigation has narrowed down the probes to GSK-J4, a histone demethylase inhibitor. The selected drugs were tested in mono-culture and co-culture with or without TMZ (Figure 3.26). MS023 or MS049 did not present a statistically significant difference in mono-culture. In contrast, GSK-J4 did present a sensitizing effect in both mono-culture and co-culture.

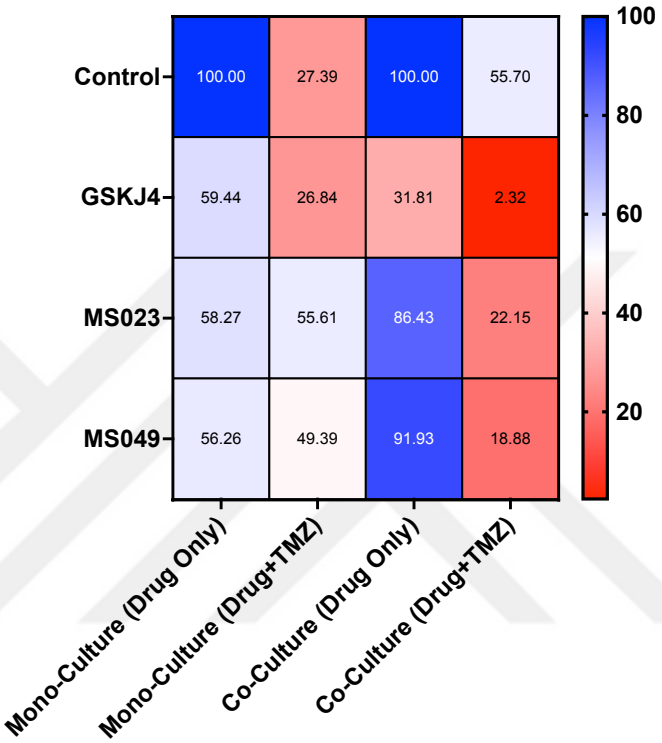

Figure 3.24 Cross-comparison validation of selected drugs. The probe and temozolomide combination did not show a statistically significant difference in mono-culture conditions. In contrast, drug-only treatment presented a slightly decreased effect for MS023 and MS049. GSK-J4 led to the expected decrease in cell viability in both drug only and drug and temozolomide combination in both mono- and co-cultures.

Since GSK-J4 presented the most promising results among the epigenetic inhibitor probes, we performed a dose-response experiment to identify the IC_{50} of GSK-J4. The cells were treated with multiplying doses between 1 and 16 µM, the cell viability was measured, and non-linear dose-response was fitted to the results. The IC_{50} of GSK-J4 was determined as 7.5 µM for U87MG cells (Figure 3.27). We also tested GSK-J5, the inactive form of GSK-J4, in mono- and co-culture with and without TMZ treatment. The mono-culture presented all the expected results, such as sensitization or non-activity of

GSK-J5 with and without temozolomide. The co-culture presented similar results. When the mono- and co-culture were compared, we observed the temozolomide resistance and sensitizer effect of combination therapy. The GSK-J5 did not have an impact as expected.

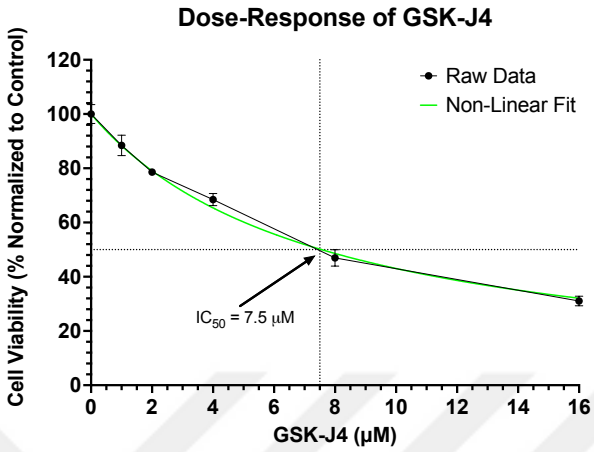

Figure 3.25 GSK-J4 dose-response assay. The increasing dose of GSK-J4 decreased the cell viability of U87MG cells. 1 μM led to a 10% decrease, while 16 μM led to a 65% decrease in cell viability. The non-linear fit of inhibitory drug calculated the IC_{50} as 7.5 μM for U87MG cells.

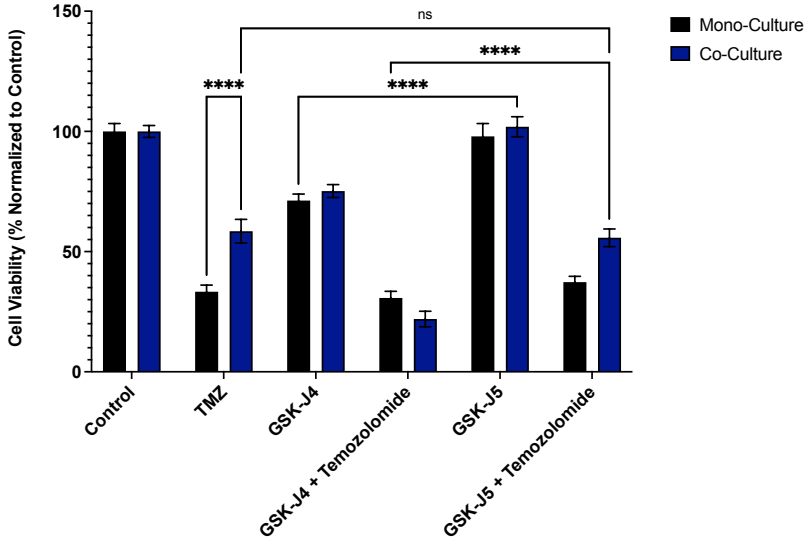

Figure 3.26 GSK-J4 and GSK-J5 response of mono- and co-culture samples. Mono- and co-culture comparisons showed significant co-culture protection against temozolomide and GSK-J4 sensitizing effect, but no significant effects of GSK-J5 was observed, as expected.

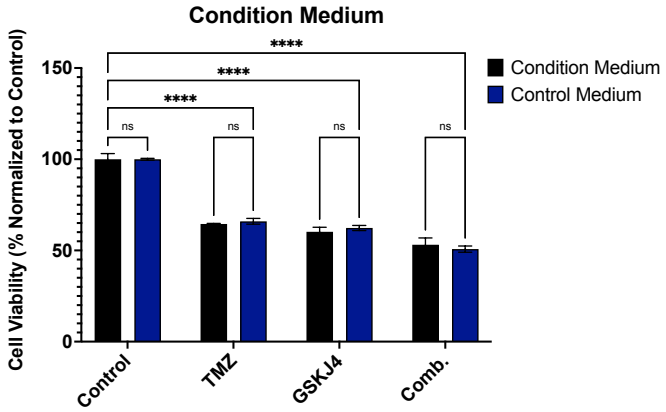

Figure 3.27 Condition medium assay of temozolomide and GSK-J4 combinations. Condition medium assay of temozolomide, GSK-J4 or temozolomide and GSK-J4 combination therapy. The control and condition medium individual drug treatment or combination therapy results presented a statistically significant decrease. However, no statistically significant difference was observed when the control and condition medium results were compared.

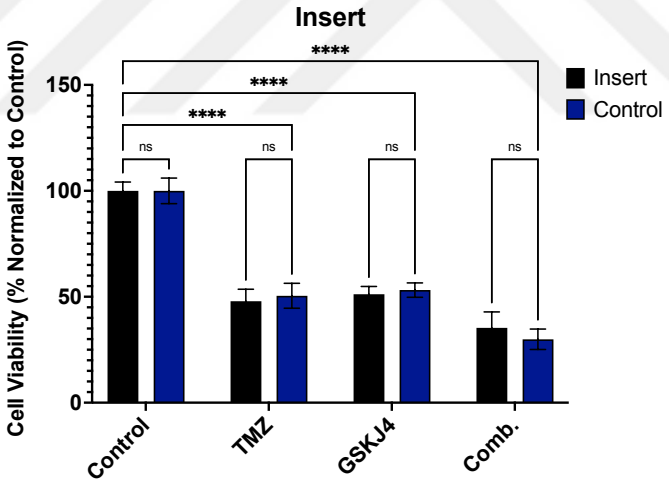

Figure 3.28 Transwell (insert) assay of temozolomide and GSK-J4 combinations. Transwell insert assay of temozolomide, GSK-J4 or temozolomide and GSK-J4 combination therapy. The control and insert comparison for individual drug treatment or combination therapy results presented a statistically significant decrease. However, no statistically significant difference was observed when the control and transwell results were compared.

3.2.3 GSK-J4 presented sensitising effect in contact-dependent co-culturing only

Even though we showed a contact-dependent protective effect in co-cultures, we did not know the working mode of GSK-J4. Therefore, we suspected that the GSK-J4 treatment could act and sensitize temozolomide contact independently, or the effect could be U87MG specific only.

In order to answer these questions, we performed another contact-independent cell viability assay. Since we did not observe any significant differences between U87MG or astrocyte treatment (Figure 3.2 and Figure 3.3), we only focused on U87MG cells. Our results did not present a statistically significant differential response to temozolomide, GSK-J4 or temozolomide and GSK-J4 combination treatment (figure 3.29). Nor did the transwell assay we applied present statistically significant changes upon treatment (Figure 3.30).

To test whether GSK-J4 is a U87MG-specific sensitizer or not, we prepared suspension FMC^{+}-U87MG cells with limited cell-to-cell interaction and FMC^{+}-T98G cells to contact-dependent co-culture with GFP^{+}-astrocytes. Suspension cells did not present astrocytic protection even though the sensitizing effect was observed (Figure 3.31). In contrast, the T98G experiment demonstrated statistically significant temozolomide resistance in T98G-astrocyte co-culture compared to mono-culture. Also, we observed individual GSK-J4 and sensitizing effects both in mono- and co-cultures. In parallel, mono- and co-culture comparison of combination therapy showed statistically significant sensitizing effects (Figure 3.32).

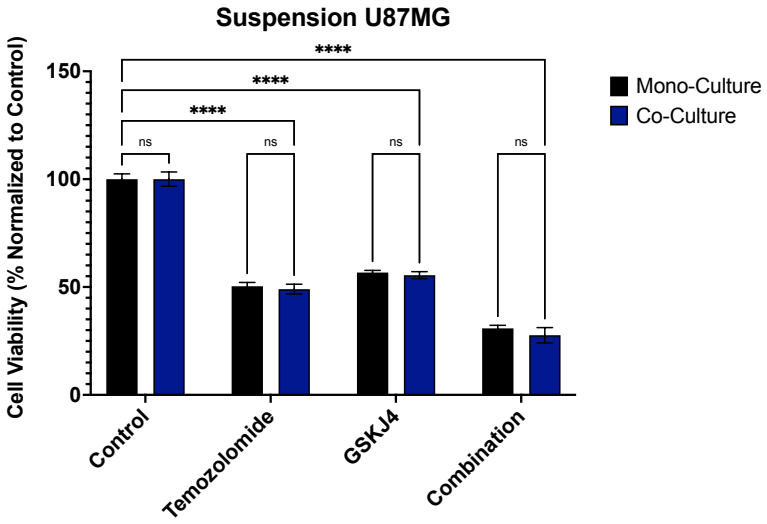

Figure 3.29 Temozolomide and GSK-J4 combinations on suspension co-cultures. Suspension mono- and co-culture treated with temozolomide, GSK-J4 and temozolomide and GSK-J4 combination. The drug response of mono- and co-cultures were as expected.

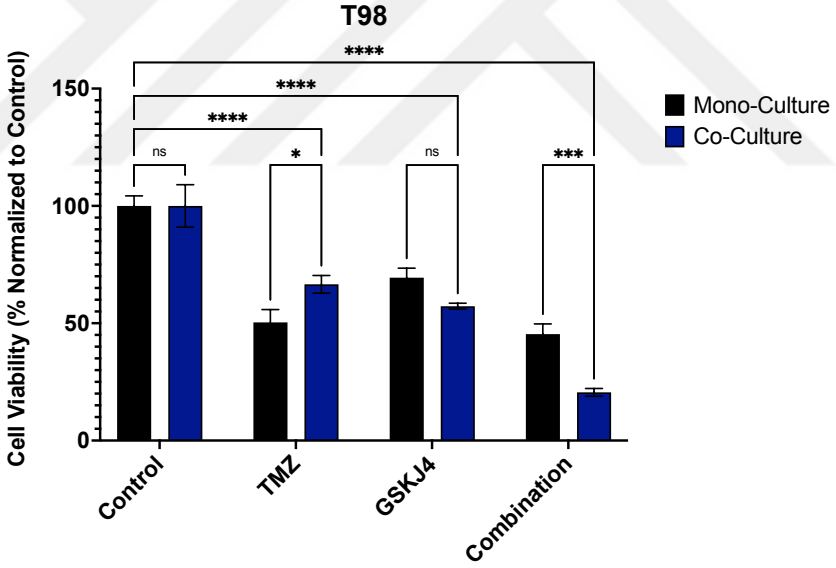

Figure 3.30 T98G – astrocyte contact-dependent co-culture drug responses. Both mono- and co-cultures did present all expected treatment responses. Temozolomide response of co-cultures demonstrated statistically significant resistance compared to mono-culture, and GSK-J4 and temozolomide combination treatment showed a sensitizing effect.

Further investigation of U87MG – astrocyte co-cultures with temozolomide, GSK-J4 or temozolomide and GSK-J4 combination treatment was performed by imaging

with intervals followed by quantification. Also, a drug-treated SEM of co-cultures was performed.

Dual colour imaging with interval images from different sections (Figure 3.33) were quantified (Figure 3.34). The individual temozolomide and GSK-J4 treatment presented approximately a 50% cell population survival in both mono- and co-culture. In parallel, temozolomide and GSK-J4 combination therapy showed 30% cell survival. When mono- and co-cultures were compared, co-culture cell survival was 15% more compared to mono-culture. However, individual GSK-J4 or temozolomide and GSK-J4 combination treatment did not present an altered response. Still, the combination therapy overcame the temozolomide resistance and decreased the cell survival to 30%.

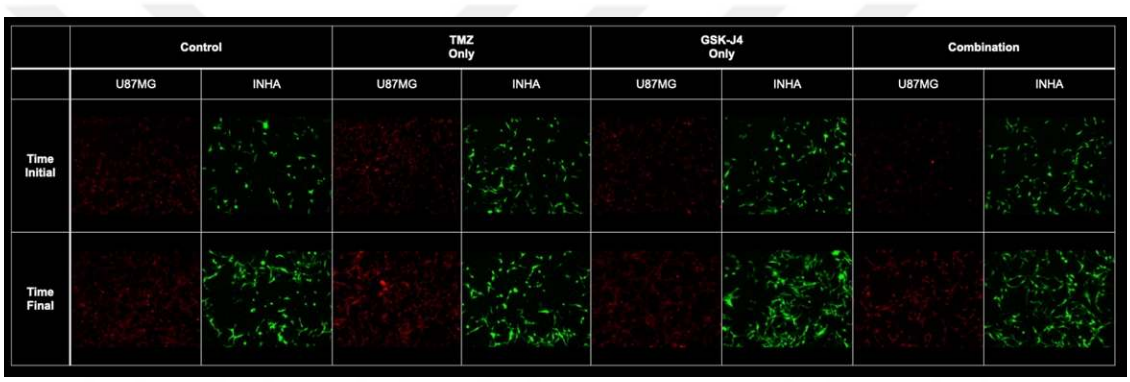

Figure 3.31 The representative images of dual colour interval imaging. Time initial and time final images present, all combinations of treatment regimens.

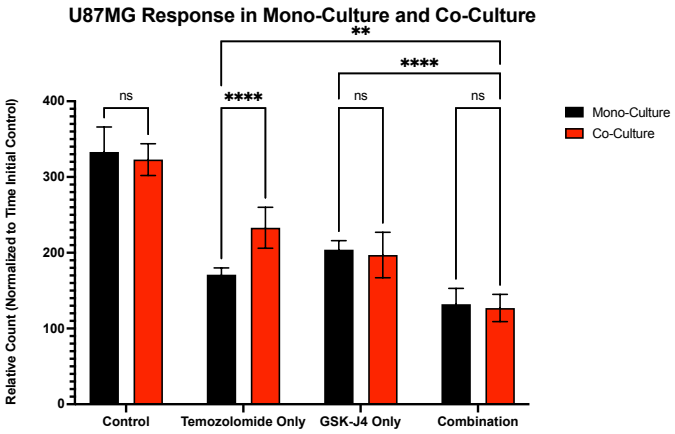

Figure 3.32 The quantification of dual colour imaging. The control did not present altered proliferation between mono- and co-culture. Temozolomide response of mono-culture was 50% cell survival; in parallel, the co-culture demonstrated 65% survival. GSK-J4 presents 50% survival for both conditions. Similar to GSK-J4, both conditions present 30% survival.

We suspected that GSK-J4 could interrupt the cell-to-cell contact to alter the sensitizing effect. Therefore, we conducted SEM imaging to observe the cell-to-cell interactions after drug treatment. The cells were observed with different magnifications for temozolomide, GSK-J4 or temozolomide and GSK-J4 combination therapy, and they did not present altered cell-to-cell interaction (Figure 3.33).

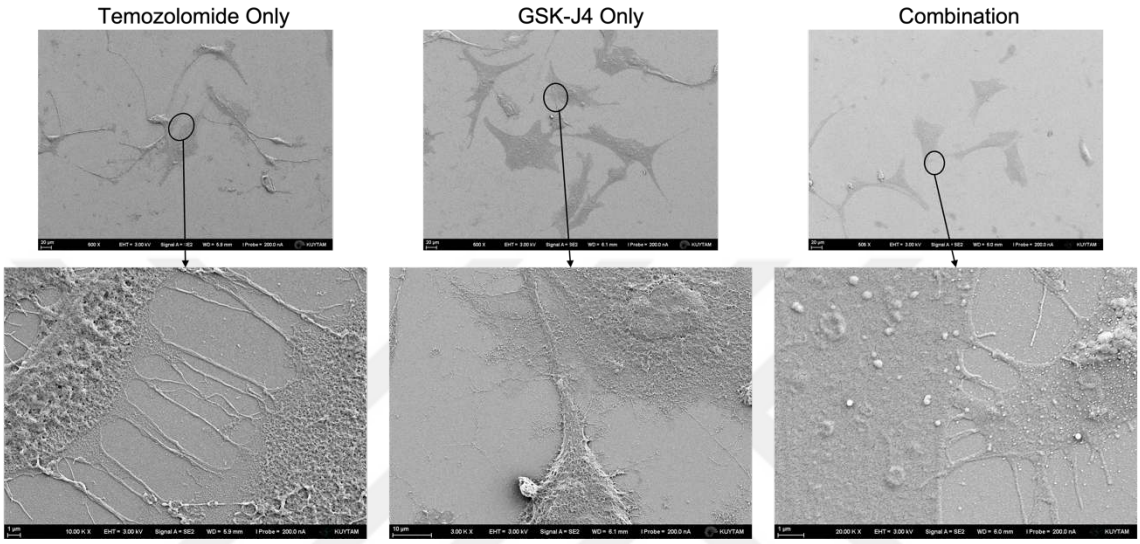

Figure 3.33 SEM images of drug-treated co-culture samples. The first panel presents temozolomide treated samples, the second presents GSK-J4 treated samples, and the third presents temozolomide and GSK-J4 combination therapy. All the samples exhibited close-contact cell-to-cell interaction structures.

3.2.4 KDM6A knockdown phenocopied sensitising effect of GSK-J4

GSK-J4 is a selective dual jumonji H3K27me3/me2 histone lysine demethylase inhibitor. It is well known that KDM6B (UTR/JMJD3) and KDM6A (UTX) are inhibited with GSK-J4 treatment. Therefore, we hypothesized that individual KDM6A or KDM6B knockdown could mimic the GSK-J4 effects and sensitize glioblastoma cells to temozolomide.

We designed the KDM6A or KDM6B promoter region targeting sgRNAs along with non-targeting (NT) sgRNAs. The sgRNAs were transduced to stable death-Cas9 (dCas9) expressing cells, and the relative gene expression levels of wild-type or knockdown cells were validated with qPCR experiments. qPCR results presented a 0.7-

fold decrease in KDM6A and a 0.65-fold decrease in KDM6B, while the NT and Cas9 did not demonstrate significant gene expression alteration (Figure 3.34).

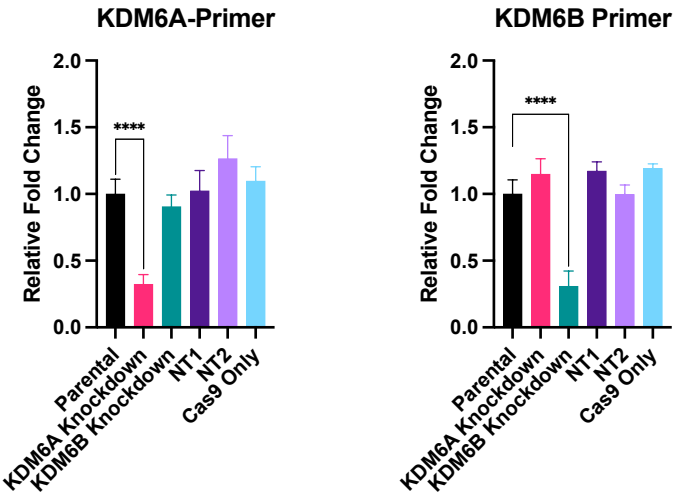

Figure 3.34 qRT-PCR validation of KDM6A and KDM6B knockdown cells. The qPCR was performed either for KDM6A (left) or KDM6B (right) mRNA measurement. KDM6A silencing presented a 0.7-fold decrease, while the KDM6B, NT1, NT2, and Cas9 only cells did not show significantly altered expression in KDM6A detection. In parallel, KDM6B silencing presented a 0.65-fold decrease, while KDM6A, NT1, NT2, and Cas9 only cells did not demonstrate altered expression in KDM6B detection.

In order to understand KDM6A and KDM6B's involvement in TMZ sensitization, we performed a drug-response assay. The knockdown cells and proper controls were seeded, treated with TMZ, and cell viability was measured (Figure 3.35). The cells did not present altered proliferation compared to wild type, while the temozolomide treatment demonstrated a 50% viability decreased in all groups except KDM6A knockdown. KDM6A silencing showed a 60% decrease in cell viability and approximately 10% less resistance compared to other conditions.

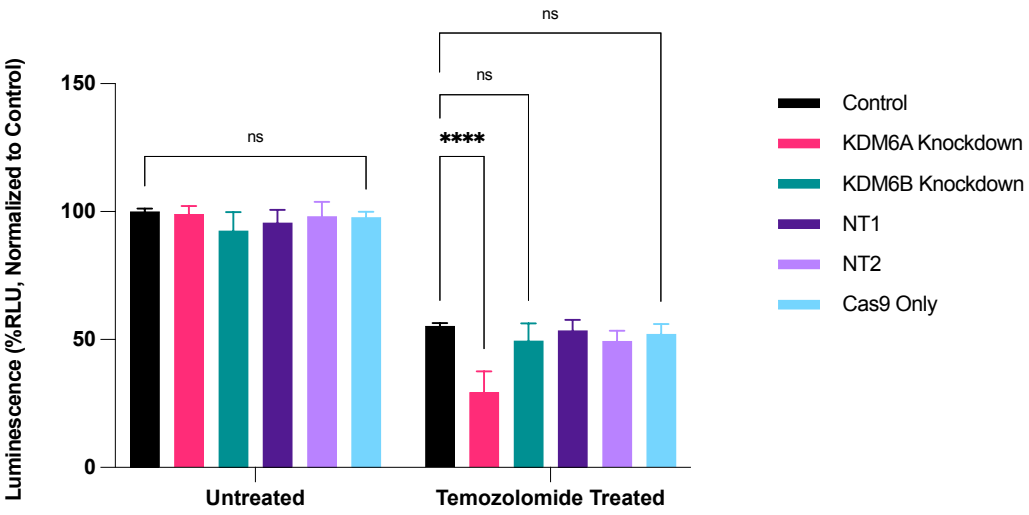

Figure 3.35 Temozolomide response of KDM6A and KDM6B knockdown cells. The untreated cells did not present altered cell proliferation. Temozolomide treatment halved the cell population of control, KDM6B knockdown, NT1, NT2, and Cas9 only. In parallel, KDM6A presented 60% cell death.

3.2.5 Single cell transcriptomics reveals mitochondrial dysregulation in co-cultures

GSK-J4's temozolomide sensitizing effect was validated with chemical probes and transcriptomic changes. Therefore, we wanted to understand and identify the whole transcriptome changes with GSK-J4 treatment. We applied a combined multimodal – CITEseq method to vehicle or GSK-J4 treated FMC^{+}-U87MG – GFP^{+}-astrocyte co-cultures. The conditions vehicle and GSK-J4 were tagged and pooled before single-cell library preparation. The hashtags on read 1 were identified and associated with unique molecular identifiers (UMIs), followed by UMI pairing of read 1 and read 2. This information is used to watermark and separate the conditionally different reads.

The split files were used for quality control, which identified approximately 5000 cells in control, and 6000 cells in the GSK-J4 treatment conditions. The UMI counts per cell was around 10000, along with gene counts per cell of 7000 in both conditions. UMI counts versus gene counts graphs presented good quality and perfectly sequenced samples, and the slopes of the samples were similar for both samples (Figure 3.36). Whole data was filtered with a minimum of 300 UMIs and eliminated the cells without the necessary UMIs. The single-cell data is high-dimensional, noisy, and sparse data. After

dimension reduction, our data presented a decreasing standard deviation and p-value close to zero for all the principal components (PCs) of the JackStraw plot (Figure 3.37).

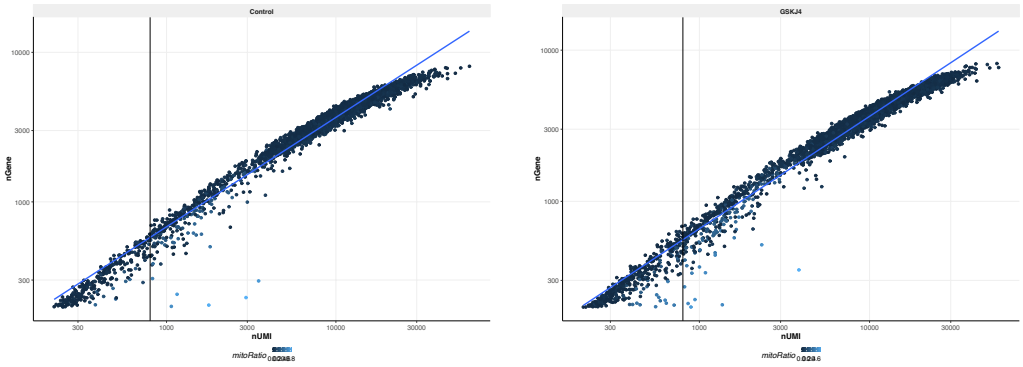

Figure 3.36 Count of genes versus count of UMIs. The graph presents each gene and UMI identified for each cell. The dispersion for both conditions presented the samples are sequenced deep enough. Also, the linearity and slopes were similar to each other.

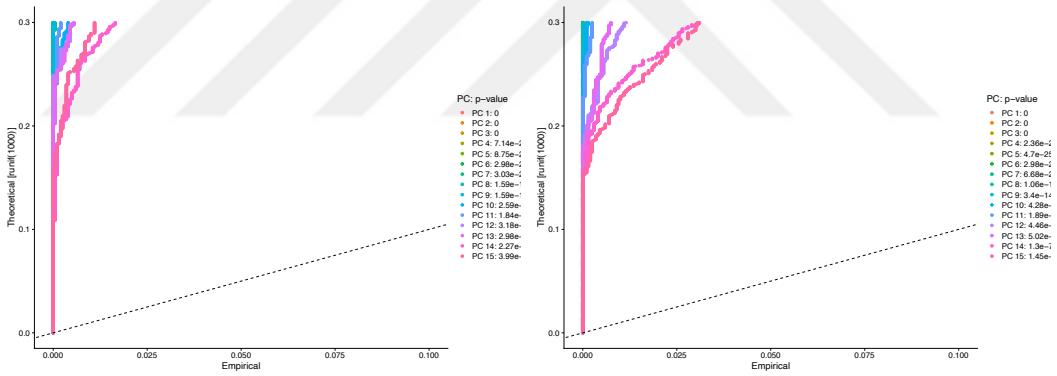

Figure 3.37 JackStraw plot of PC distributions. The control samples presented < 3.99e-76 p-value, while GSK-J4 samples demonstrated <1.45e-73 p-value. Both conditions presented good filtering with a p-value close to 0, which was an indicator of good filtering.

The filtered results were used for doublet detection and elimination. Our samples presented less than 1% doublets, which were eliminated from the further analysis. Still, the data demonstrated high dimensionality and needed further dimension reduction. Two different methods were used for dimension reduction, 1) uniform manifold approximation (UMAP) and 2) t-stochastic neighbour embedding (t-SNE). Both methods identify and

divide the cells into mutually equidistant groups. The control presented 11 clusters, while GSK-J4 presented 12 clusters for t-SNE and UMAP (Figure 3.38).

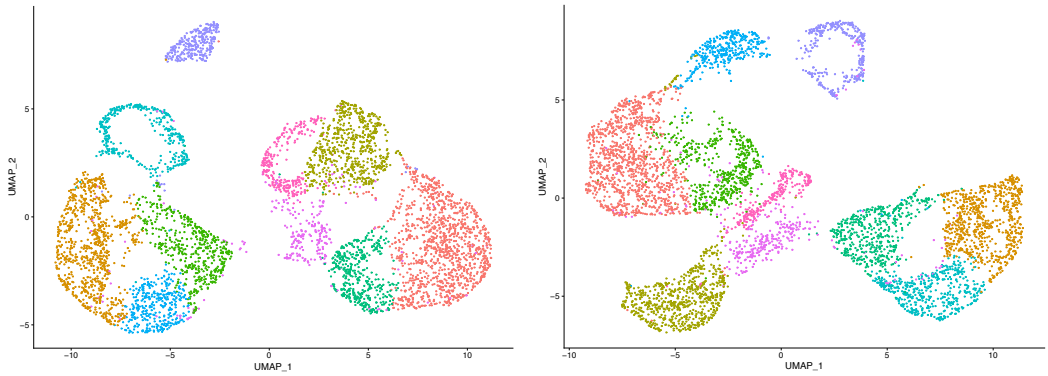

Figure 3.38 Dimension reduction of control and GSK-J4. Control presents 11, and GSK-J4 presents 12 distinguishable clusters.

A better understanding of the clusters and the cellular distribution was achieved by looking into U87MG and astrocyte-specific molecular markers. We tested more than 20 markers. The markers and associated clusters were compared with the negative binomial test and likelihood-ratio test to select the most overlapping features for astrocytes and U87MG cells. ITGA6 (CD49f) and SYNM features for astrocytes, and CD68 and ENG(CD105) were identified as U87MG features. The markers' distribution and similarity were graphed with a blend graph (Figure 3.39). The ITGA6 and SYNM, as well as CD68 and ENG, have shown the cluster and cell-type distribution.

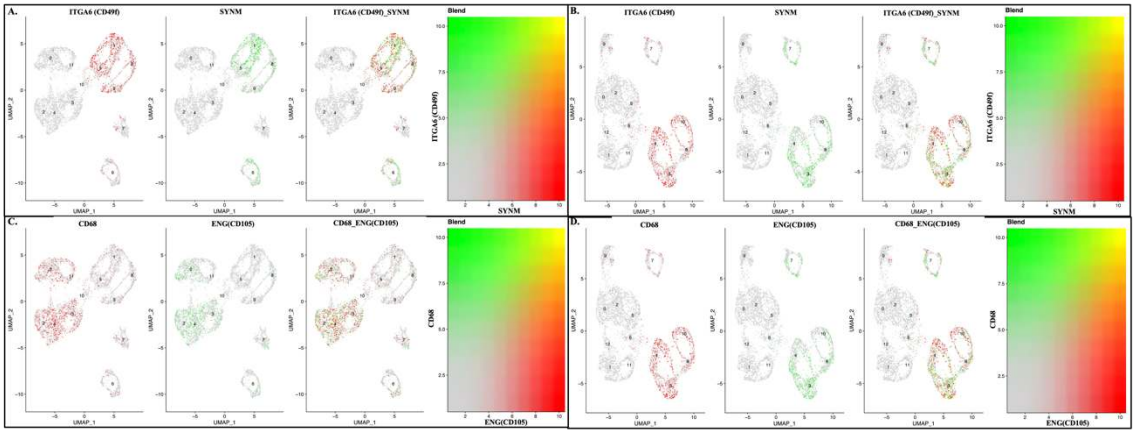

Figure 3.39 Blend graph of astrocyte and U87MG features. A. The distribution of the control group for astrocytic features. **B.** The distribution of GSK-J4 for astrocytic

features. **C.** The control group distribution for U87MG features. **D.** GSK-J4 distribution for U87MG features.

The data clustering allowed us to reduce the dimensions, understand the outcomes better and identify the features of our cell-types. However, to produce a self-consistent version of the data, we combined the samples with Seurat and harmony. Then we identified our distinct cell types with the pre-determined features (Figure 3.40). Most of the clusters presented either astrocytic features or U87MG features, but the minority which presented both (Figure 3.40, clusters 7 and 8) were named "Unknown", while the rest were named according to their features (Figure 3.41).

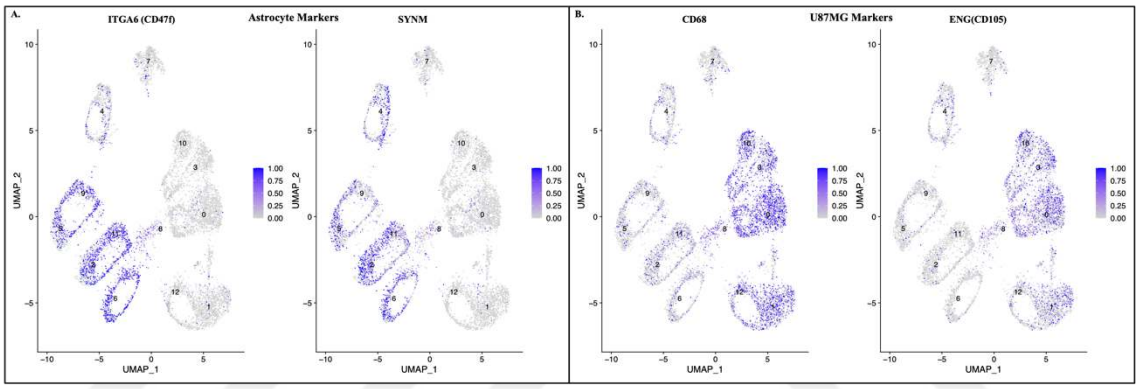

Figure 3.40 Feature marking of integrated data. The clusters present significant dispersion according to the features, except clusters 7 and 8. **A.** Astrocytic features were observed at clusters 2, 4, 5, 6, 7, 8, 9, and 11. **B.** U87MG features were observed at clusters 0, 1, 3, 7, 8, 10, and 12.

We further investigated the effects of cell cycle heterogeneity in scRNA-seq data by calculating cell cycle phase scores based on canonical markers. Cell cycle variation is a common source of uninteresting variation in scRNA-seq. The Seurat makes a list of cell cycle phase marker genes available for humans and performs phase scoring according to their expression. Taking the phase markers for the cell cycle genes, we scored each cell based on which stage of the cell cycle it is most likely to be in, without performing the regression. PC scores presented a slight increase in the G2M phase compared to control, alongside a slight decrease in the S phase (Figure 3.42). The phase transition presented itself among several clusters also (Figure 3.43). However, no statistically significant difference was observed when the control and condition medium results were compared.

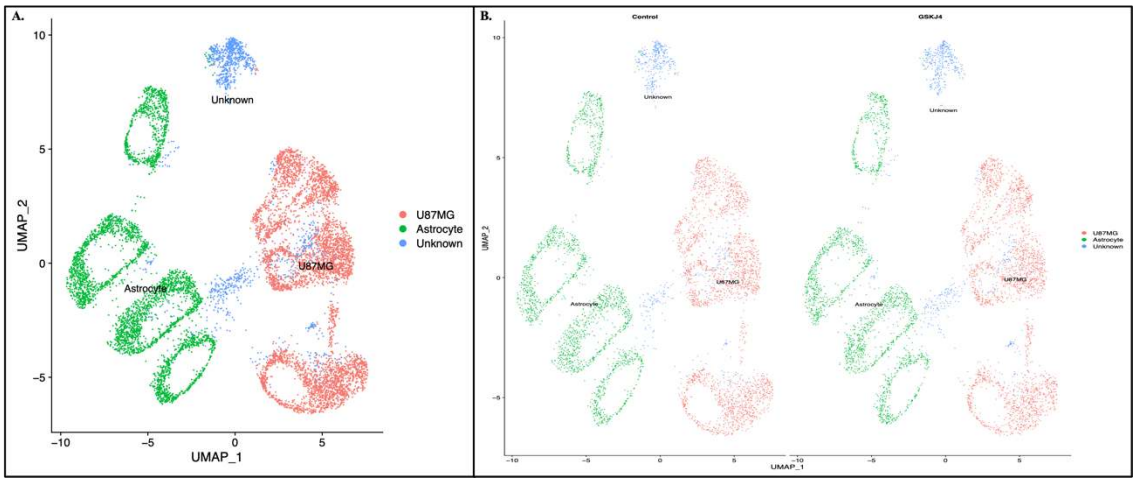

Figure 3.41 Cluster separation according to their features. A. Control and GSK-J4 integrated data present distinct separation. Astrocytes were on the left, while the U87MG cells were on the right. The cells which showed both features were named "Unknown". **B.** Individual Control and GSK-J4 clusters are named according to their features.

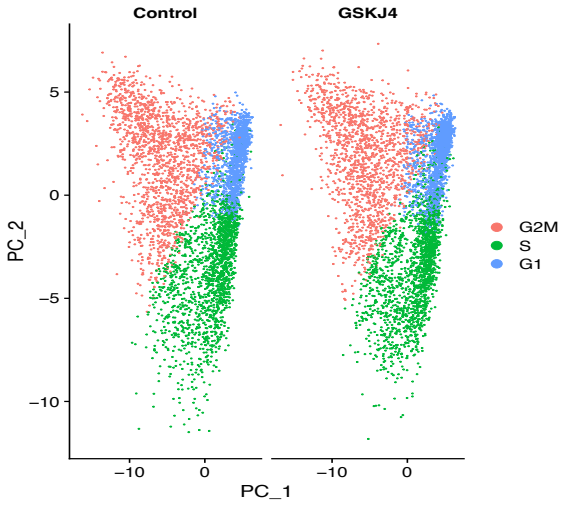

Figure 3.42 Principal component analysis of cell cycle scoring. The PC variations present the S phase transition into the G2M accumulation with GSK-J4 treatment.

The cell cycle scoring of control and the effect of GSK-J4 were examined thoroughly, whereas the cell cycle phase of distinct cell types was not observed due to the multilevel state of our data. Therefore, we separated the cells according to their features and calculated cell cycle scores in control and GSK-J4 conditions (Figure 3.43). The astrocytes presented an even distribution of cell cycle in control and GSK-J4 (Figure 3.44.A). GSK-J4 treatment of U87MG cells demonstrates decreased S phase cells and increased G2M cell phase characteristics.

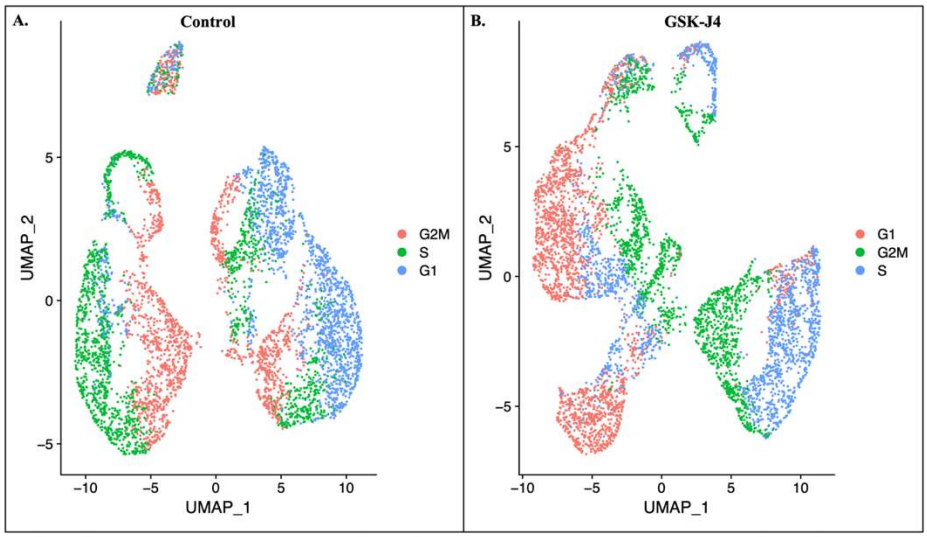

Figure 3.43 Cell cycle scoring of clusters. A. The cell cycle distribution of the control group. G1 and S phase cells were observed more compared to G2M. **B.** GSK-J4 treated cell cycle distribution. G2M accumulation and S phase cell count decrease were observed upon GSK-J4 treatment.

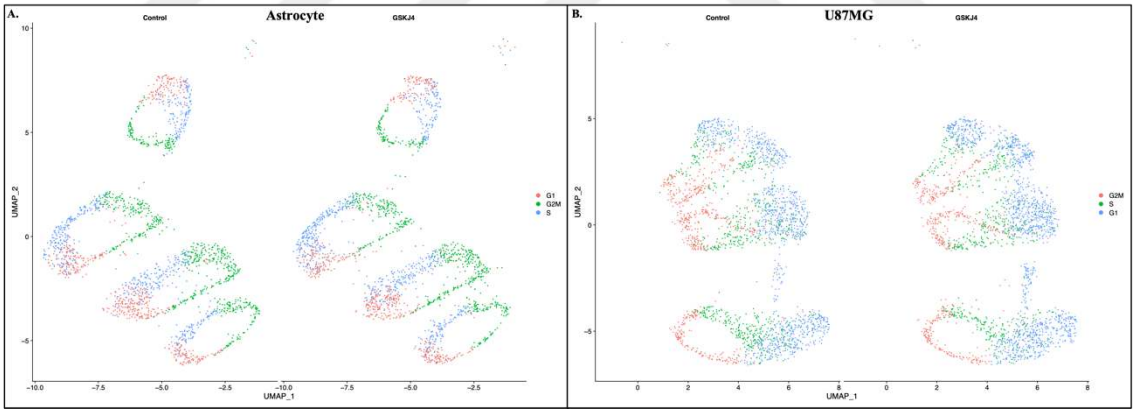

Figure 3.44 The cell cycle scoring of astrocytes and U87MG cells. A. Astrocytes did not present altered cell cycle characteristics. **B.** U87MG cells demonstrate accumulation of G2M phase and a decrease in S phase upon GSK-J4 treatment.

The genomic landscape changes of astrocytes and U87MG cells with GSK-J4 treatment were essential to understanding and identifying the vulnerabilities of U87MG cells. Therefore, we conducted differential expression (DE) analysis for astrocytes and U87MG cells individually, comparing GSK-J4 with control. The differential expression revealed 40 DE genes for astrocytes and 38 DE genes for U87MG cells. As top DE genes,

the astrocytes presented *MTRNR2L10* (Figure 3.45) up-regulation and *MT-CYB* (Figure 3.46) down-regulation. Meanwhile, *MT-ND4L* (Figure 3.47) and *BNIP3* (Figure 3.48) were the top up- and down-regulated genes among U87MG, respectively.

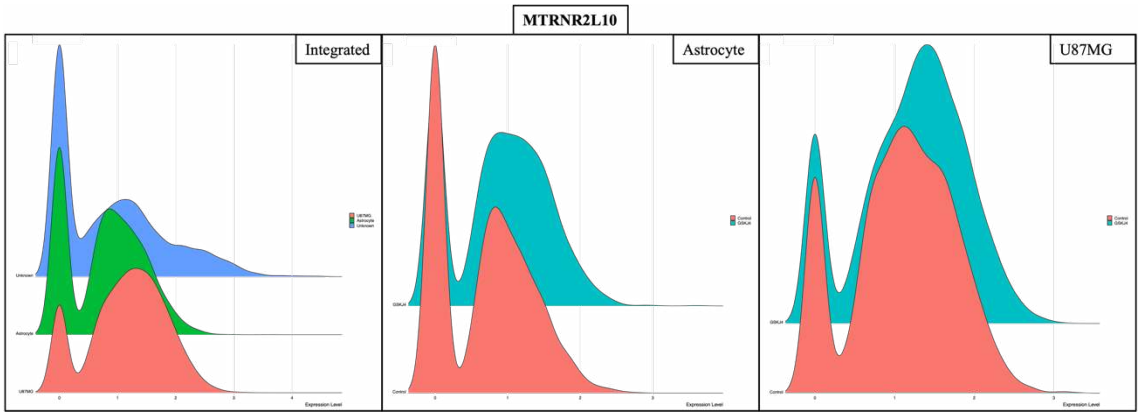

Figure 3.45 Differential expression of MTRNR2L10. A. The differential expression comparison of cell types, astrocytes present elevated expression compared to other cell types. **B.** Gene expression of *MTRNR2L10* presents elevated expression in GSK-J4 compared to control in astrocytes. **C.** *MTRNR2L10* did not present altered expression in GSK-J4 treated samples compared to control in U87MG cells.

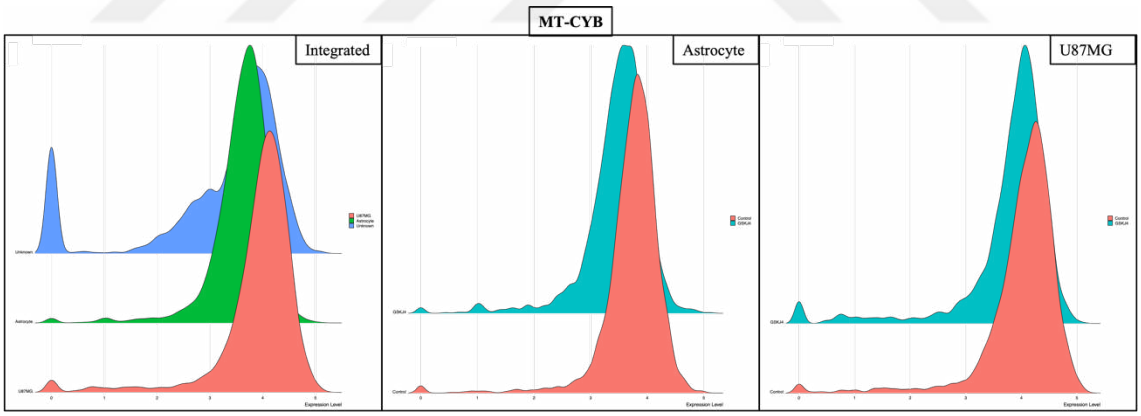

Figure 3.46 Differential expression of MT-CYB. A. The differential expression comparison of cell types, astrocytes present decreased expression compared to other cell types. **B.** Gene expression of *MT-CYB* present decreased expression in GSK-J4 compared to control in astrocytes. **C.** *MT-CYB* did not present differential expression in GSK-J4 treated samples compared to control in U87MG cells.

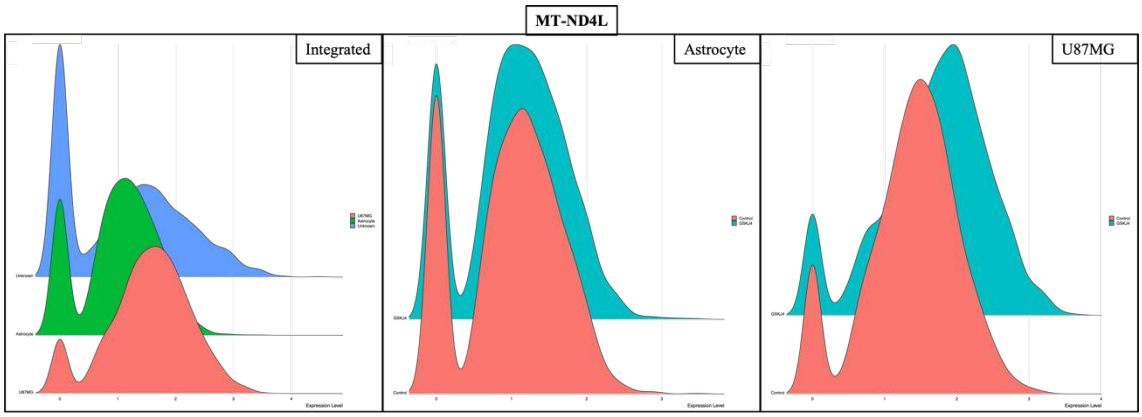

Figure 3.47 Differential expression of MT-ND4L. A. The differential expression comparison of cell types, astrocytes present decreased expression compared to other cell types. **B.** Gene expression of *MT-ND4L* did not present differential expression in GSK-J4 compared to control in astrocytes. **C.** *MT-ND4L* presents inclined expression in GSK-J4 treated samples compared to control in U87MG cells.

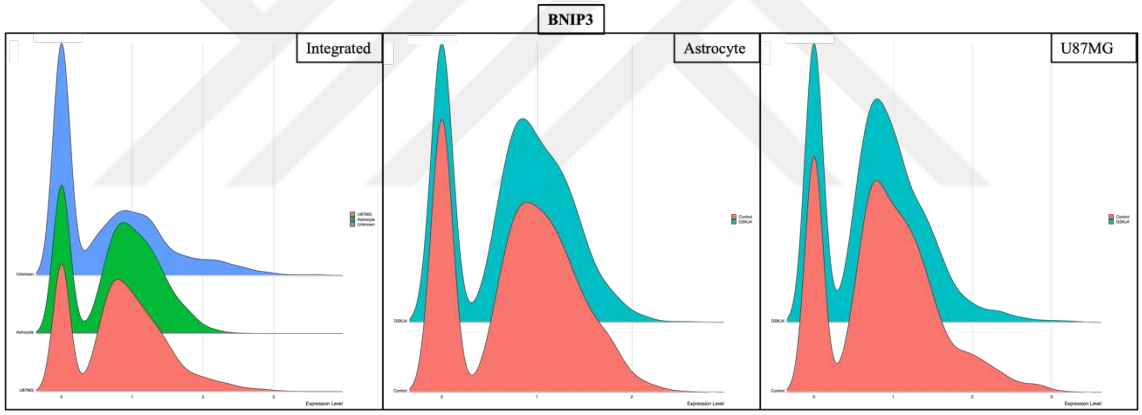

Figure 3.48 Differential expression of BNIP3. A. The differential expression comparison of cell types, U87MG cells present decreased expression compared to other cells. **B.** Gene expression of *BNIP3* did not present altered expression in GSK-J4 compared to control in astrocytes. **C.** *BNIP3* presents decreased expression in GSK-J4 treated samples compared to control in U87MG cells.

Astrocytes and U87MG cells shared only 4 genes *MT-CYB*, *MT-CO2*, *MT-ND2*, and *MTRNR2L10*. Even though the rest of the DE genes were not common, most of the genes in both groups were directly or indirectly involved in mitochondrial regulation. Detailed gene set enrichment analysis (GSEA) of common and uncommon genes among astrocytes and U87MG cells revealed approximate 30 altered pathways for astrocytes and

22 altered pathways for U87MG cells. Predominantly, oxidative respiration in mitochondria pathways were up-regulated, and the apoptosis pathway was downregulated in astrocytes. U87MG cells presented upregulated glycolysis and protection from hypoxia genes and downregulated oxidative respiration pathways (Figure 3.49).

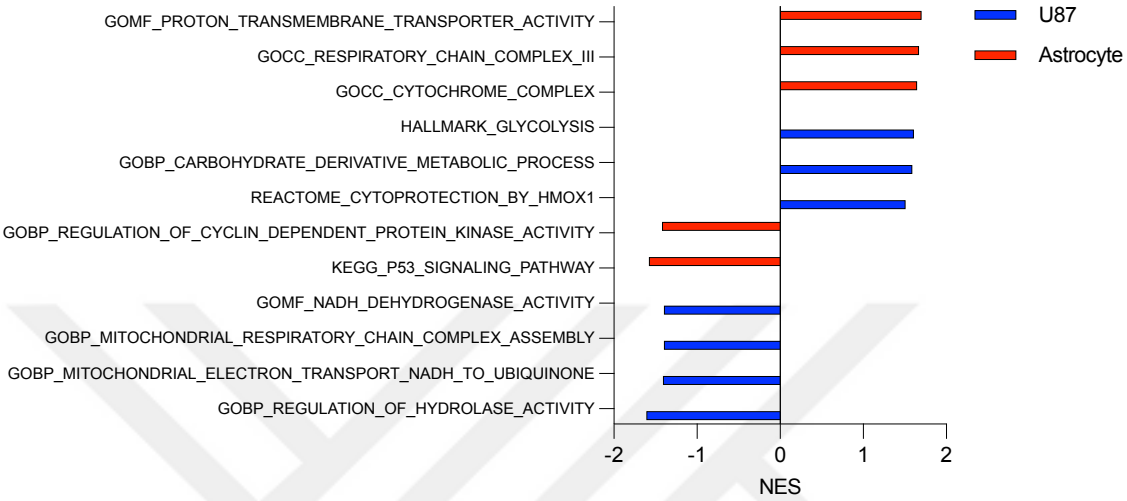

Figure 3.49 Gene Set Enrichment Analysis (GSEA) of differentially expressed genes from astrocytes and U87MG cells. The astrocytes did present elevated oxidative respiration while decreased cell death. In contrast, U87MG cells demonstrated an anaerobic respiration increase and inhibition of aerobic respiration.

The single cell result was validated with qRT-PCR. The top differentially expressed genes were selected, astrocyte and U87MG common or uncommon. The top upregulated MT-CO2, MT-CYB, down-regulated MTRNR2L10, and MT-ND2 were selected. Since these genes presented similar expression patterns (Figure 3.45, 3.46), the gene expressions of unsorted co-culture (U87MG-astrocyte), U87MG and astrocytes sorted from co-culture, and mono-culture U87MG and astrocytes, GSK-J4 treated and untreated, were used in qRT-PCR. The results confirmed single-cell results (Figure 3.50 A., B., C.). Upregulated MT-CO2 and MT-CYB and downregulated MTRNR2L10 and MT-ND2 presented differential expression, whereas mono-cultured U87MG and INHA did not present differential expression of these genes (Figure 3.50).

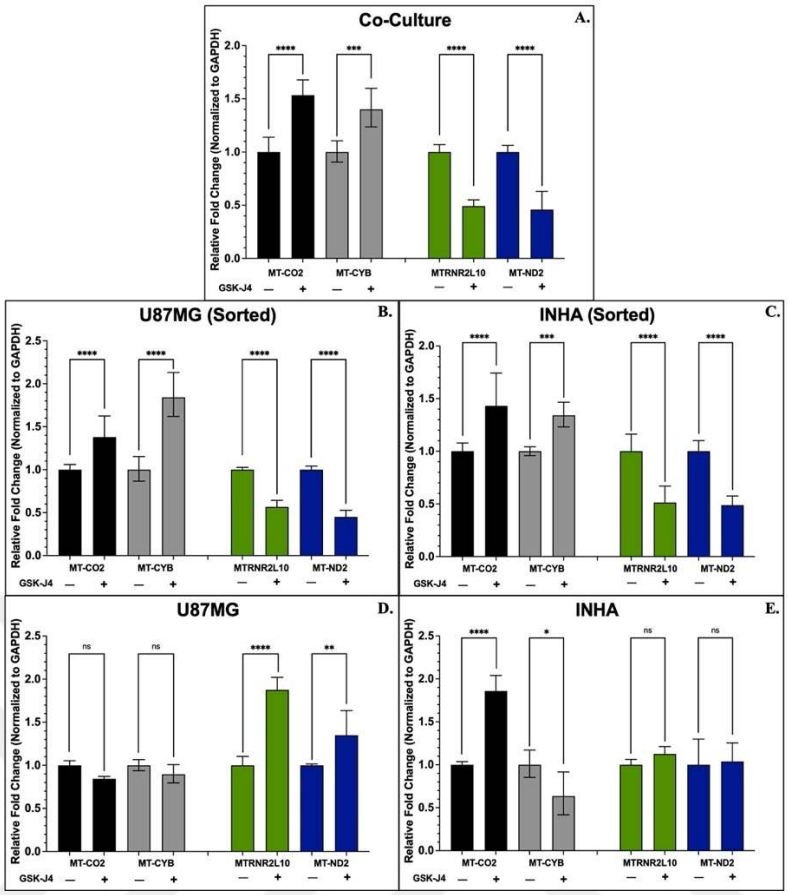

Figure 3.50 qRT-PCR results of top differentially expressed genes. A. Co-cultured U87MG and INHA cells presented significant upregulation of MT-CO2, MT-CYB, and downregulation of MTRNR2L10 and MT-ND2 when treated with GSK-J4. **B.** GSK-J4 treated U87MG cells sorted from co-culture presented significant upregulated MT-CO2, MT-CYB, and downregulated MTRNR2L10 and MT-ND2. **C.** GSK-J4 treated INHA cells sorted from co-culture presented significant upregulated MT-CO2, MT-CYB, and downregulated MTRNR2L10 and MT-ND2. **D.** Mono-cultured U87MG cells treated with GSK-J4 presented non-significant difference of MT-CO2, MT-CYB, and upregulation of MTRNR2L10 and MT-ND2. **E.** Mono-cultured INHA cells treated with GSK-J4 presented upregulation of MT-CO2, downregulation of MT-CYB, and a non-significant difference of MTRNR2L10 and MT-ND2.

Glycolysis-related genes presented the top upregulated genes for U87MG cells (Figure 49). Genes such as ENO1, P4HA1, TPI1, HIF1A, MT-CO2, and MT-ND4L expressions were investigated with qRT-PCR. The U87MG and astrocyte co-cultures, and U87MG and astrocytes sorted from co-cultures (Figure 3.51) did present similar

expression patterns as single cell results. However, mono-cultured U87MG cells or astrocytes demonstrated opposite or non-significant expression differences (Figure 3.51).

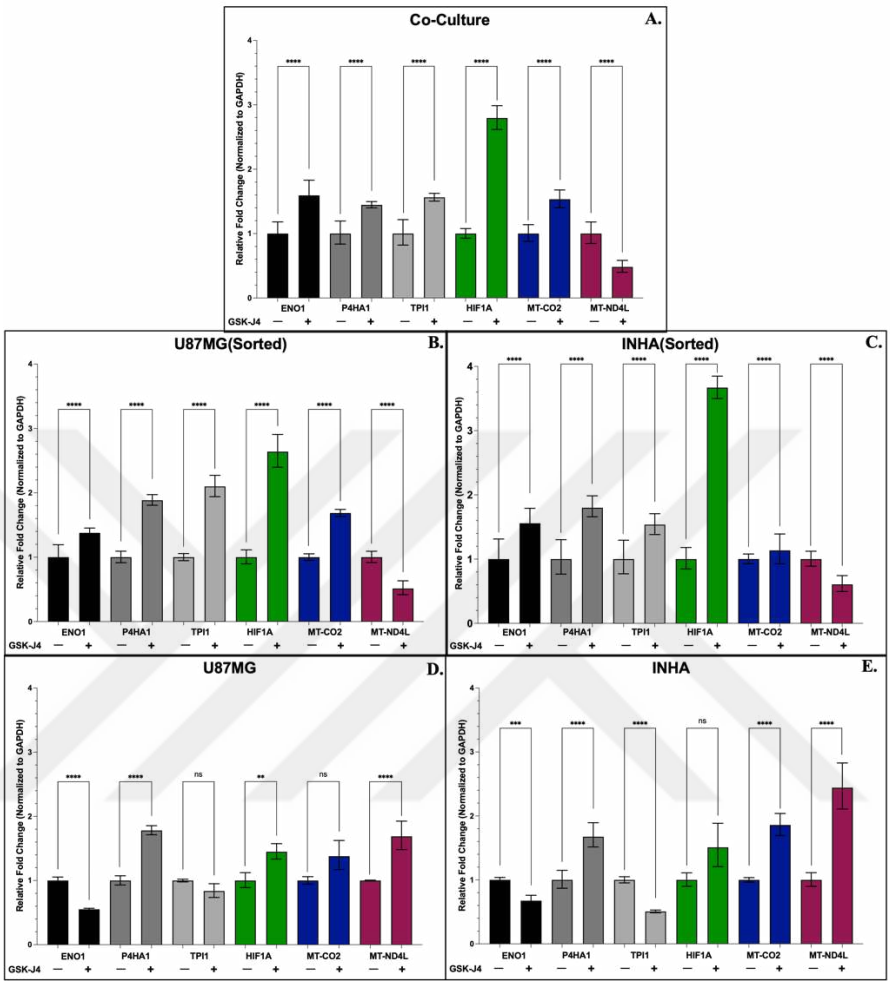

Figure 3.51: qRT-PCR results of glycolysis-related genes. A. Co-cultured U87MG and INHA cells presented significant upregulation of ENO1, P4HA1, TPI1, HIF1A, and MT-CO2, and downregulation of MT-ND4L when treated with GSK-J4. **B.** GSK-J4 treated U87MG cells sorted from co-culture presented significant upregulated ENO1, P4HA1, TPI1, HIF1A, and MT-CO2, and downregulated MT-ND4L. **C.** INHA cells treated with GSK-J4 sorted from co-culture presented significant upregulated ENO1, P4HA1, TPI1, HIF1A, and MT-CO2, and downregulated MT-ND4L. **D.** Mono-cultured U87MG cells treated with GSK-J4 presented non-significant difference of MT-CO2, TPI1, upregulation of P4HA1, HIF1A, MT-CO2 and MT-ND4l, and downregulation of ENO1. **E.** Mono-cultured INHA cells treated with GSK-J4 presented upregulation of MT-CO2, HIF1A, and P4HA1, downregulation of ENO1 and TPI1, and a non-significant difference of HIF1A.

4 Discussion

Glioblastoma (GBM) is a malignant central nervous system (CNS) tumour with a median survival of 16 months. Treatment options for GBM have remained unchanged in the last 25 years, and it consists of surgery, ionizing radiation, and chemotherapy with temozolomide (J. H. Lee et al., 2018b; Martínez-Jiménez et al., 2020; *The Development and Causes of Cancer - The Cell - NCBI Bookshelf*, n.d.). The location of GBM, the brain, is a highly protective environment with microglial cells and a blood-brain barrier, which also limits the efficient delivery of therapeutic agents to tumours. However, even the therapeutics that could overcome these obstacles may not act as efficient as expected due to the interactions in the microenvironment. Healthy cells in the tumour microenvironment have a different response to the chemotherapeutics and they can participate in the development of resistance. Therefore, understanding the drug response, cell-to-cell interaction, and interaction-derived resistance are important to develop more effective targeting of the tumours (Berger, 2007; Falkenberg & Johnstone, 2014; Fiacco et al., 2009; Jiang et al., 2020; Saha et al., 2021; Watson et al., 2021).

This thesis investigated temozolomide resistance acquired with astrocyte interactions by establishing and characterising a co-culture model. In addition, epigenetic vulnerabilities were thoroughly examined.

4.1 Tumour chemoresistance in the tumour microenvironment

The fundamentals of the modern chemotherapy agent can be traced back to chemical warfare during World War II. In 1943, Dr. Stewart Francis Alexander investigated a mustard gas aftermath, and found lymphoid and myeloid suppression in autopsies of the victims. Since the mustard gas killed fast-dividing cells, Dr. Alexander suggested that it could be a potential cancer therapy. Dr. Louis S. Goodman and Dr. Alfred Gilman tried to treat non-Hodgkin's lymphoma using this information. Even though the patient died of cancer, the doctors observed a dramatic reduction in tumour mass and reported this clinical trial in 1946. Until 1955, different researchers demonstrated chemical targeting of tumours, which is currently known as first-generation chemotherapy (Farber et al., 2010; Fenn & Udelsman, 2011; Weisse, 1991).

In 1955, the United States Congress financially supported the production of second-generation chemotherapy research and created National Cancer Chemotherapy Service Centre (NCCSC). NCCSC has collected, evaluated, and defined the boundaries of the research methodologies (DeVita & Chu, 2008). In the 1960s, two research groups in different countries tried to combine chemotherapy agents with different mechanisms of action. Both groups observed amplified mass reduction in tumours compared to the mono-therapy applications of chemotherapy (Bonadonna et al., 2009). This harsh combined therapy did not prevent the recurrence of tumour, the therapy resistance, and the death of the patients. Even after a decade, the advanced therapy regimens could not overcome the therapy resistance of tumour cells (Anand et al., 2022; DeVita & Chu, 2008; Hoverman, 2021).

Therapy resistance in cancer is a well-known phenomenon, which could create chemotherapy-tolerant cancer cells. Based on the time of development, drug resistance could be categorized as innate (intrinsic) or acquired resistance. Innate resistance exists before drug treatment as part of the heterogeneity of the tumours. However, the cytotoxicity of the chemotherapy agents, action and reaction of treatment, and changes of tumour microenvironment leads to increased genomic instability or activation of other mechanisms in cancer cells, and eventually development of acquired resistance(Alfarouk et al., 2015; Housman et al., 2014). For example, cytotoxicity could lead to cell death by death receptor-mediated cytotoxicity. TRAIL targets death receptor 4 or 5 (DR4-5) or Fas ligand (FasL) target Fas receptor promote downstream mechanisms and eventually lead to cell death. However, cancer cells tend to escape from cell death, and one of these escape mechanisms is downregulation of apoptosis initiator ligands. Therefore, upon TRAIL and FasL combined treatment, the cells without corresponding ligands would survive the treatment regimen. Furthermore, these survived cells would proliferate and create resistant cancer (Wilson et al., 2009). Unfortunately, recurrent tumours are not a specific homogeneous cell population derived from a single cell. The heterogeneous profile of tumours are more complex with the cells in the microenvironment.

The solid tumour environment consists of extracellular matrix (ECM), immune cells, and blood vessels, among other tissue-specific cells. Depending on the cancer type, the tumour microenvironment contains numerous non-malignant cells. The

environmental cells promote tumour proliferation and survival (Li et al., 2017; Lucas et al., 2017; Perrin et al., 2019; X. Zhang et al., 2019). For example, neuroblastoma cells (NBLs) could develop cisplatin resistance with the help of tumour-associated macrophages (TAMs). When NBLs are treated with cisplatin, miR21/TLR8-NF-kB exosomes are released into the microenvironment. miR21 exosomes promote miR155 exosome production in TAMs by TLR8-NF-kB inhibition. miR155 containing exosomes interact with NBLs and inhibit *TERF1*. Then downstream mechanisms of *TERF1* inhibition in NBLs lead to cisplatin resistance (Challagundla et al., 2015). The tumours do not only interact with the surrounding cells but also shape the environment according to their needs.

The pH balance is an essential factor in the microenvironment. Under normal conditions, the intracellular pH (pH 6.7-7.3) is slightly less than the extracellular pH (pH 7.2-7.6) (Casey et al., 2010). The tumour cells reverse the pH gradient and create an acidic extracellular pH by proton pumping and the Warburg effect (Sharma et al., 2015). An altered environment promotes the destruction of healthy surrounding cells opening up spaces to be occupied by tumour cells, which supports further pH alteration. The acidic pH accumulation decreases the efficacy of some chemotherapy agents by ion trapping (Taylor et al., 2015). The proton pump inhibition in melanoma cells demonstrated synergistic effects in combination with paclitaxel (Wojtkowiak et al., 2011). Contact independent secretion of regulative factors or exosome transfers could be targeted for tumour treatment. However, it is well known that the tumour cells directly communicate with each other.

Contact-dependent communication could be classified in gap junctions, ligand-receptor pair mediated cell adhesion, and tunnel nanotubes. Gap junctions are significant contributors of direct cell-to-cell contact. Gap junctions appear in a short distance apart and connect two cells' cytoplasm directly, allowing anything that could fit into the junction structure a direct passage. The gap junctions are composed of two connexons formed by transmembrane protein connexins. Cancer cells usually downregulate connexins. Depending on the tumour type, connexin downregulation is associated with increased proliferation (Leithe et al., 2006). However, especially in metastatic borders of breast cancer and melanomas, connexin 43 (Cx43) upregulation has been documented,

and inhibition of Cx43 was associated with decreased metastatic ability (Alaga et al., 2017; Ming et al., 2015). Another approach presents *herpes simplex virus thymidine kinase (TK)* local delivery paired with ganciclovir (GCV) treatment for glioblastomas. The *TK* delivery sensitizes the tumour cells to GCV by phosphorylating the GCV to a toxic component for cells (Immonen et al., 2004). Further investigation demonstrated Cx43 upregulation by *TK* delivery, associated with increased gap junction formation and diffusion of phosphorylated GCV, eventually leading to an increased area of effect. While gap junctions need a relatively short distance to appear, nanotubes can form from further distances.

Long-distance cell interactions are possible with tunnelling nanotubes (TNTs) or tumour microtubes (TMs), which have been discovered relatively recently. Instead of short bridges, TNTs are long and thin extensions formed by F-actin filaments. They occur in various types of cells and are extensively used for tumour cell communication. The nanotubes formation was observed in MDA-MB-231 breast cancer cells and connected cancer cells together; another study presented cancer – healthy cell interactions between carcinoma-associated fibroblast (CAF) and prostate cancer cells DU145 cells 2013). Studies have demonstrated organelle, miRNA, particles and some proteins transfer, and they are widely accepted as a novel mode of intercellular interaction s in tumour cells, tumour survival and proliferation, tumour progression, and chemoresistance (Qin et al., 2021; Zampieri et al., 2021). Tumour survival, especially escaping from immune destruction, was associated with alternative tumour antigen-presenting mechanisms. In contrast, recent studies of TME-tumour interactions presented evidence of another mechanism, mitochondria hijacking (Marti Gutierrez et al., 2022; Thayanithy et al., 2014; Torralba et al., 2016). The breast cancer cells, MDA-MB-231, form more than one nanotubule with natural killer (NK) immune cells and hijack mitochondria of immune cells. After 16 hours, the NK cells lose more than 60% of the mitochondria, which decreases the respiration of these cells by 90% and suspend NK cell metabolism and activity (Baldwin & Gattinoni, 2021; Saha et al., 2021). This evidence suggests an alternative immune escape mechanism as well as the importance of mitochondrial regulation in TME. A similar mechanism was observed in glioblastoma cells, microglia, and astrocytes (Watson et al., 2021). Even though the tunnelling nanotubes have been

known since 1999, the nanotubular interconnection in tumours and surrounding healthy cells is a relatively recent concept (Davis & Sowinski, 2008).

The human astrocytoma transplanted to xenograft models was followed up for one year. This long-term study, supported by other reports, demonstrated homotypic interactions (among homogenous cancer cells) and heterotypic interactions (among heterogeneous cancer cells and TME cells) (Jung et al., 2017; Osswald et al., 2015; Venkataramani et al., 2019; Weil et al., 2017). TNT functions in cancer are characterized by four groups: 1) tumour dissemination, 2) tumour cell survival, 3) modulation of tumour cells and environment, and 4) tumour angiogenesis. One of the studies presented a very rare but exciting cell alteration and resurrection mechanism. Brain tumour propagating cells (BTPCs) were treated with lethal ionising laser radiation, and GBM TNTs approached the dead cells. A new nucleus diffused to the death cell from the connected GBM cells, eventually leading to the death cell's rise as a new cancer cell; furthermore, this resurrected cell was supported until the cell's total recovery.

Other studies presented novel surgical, chemotherapy, and radiotherapy treatment resistance mechanisms in various cancer types. Patient-derived BTPCs were transplanted into xenograft models. After the lesion, the glioblastoma cells demonstrated increased TNTs and colonization into the lesion sites. Further investigation showed that *GAP-43* inhibition leads to TNT impairment and reduced tumour recurrence (Weil et al., 2017). It was observed that TNTs were shown to involve chemoresistance in breast, pancreatic, leukaemia, and glioblastoma cells s (Desir et al., 2016). Mitochondrial dysregulation and trafficking in MCF7 breast cancer, hematopoietic malignancies, leukemia and glioblastoma (Burt et al., 2019; Desir et al., 2018; Wang et al., 2018). TNT and radiotherapy association is not widely studied yet; however, cellular stress accumulation by reactive oxygen species (ROS) is a suspected TNT trigger (Pouget & Mather, 2001).

The evidence support tumour microenvironment also supports tumour heterogeneity. The pH alterations, dynamic vasculature, fluctuating hypoxia, and contact-dependent or independent interactions create stress on tumour cells, which could induce DNA damage. DNA damage contributes to genetic instability, accumulates divergent mutations, and produces genetically diverse populations (Bindra & Glazer, 2005; Y. A.

Zhang et al., 2000). The tumour heterogeneity, increasing evidence of TME involvement in tumour formation, and recurrence play essential roles in cancer-related deaths. The cumulative knowledge about the complexity of cancer and highly possible interactions in the tumour microenvironment has reshaped the research questions. More interactive and outgoing tumour models are produced instead of highly isolated and withdrawn tumour models.

The tumour models have been developed to provide insight into tumour mechanisms. The most commonly used models are *in vivo* and *in vitro* models and vary in complexity and range from homogenous cell lines to 3D microenvironment models (Greshock et al., 2007). The complexity of the model is largely shaped by the objectives and resources. For example, drug discovery screening can be performed in cell culture; however, it would not represent the environmental interactions of the drug. Extracellular matrix embedded cell lines would provide insights into the invasion, proliferation profiles, and many more; however, they would not present the flow through vasculature. The advantages and disadvantages of the models mainly depend on the research question; however, one of the critical components of any model is the source of cancer cells (Hulkower & Herber, 2011; Vidi et al., 2013). The most widely used source of cells is cancer cell lines due to their easy maintenance, cost-effectiveness, and easy replicative results. GBM co-culture studies discussed above have used commercially available cancer and astrocyte cell lines. However, those studies either estimated the cell viability according to control proliferation or hard-to-quantify staining methods (Pustchi et al., 2020).

The cell quantifying methods of co-culture models established in this thesis would provide a new cost-effective method for researchers. While the luciferin/luciferase method would provide a quantitative method, alternative use combined with selective fluorescence marker and imaging allows both quantification and visual confirmation. These established methods demonstrated astrocyte-related resistance in co-culture upon temozolomide treatment repeatedly. Further investigation showed expected elevated cell-to-cell interactions in tumour cells from a co-culture environment compared to mono-cultured tumour cells.

4.2 Epigenetic targeting of contact-dependent astrocyte-related protection

Chemical targeting of cancer is a crucial step in cancer treatment. Even though the chemotherapies originated with toxic drug derivatives, the advancements in biotechnology and genetics allowed for the development of more effective and less dangerous drugs. Especially the epigenetic marks discovered in cancer research and the reversibility of epigenetic alterations attracted extensive attention to epigenetic drugs (Cheng et al., 2019).

The early drug discovery studies were solely based on the demonstration of efficacy instead of knowing and targeting precise targets. For example, around the 1940s, 5-azacytidine (Píškala & Šorm, 1964) and derivatives demonstrated high antibacterial activity (Šorm et al., 1964), followed by a successful inhibitory effect on lymphoid leukaemia in xenograft models. Around the 1970s, the first clinical trials were started for 5-azacytidine in acute myeloid leukaemia (AML); however, no inhibitory effect was observed on other cancers (Veselý & Čihák, 1978). Even though 5-azacytidine was studied for more than 40 years, and its impact in cancer was studied for 9 years, the underlying epigenetic mechanisms were first demonstrated in the 1980s (P. A. Jones & Taylor, 1980). This example was a representation of the first wave of epigenetic drugs. The second wave of epigenetic drug discoveries revolved around analogue-based drugs. Taking advantage of recent studies, DNA methyltransferase (DNMT) and histone deacetylase (HDAC) became attractive targets for drug discovery. More than 20 clinical trials were conducted, and 3 HDAC inhibitors were approved (Juergens et al., 2011; Mottamal et al., 2015). In the last decade, an increasing number of epigenetic drugs have been approved, and the studies were changed slightly compared to the first wave. The success stories have validated the epigenetic targeting of cancers and inspired more epigenetic drug studies. The drug discovery or repurposing involves a very tightly controlled experimental procedure series. The direct impact demonstrates the possibility of the drug's use in treatment. In parallel, the indirect effect of the drug discovery studies presents knowledge on the vulnerabilities of cancer.

Targeting cell-to-cell interactions provided promising results; however, these studies directly interrupted the interaction mechanisms (Burt et al., 2019; Desir et al.,

2016, 2018; Pouget & Mather, 2001; Wang et al., 2018; Wu et al., 2014). We observed the interaction between tumour and astrocytes led to temozolomide resistance in the co-culture model. Therefore, in this thesis, as far as we know, an epigenetic inhibitory drug screen has been conducted in a co-culture model for the first time. Our study revealed the sensitizing effect of a UTR/UTX histone demethylase inhibitor, GSK-J4. GSK-J4 has demonstrated high efficacy and sensitizing effect combined with temozolomide.

As explained before, many epigenetic mechanisms play a role in various tumours. DNA wrapping and loosening are controlled by histone methylation and demethylation. These alterations are regulated by the polycomb group (PcG) proteins. While histone methylation is regulated by polycomb repressive complexes (PRC), the reverse mechanism, histone demethylation, is controlled by KDMs and JmjC domain-containing histone demethylases (Kooistra & Helin, 2012; van Haaften et al., 2009).

Research demonstrated lysine (K) demethylation of H3K4, H3K36 and H3K79 are associated with transcriptional activation, while H3K9 and H3K27 methylation has been found in silenced chromatin structures. However, opposite characteristics emerged with a more detailed understanding of methylation/demethylation. For example, transcriptionally active genes present H3K9 methylation, or H3K36 is associated with transcription repression. Even though the exact role in activation/repression of methylation/demethylation is still emerging, the complexes and proteins are well studied (Barski et al., 2007). The ubiquitously transcribed tetratricopeptide repeat (TPR) *KDM6A* (*UTX/UTY*) and their homolog *KDM6B* (*UTR*) are histone demethylases. KDM6A and KDM6B have been associated with numerous mechanisms such as development, cell plasticity, neurodegenerative diseases, and cancer. Therefore, targeting KDM6 is a potential treatment for various diseases, including cancer. A dual KDM6A and KDM6B inhibitor GSK-J4 promoted apoptosis (Sui et al., 2017), endoplasmic reticulum (ER) stress (Lochmann et al., 2018), and hypoxia-like methylation accumulation (Yin et al., 2019).

As discussed, several studies demonstrated hypoxic conditions and HIF-mediated hypoxic transcriptional changes. Altered gene expression and histone methylation patterns in hypoxic conditions made the KDM involvement important in hypoxic

conditions (Hancock et al., 2015). For example, a recent study presented KDM6A dependency on transcription activating factor 4 (*ATF4*) gene, and heme-regulated eIF2α kinase (*HRI*) – *ATF4* regulates hypoxia. The mechanism has been suggested as GSK-J4-related mitochondrial stress occupies *HRI*, and since *HRI* is an unchangeable *ATF4* activator, *ATF4* could not be activated. Inactive *ATF4* could not stabilize hypoxia-inducible factors and initiate hypoxia (Kitajima et al., 2021). Another study revealed that KDM6A, but not its paralog KDM6B, is oxygen-sensitive, and KDM6A loss-related H3K27 hypermethylation controls cell differentiation fate. mHepa-1 c4 cells presented H3K27 methylation accumulation under hypoxic conditions. In parallel, down-regulation of KDM6A and KDM6B has been observed. The recovery of KDM6A, but not KDM6B, by ectopic overexpression demonstrated normal methylation levels of H3K27 in hypoxia. Also, KDM6B-silenced mHepa-1 c4 cells, presented normal levels of KDM6A expression and release from the H3K27 methylation accumulation under normoxic conditions. As supporting evidence, hypoxia or KDM6A inhibition was associated with blocked myogenic differentiation in C2C12 cells. Therefore, authors concluded that KDM6A is oxygen-sensitive and presents hypoxia-like H3K27 hypermethylation, which could block cell differentiation (Chakraborty et al., 2019).

In this thesis, we demonstrated the marked effect of GSK-J4 and temozolomide sensitization in co-culture conditions. We combined two single-cell approaches to track the underlying mechanisms of GSK-J4 in co-culture conditions. The CITE-seq and Multimodal single-cell combined method allowed us to track the differential expression of individual cell groups, U87MG and astrocytes simultaneously. The differential expression pointed to mitochondrial dysregulation, glycolysis induction and p53 signalling pathway down-regulation. In parallel, we showed that GSK-J4 treatment did not alter the cell cycle in astrocytes; however, U87MG cells demonstrated G2M accumulation upon GSK-J4 treatment. Another result indicated KDM6A silencing present, GSK-J4 similar, temozolomide sensitization on U87MG cells.

Throughout the thesis, we demonstrated that astrocytes present a protective effect for temozolomide treatment to U87MG cells. However, KDM6A inhibition might lead to hypermethylation in U87MG cells even in the astrocyte presence. Then U87MG cells could not respond to temozolomide treatment because hypermethylation could prevent

the induction of rescue mechanisms. In parallel, the astrocytes could not protect the U87MG cells because GSK-J4 might induce mitochondrial stress and dysregulation in astrocytes, and to turn the tides, the protective effect was sacrificed. These speculations need to be studied experimentally in the future.

In conclusion, we suggest that astrocyte – U87MG cell interaction and temozolomide resistance could be altered by GSK-J4 treatment, which might be due to mitochondrial dysregulation. Therefore, further understanding of crosstalk in astrocyte – U87MG co-cultures and mitochondria involvement in the underlying mechanisms upon GSK-J4 treatment could provide new targets for drug discoveries.

To our knowledge, this thesis presents one of the first studies with epigenetic screens in co-culture environments and single cell sequencing in Turkey; and may open new avenues for further related research.

5 REFERENCES

Alaga, K. C., Crawford, M., Dagnino, L., & Laird, D. W. (2017). Aberrant Cx43 Expression and Mislocalization in Metastatic Human Melanomas. *Journal of Cancer*, *8*(7), 1123–1128. https://doi.org/10.7150/JCA.18569

Alfarouk, K. O., Stock, C. M., Taylor, S., Walsh, M., Muddathir, A. K., Verduzco, D., Bashir, A. H. H., Mohammed, O. Y., Elhassan, G. O., Harguindey, S., Reshkin, S. J., Ibrahim, M. E., & Rauch, C. (2015). Resistance to cancer chemotherapy: failure in drug response from ADME to P-gp. *Cancer Cell International*, *15*(1). https://doi.org/10.1186/S12935-015-0221-1

Allen, N. J. (2014). Astrocyte regulation of synaptic behavior. *Annual Review of Cell and Developmental Biology*, *30*(1), 439–463. https://doi.org/10.1146/ANNUREV-CELLBIO-100913-013053

ALLFREY, V. G., FAULKNER, R., & MIRSKY, A. E. (1964). ACETYLATION AND METHYLATION OF HISTONES AND THEIR POSSIBLE ROLE IN THE. *Proceedings of the National Academy of Sciences of the United States Of*, *51*, 786–794. https://doi.org/10.1073/PNAS.51.5.786/ASSET/8C54DEE7-DD18-4CC2-86A1-BD41B3751D13/ASSETS/PNAS.51.5.786.FP.PNG

Allis, C. D., & Jenuwein, T. (2016). The molecular hallmarks of epigenetic control. In *Nature Reviews Genetics* (Vol. 17, Issue 8, pp. 487–500). Nature Publishing Group. https://doi.org/10.1038/nrg.2016.59

Anand, U., Dey, A., Chandel, A. K. S., Sanyal, R., Mishra, A., Pandey, D. K., de Falco, V., Upadhyay, A., Kandimalla, R., Chaudhary, A., Dhanjal, J. K., Dewanjee, S., Vallamkondu, J., & Pérez de la Lastra, J. M. (2022). Cancer chemotherapy and beyond: Current status, drug candidates, associated risks and progress in targeted therapeutics. *Genes & Diseases*. https://doi.org/10.1016/J.GENDIS.2022.02.007

Bachiller, S., Jiménez-Ferrer, I., Paulus, A., Yang, Y., Swanberg, M., Deierborg, T., & Boza-Serrano, A. (2018). Microglia in neurological diseases: A road map to brain-disease dependent-inflammatory response. *Frontiers in Cellular Neuroscience*, *12*, 488. https://doi.org/10.3389/FNCEL.2018.00488/BIBTEX

Bakhoum, S. F., Silkworth, W. T., Nardi, I. K., Nicholson, J. M., Compton, D. A., & Cimini, D. (2014). The mitotic origin of chromosomal instability. *Current Biology*, *24*(4), R148–R149. https://doi.org/10.1016/J.CUB.2014.01.019

Baldwin, J. G., & Gattinoni, L. (2021). Cancer cells hijack T-cell mitochondria. *Nature Nanotechnology 2021 17:1*, *17*(1), 3–4. https://doi.org/10.1038/s41565-021-01006-y

Bamford, S., Dawson, E., Forbes, S., Clements, J., Pettett, R., Dogan, A., Flanagan, A., Teague, J., Futreal, P. A., Stratton, M. R., & Wooster, R. (2004). The COSMIC (Catalogue of Somatic Mutations in Cancer) database and website. *British Journal of Cancer*, *91*(2), 355–358. https://doi.org/10.1038/sj.bjc.6601894

Bao, S., Wu, Q., McLendon, R. E., Hao, Y., Shi, Q., Hjelmeland, A. B., Dewhirst, M. W., Bigner, D. D., & Rich, J. N. (2006). Glioma stem cells promote radioresistance by preferential activation of the DNA damage response. *Nature*, *444*(7120), 756–760. https://doi.org/10.1038/NATURE05236

Bar, E. E. (2011). Glioblastoma, cancer stem cells and hypoxia. *Brain Pathol*, *21*(2), 119–129. https://doi.org/10.1111/j.1750-3639.2010.00460.x

Bar, E. E., Lin, A., Mahairaki, V., Matsui, W., & Eberhart, C. G. (2010). Hypoxia increases the expression of stem-cell markers and promotes clonogenicity in glioblastoma neurospheres. *Am J Pathol*, *177*(3), 1491–1502. https://doi.org/10.2353/ajpath.2010.091021

Barski, A., Cuddapah, S., Cui, K., Roh, T. Y., Schones, D. E., Wang, Z., Wei, G., Chepelev, I., & Zhao, K. (2007). High-Resolution Profiling of Histone Methylations in the Human Genome. *Cell*, *129*(4), 823–837. https://doi.org/10.1016/J.CELL.2007.05.009

Beier, D., Hau, P., Proescholdt, M., Lohmeier, A., Wischhusen, J., Oefner, P. J., Aigner, L., Brawanski, A., Bogdahn, U., & Beier, C. P. (2007). CD133+ and CD133− Glioblastoma-Derived Cancer Stem Cells Show Differential Growth Characteristics and Molecular Profiles. *Cancer Research*, *67*(9), 4010–4015. https://doi.org/10.1158/0008-5472.CAN-06-4180

Benedí, V. J., Jofre, J., & Tomás, J. M. (1986). Klebsiella pneumoniae C3 lipopolysaccharide mutants obtained by resistance to bacteriophage FC3-9. *Annales de l'Institut Pasteur. Microbiologie*, *137B*(1), 29–36. https://doi.org/10.1016/S0769-2609(86)80091-6

Berger, S. L. (2007). The complex language of chromatin regulation during transcription. *Nature 2007 447:7143*, *447*(7143), 407–412. https://doi.org/10.1038/nature05915

Biasoli, D., Kahn, S. A., Cornélio, T. A., Furtado, M., Campanati, L., Chneiweiss, H., Moura-Neto, V., & Borges, H. L. (2013). Retinoblastoma protein regulates the crosstalk between autophagy and apoptosis, and favors glioblastoma resistance to etoposide. *Cell Death and Disease*, *4*(8), 1–11. https://doi.org/10.1038/cddis.2013.283

Bindra, R. S., & Glazer, P. M. (2005). Genetic instability and the tumor microenvironment: towards the concept of microenvironment-induced mutagenesis. *Mutation Research*, *569*(1–2), 75–85. https://doi.org/10.1016/J.MRFMMM.2004.03.013

BLAST: Basic Local Alignment Search Tool. (n.d.). Retrieved May 19, 2022, from https://blast.ncbi.nlm.nih.gov/Blast.cgi

Bonadonna, G., Brusamolino, E., Valagussa, P., Rossi, A., Brugnatelli, L., Brambilla, C., de Lena, M., Tancini, G., Bajetta, E., Musumeci, R., & Veronesi, U. (2009). Combination Chemotherapy as an Adjuvant Treatment in Operable Breast Cancer. *Http://Dx.Doi.Org/10.1056/NEJM197602192940801*, *294*(8), 405–410. https://doi.org/10.1056/NEJM197602192940801

Bozic, I., Antal, T., Ohtsuki, H., Carter, H., Kim, D., Chen, S., Karchin, R., Kinzler, K. W., Vogelstein, B., & Nowak, M. A. (2010). Accumulation of driver and passenger mutations during tumor progression. *Proceedings of the National Academy of Sciences of the United States of America*, *107*(43), 18545–18550. https://doi.org/10.1073/PNAS.1010978107/SUPPL_FILE/APPENDIX.PDF

Bradl, M., & Lassmann, H. (2010). Oligodendrocytes: biology and pathology. *Acta Neuropathologica*, *119*(1), 37. https://doi.org/10.1007/S00401-009-0601-5

Brat, D. J., Verhaak, R. G., Aldape, K. D., Yung, W. K., Salama, S. R., Cooper, L. A., Rheinbay, E., Miller, C. R., Vitucci, M., Morozova, O., Robertson, A. G., Noushmehr, H., Laird, P. W., Cherniack, A. D., Akbani, R., Huse, J. T., Ciriello, G., Poisson, L. M., Barnholtz-Sloan, J. S., … Zhang, J. (2015). Comprehensive, integrative genomic analysis of diffuse lower-grade gliomas. *N. Engl. J. Med*, *372*, 2481–2498.

Brennan, C. W., Verhaak, R. G., McKenna, A., Campos, B., Noushmehr, H., Salama, S. R., Zheng, S., Chakravarty, D., Sanborn, J. Z., Berman, S. H., Network, T. R., & al., et. (2013). The somatic genomic landscape of glioblastoma. *Cell*, *155*, 462–477.

Brennan, C. W., Verhaak, R. G. W., McKenna, A., Campos, B., Noushmehr, H., Salama, S. R., Zheng, S., Chakravarty, D., Sanborn, J. Z., Berman, S. H., Beroukhim, R., Bernard, B., Wu, C.-J., Genovese, G., Shmulevich, I., Barnholtz-Sloan, J., Zou, L., Vegesna, R., Shukla, S. A., … Chin, L. (2014). The Somatic Genomic Landscape of Glioblastoma. *Cell*, *157*(3), 753. https://doi.org/10.1016/j.cell.2014.04.004

Burt, R., Dey, A., Aref, S., Aguiar, M., Akarca, A., Bailey, K., Day, W., Hooper, S., Kirkwood, A., Kirschner, K., Lee, S. W., Celso, C. lo, Manji, J., Mansour, M. R., Marafioti, T., Mitchell, R. J., Muirhead, R. C., Ng, K. C. Y., Pospori, C., … Fielding, A. K. (2019). Activated stromal cells transfer mitochondria to rescue acute lymphoblastic leukemia cells from oxidative stress. *Blood*, *134*(17), 1415–1429. https://doi.org/10.1182/BLOOD.2019001398

Butowski, N. A. (2015). Epidemiology and diagnosis of brain tumors. *CONTINUUM Lifelong Learning in Neurology*, *21*(2), 301–313. https://doi.org/10.1212/01.CON.0000464171.50638.fa

Cai, X., & Sughrue, M. E. (2018). Glioblastoma: new therapeutic strategies to address cellular and genomic complexity. *Oncotarget*, *9*(10), 9540–9554. https://doi.org/10.18632/oncotarget.23476

Candeias, S. M., & Gaipl, U. S. (2016). The Immune System in Cancer Prevention, Development and Therapy. *Anti-Cancer Agents in Medicinal Chemistry*, *16*(1), 101–107. http://www.ncbi.nlm.nih.gov/pubmed/26299661

Casey, J. R., Grinstein, S., & Orlowski, J. (2010). Sensors and regulators of intracellular pH. *Nature Reviews. Molecular Cell Biology*, *11*(1), 50–61. https://doi.org/10.1038/NRM2820

Ceccarelli, M., Barthel, F. P., Malta, T. M., Sabedot, T. S., Salama, S. R., Murray, B. A., Morozova, O., Newton, Y., Radenbaugh, A., Pagnotta, S. M., Anjum, S., Wang, J., Manyam, G., Zoppoli, P., Ling, S., Rao, A. A., Grifford, M., Cherniack, A. D., Zhang, H., … Verhaak, R. G. W. (2016). Molecular Profiling Reveals Biologically Discrete Subsets and Pathways of Progression in Diffuse Glioma. *Cell*, *164*(3), 550–563. https://doi.org/10.1016/j.cell.2015.12.028

Chakraborty, A. A., Laukka, T., Myllykoski, M., Ringel, A. E., Booker, M. A., Tolstorukov, M. Y., Meng, Y. J., Meier, S. R., Jennings, R. B., Creech, A. L., Herbert, Z. T., McBrayer, S. K., Olenchock, B. A., Jaffe, J. D., Haigis, M. C., Beroukhim, R., Signoretti, S., Koivunen, P., & Kaelin, W. G. (2019). Histone

demethylase KDM6A directly senses oxygen to control chromatin and cell fate. *Science (New York, N.Y.)*, *363*(6432), 1217. https://doi.org/10.1126/SCIENCE.AAW1026

Challagundla, K. B., Wise, P. M., Neviani, P., Chava, H., Murtadha, M., Xu, T., Kennedy, R., Ivan, C., Zhang, X., Vannini, I., Fanini, F., Amadori, D., Calin, G. A., Hadjidaniel, M., Shimada, H., Jong, A., Seeger, R. C., Asgharzadeh, S., Goldkorn, A., & Fabbri, M. (2015). Exosome-Mediated Transfer of microRNAs Within the Tumor Microenvironment and Neuroblastoma Resistance to Chemotherapy. *JNCI Journal of the National Cancer Institute*, *107*(7), 135. https://doi.org/10.1093/JNCI/DJV135

Chan, C. S., Rastelli, L., & Pirrotia, V. (1994). A Polycomb response element in the Ubx gene that determines an epigenetically inherited state of repression. *The EMBO Journal*, *13*(11), 2553–2564. https://doi.org/10.1002/J.1460-2075.1994.TB06545.X

Chen, W., Wang, D., Du, X., He, Y., Chen, S., Shao, Q., Ma, C., Huang, B., Chen, A., Zhao, P., Qu, X., & Li, X. (2015). Glioma cells escaped from cytotoxicity of temozolomide and vincristine by communicating with human astrocytes. *Medical Oncology*, *32*(3). https://doi.org/10.1007/s12032-015-0487-0

Cheng, Y., He, C., Wang, M., Ma, X., Mo, F., Yang, S., Han, J., & Wei, X. (2019). Targeting epigenetic regulators for cancer therapy: mechanisms and advances in clinical trials. *Signal Transduction and Targeted Therapy 2019 4:1*, *4*(1), 1–39. https://doi.org/10.1038/s41392-019-0095-0

Chitambar, C. R., Libnoch, J. A., Matthaeus, W. G., Ash, R. C., Ritch, P. S., & Anderson, T. (1991). Evaluation of continuous infusion low-dose 5-azacytidine in the treatment of myelodysplastic syndromes. *American Journal of Hematology*, *37*(2), 100–104. https://doi.org/10.1002/AJH.2830370207

CHOPCHOP. (n.d.). Retrieved May 19, 2022, from https://chopchop.cbu.uib.no/

Clarke, J., Penas, C., Pastori, C., Komotar, R. J., Bregy, A., Shah, A. H., Wahlestedt, C., & Ayad, N. G. (2013). Epigenetic pathways and glioblastoma treatment. *Https://Doi.Org/10.4161/Epi.25440*, *8*(8), 785–795. https://doi.org/10.4161/EPI.25440

Cloud-based platform for biotech R&D | Benchling. (n.d.). Retrieved May 19, 2022, from https://www.benchling.com/

Condorelli, D. F., Albani, P. D., Conticello, S. G., Bernesi, V., Nicoletti, V. G., Caruso, A., Vacanti, M., Albanese, V., Vellis, J. de, & Giuffrid, A. M. S. (1997). A Neural-Specific Hypomethylated Domain in the 5' Flanking Region of the Glial Fibrillary Acidic Protein Gene. *Developmental Neuroscience*, *19*(5), 446–456. https://doi.org/10.1159/000111242

Condorelli, D. F., Nicoletti, V. G., Barresi, V., Caruso, A., Conticello, S., de Vellis, J., & Stella, A. M. G. (1994). Tissue-specific DNA methylation patterns of the rat glial fibrillary acidic protein gene. *Journal of Neuroscience Research*, *39*(6), 694–707. https://doi.org/10.1002/JNR.490390610

Constantinides, P. G., Taylor, S. M., & Jones, P. A. (1978). Phenotypic conversion of cultured mouse embryo cells by aza pyrimidine nucleosides. *Developmental Biology*, *66*(1), 57–71. https://doi.org/10.1016/0012-1606(78)90273-7

Cytoplasmic bridges, intercellular junctions, and individualization of germ cells during spermatogenesis in Dermatobia hominis (Diptera: Cuterebridae). (n.d.). Retrieved May 18, 2022, from https://onlinelibrary.wiley.com/doi/epdf/10.1002/%28SICI%291097-4687%28199602%29227%3A2%3C145%3A%3AAID-JMOR2%3E3.0.CO%3B2-8

Das, S., & Marsden, P. A. (2013). Angiogenesis in Glioblastoma. *New England Journal of Medicine*, *369*(16), 1561–1563. https://doi.org/10.1056/NEJMcibr1309402

Davis, D. M., & Sowinski, S. (2008). Membrane nanotubes: dynamic long-distance connections between animal cells. *Nature Reviews Molecular Cell Biology 2008 9:6*, *9*(6), 431–436. https://doi.org/10.1038/nrm2399

Dawson, M. A., & Kouzarides, T. (2012). Cancer epigenetics: From mechanism to therapy. In *Cell* (Vol. 150, Issue 1, pp. 12–27). Cell Press. https://doi.org/10.1016/j.cell.2012.06.013

Desir, S., Dickson, E. L., Vogel, R. I., Thayanithy, V., Wong, P., Teoh, D., Geller, M. A., Steer, C. J., Subramanian, S., & Lou, E. (2016). Tunneling nanotube formation is stimulated by hypoxia in ovarian cancer cells. *Oncotarget*, *7*(28), 43150–43161. https://doi.org/10.18632/ONCOTARGET.9504

Desir, S., O'Hare, P., Vogel, R. I., Sperduto, W., Sarkari, A., Dickson, E. L., Wong, P., Nelson, A. C., Fong, Y., Steer, C. J., Subramanian, S., & Lou, E. (2018). Chemotherapy-Induced Tunneling Nanotubes Mediate Intercellular Drug Efflux in

Pancreatic Cancer. *Scientific Reports*, *8*(1). https://doi.org/10.1038/S41598-018-27649-X

DeVita, V. T., & Chu, E. (2008). A History of Cancer Chemotherapy. *Cancer Research*, *68*(21), 8643–8653. https://doi.org/10.1158/0008-5472.CAN-07-6611

Djuric, U., Brian Lam, K. H., Kao, J., Batruch, I., Jevtic, S., Papaioannou, M. D., & Diamandis, P. (2019). Defining protein pattern differences among molecular subtypes of diffuse gliomas using mass spectrometry. *Molecular and Cellular Proteomics*, *18*(10), 2029–2043. https://doi.org/10.1074/MCP.RA119.001521/ATTACHMENT/F4CE375A-1737-4D3F-857B-DD8D08C318C0/MMC1.ZIP

Dong, Z., & Cui, H. (2019). Epigenetic modulation of metabolism in glioblastoma. *Seminars in Cancer Biology*, *57*, 45–51. https://doi.org/10.1016/J.SEMCANCER.2018.09.002

Dupont, C., Armant, D. R., & Brenner, C. A. (2009). Epigenetics: Definition, mechanisms and clinical perspective. *Seminars in Reproductive Medicine*, *27*(5), 351–357. https://doi.org/10.1055/S-0029-1237423/ID/46

Eberhart, C. G., & Bar, E. E. (2020). Spatial enrichment of cellular states in glioblastoma. *Acta Neuropathologica 2020 140:1*, *140*(1), 85–87. https://doi.org/10.1007/S00401-020-02165-3

Ellis, L., Atadja, P. W., & Johnstone, R. W. (2009). Epigenetics in cancer: Targeting chromatin modifications. In *Molecular Cancer Therapeutics* (Vol. 8, Issue 6, pp. 1409–1420). American Association for Cancer Research. https://doi.org/10.1158/1535-7163.MCT-08-0860

Ene, C. I., Edwards, L., Riddick, G., Baysan, M., Woolard, K., Kotliarova, S., Lai, C., Belova, G., Cam, M., Walling, J., Zhou, M., Stevenson, H., Kim, H. S., Killian, K., Veenstra, T., Bailey, R., Song, H., Zhang, W., & Fine, H. A. (2012). Histone Demethylase Jumonji D3 (JMJD3) as a Tumor Suppressor by Regulating p53 Protein Nuclear Stabilization. *PLOS ONE*, *7*(12), e51407. https://doi.org/10.1371/JOURNAL.PONE.0051407

EPD The Eukaryotic Promoter Database. (n.d.). Retrieved May 19, 2022, from https://epd.epfl.ch//index.php

Falkenberg, K. J., & Johnstone, R. W. (2014). Histone deacetylases and their inhibitors in cancer, neurological diseases and immune disorders. *Nature Reviews. Drug Discovery*, *13*(9), 673–691. https://doi.org/10.1038/NRD4360

Fan, G., Beard, C., Chen, R. Z., Csankovszki, G., Sun, Y., Siniaia, M., Biniszkiewicz, D., Bates, B., Lee, P. P., Kühn, R., Trumpp, A., Poon, C. S., Wilson, C. B., & Jaenisch, R. (2001). DNA Hypomethylation Perturbs the Function and Survival of CNS Neurons in Postnatal Animals. *Journal of Neuroscience*, *21*(3), 788–797. https://doi.org/10.1523/JNEUROSCI.21-03-00788.2001

Farber, S., Diamond, L. K., Mercer, R. D., Sylvester, R. F. Jr., & Wolff, J. A. (2010). Temporary Remissions in Acute Leukemia in Children Produced by Folic Acid Antagonist, 4-Aminopteroyl-Glutamic Acid (Aminopterin). *Http://Dx.Doi.Org/10.1056/NEJM194806032382301*, *238*(23), 787–793. https://doi.org/10.1056/NEJM194806032382301

Fenn, J. E., & Udelsman, R. (2011). First use of intravenous chemotherapy cancer treatment: Rectifying the record. *Journal of the American College of Surgeons*, *212*(3), 413–417. https://doi.org/10.1016/J.JAMCOLLSURG.2010.10.018

Fiacco, T. A., Agulhon, C., & McCarthy, K. D. (2009). Sorting Out Astrocyte Physiology from Pharmacology. *Http://Dx.Doi.Org/10.1146/Annurev.Pharmtox.011008.145602*, *49*, 151–174. https://doi.org/10.1146/ANNUREV.PHARMTOX.011008.145602

Freeman, M. R., & Rowitch, D. H. (2013). Evolving Concepts of Gliogenesis: A Look Way Back and Ahead to the Next 25 Years. *Neuron*, *80*(3), 613. https://doi.org/10.1016/J.NEURON.2013.10.034

Fritsch, C., Brown, J. L., Kassis, J. A., & Müller, J. (1999). The DNA-binding polycomb group protein pleiohomeotic mediates silencing of a Drosophila homeotic gene. *Development (Cambridge, England)*, *126*(17), 3905–3913. https://doi.org/10.1242/DEV.126.17.3905

Fuertes, M. B., Kacha, A. K., Kline, J., Woo, S. R., Kranz, D. M., Murphy, K. M., & Gajewski, T. F. (2011). Host type I IFN signals are required for antitumor CD8+ T cell responses through CD8α+ dendritic cells. *Journal of Experimental Medicine*, *208*(10), 2005–2016. https://doi.org/10.1084/jem.20101159

Gallicchio, V. S. (1985). Inhibition of dimethyl sulfoxide-induced friend erythroleukemia cell differentiation in vitro by lithium chloride. *Pathobiology*, *53*(5), 287–293. https://doi.org/10.1159/000163324

GAP JUNCTIONS MEDIATING A BYSTANDER EFFECF IN VIVO lular coupling. The characteristics of these clones have been described previ ously (30). Retroviral Vector. A replication-deficient retroviral vector, containing. (n.d.). Retrieved June 10, 2022, from http://aacrjournals.org/cancerres/article-pdf/57/8/1523/2466106/cr0570081523.pdf

Gillette, T. G., & Hill, J. A. (2015a). Readers, writers and erasers: Chromatin as the Whiteboard of Heart Disease. *Circulation Research*, *116*(7), 1245. https://doi.org/10.1161/CIRCRESAHA.116.303630

Gillette, T. G., & Hill, J. A. (2015b). Readers, writers and erasers: Chromatin as the Whiteboard of Heart Disease. *Circulation Research*, *116*(7), 1245. https://doi.org/10.1161/CIRCRESAHA.116.303630

GitHub - cribbslab/deseq2_report: Deseq2 automatic report generation. (n.d.). Retrieved May 20, 2022, from https://github.com/cribbslab/deseq2_report

GitHub - cribbslab/scflow: Single cell pipelines. (n.d.). Retrieved May 20, 2022, from https://github.com/cribbslab/scflow

Gonzalez, H., Hagerling, C., & Werb, Z. (2018). Roles of the immune system in cancer: From tumor initiation to metastatic progression. *Genes and Development*, *32*(19–20), 1267–1284. https://doi.org/10.1101/GAD.314617.118

Goto, K., Numata, M., Komura, J. I., Ono, T., Bestor, T. H., & Kondo, H. (1994). Expression of DNA methyltransferase gene in mature and immature neurons as well as proliferating cells in mice. *Differentiation*, *56*(1–2), 39–44. https://doi.org/10.1046/J.1432-0436.1994.56120039.X

Greshock, J., Nathanson, K., Martin, A. M., Zhang, L., Coukos, G., Weber, B. L., & Zaks, T. Z. (2007). Cancer cell lines as genetic models of their parent histology: analyses based on array comparative genomic hybridization. *Cancer Research*, *67*(8), 3594–3600. https://doi.org/10.1158/0008-5472.CAN-06-3674

Guarino, M., Rubino, B., & Ballabio, G. (2007). The role of epithelial-mesenchymal transition in cancer pathology. *Pathology*, *39*(3), 305–318. https://doi.org/10.1080/00313020701329914

Hambardzumyan, D., & Bergers, G. (2015). Glioblastoma: Defining Tumor Niches. *Trends in Cancer*, *1*(4), 252–265. https://doi.org/10.1016/J.TRECAN.2015.10.009

Hanahan, D. (2022). Hallmarks of Cancer: New Dimensions. *Cancer Discovery*, *12*(1), 31–46. https://doi.org/10.1158/2159-8290.CD-21-1059

Hanahan, D., & Weinberg, R. A. (2011). Hallmarks of cancer: The next generation. *Cell*, *144*(5), 646–674. https://doi.org/10.1016/j.cell.2011.02.013

Hancock, R. L., Dunne, K., Walport, L. J., Flashman, E., & Kawamura, A. (2015). Epigenetic regulation by histone demethylases in hypoxia. *Epigenomics*, *7*(5), 791–811. https://doi.org/10.2217/EPI.15.24/ASSET/IMAGES/LARGE/FIGURE4.JPEG

Handy, D. E., Castro, R., & Loscalzo, J. (2011). Epigenetic Modifications: Basic Mechanisms and Role in Cardiovascular Disease. *Circulation*, *123*(19), 2145. https://doi.org/10.1161/CIRCULATIONAHA.110.956839

Heddleston, J. M., Wu, Q., Rivera, M., Minhas, S., Lathia, J. D., Sloan, A. E., Iliopoulos, O., Hjelmeland, A. B., & Rich, J. N. (2011). Hypoxia-induced mixed-lineage leukemia 1 regulates glioma stem cell tumorigenic potential. *Cell Death & Differentiation 2012 19:3*, *19*(3), 428–439. https://doi.org/10.1038/cdd.2011.109

Heiden, M. G. V., Cantley, L. C., & Thompson, C. B. (2009). Understanding the Warburg Effect: The Metabolic Requirements of Cell Proliferation. *Science*, *324*(5930), 1029–1033. https://doi.org/10.1126/SCIENCE.1160809

Herbet, G., & Duffau, H. (2020). Revisiting the functional anatomy of the human brain: Toward a meta-networking theory of cerebral functions. *Physiological Reviews*, *100*(3), 1181–1228. https://doi.org/10.1152/PHYSREV.00033.2019/ASSET/IMAGES/LARGE/Z9J003 2029460009.JPEG

Housman, G., Byler, S., Heerboth, S., Lapinska, K., Longacre, M., Snyder, N., & Sarkar, S. (2014). Drug resistance in cancer: an overview. *Cancers*, *6*(3), 1769–1792. https://doi.org/10.3390/CANCERS6031769

Hoverman, J. R. (2021). 25 Years of Cancer Chemotherapy Pathways: A Brief History with a Look to the Future. *Health*, *13*(03), 205–216. https://doi.org/10.4236/HEALTH.2021.133018

Hu, J., Sun, T., Wang, H., Chen, Z., Wang, S., Yuan, L., Liu, T., Li, H. R., Wang, P., Feng, Y., Wang, Q., McLendon, R. E., Friedman, A. H., Keir, S. T., Bigner, D. D., Rathmell, J., Fu, X. dong, Li, Q. J., Wang, H., & Wang, X. F. (2016). MiR-215 Is

Induced Post-transcriptionally via HIF-Drosha Complex and Mediates Glioma-Initiating Cell Adaptation to Hypoxia by Targeting KDM1B. *Cancer Cell*, *29*(1), 49–60. https://doi.org/10.1016/J.CCELL.2015.12.005

Hudson, A. L., Parker, N. R., Khong, P., Parkinson, J. F., Dwight, T., Ikin, R. J., Zhu, Y., Chen, J., Wheeler, H. R., & Howell, V. M. (2018). Glioblastoma recurrence correlates with increased APE1 and polarization toward an immuno-suppressive microenvironment. *Frontiers in Oncology*, *8*(AUG). https://doi.org/10.3389/fonc.2018.00314

Hulkower, K. I., & Herber, R. L. (2011). Cell migration and invasion assays as tools for drug discovery. *Pharmaceutics*, *3*(1), 107–124. https://doi.org/10.3390/PHARMACEUTICS3010107

Immonen, A., Vapalahti, M., Tyynelä, K., Hurskainen, H., Sandmair, A., Vanninen, R., Langford, G., Murray, N., & Ylä-Herttuala, S. (2004). AdvHSV-tk gene therapy with intravenous ganciclovir improves survival in human malignant glioma: a randomised, controlled study. *Molecular Therapy*, *10*(5), 967–972. https://doi.org/10.1016/J.YMTHE.2004.08.002

Iwadate, Y. (2016). Epithelial-mesenchymal transition in glioblastoma progression. In *Oncology Letters*. https://doi.org/10.3892/ol.2016.4113

Jiang, H., White, E. J., Conrad, C., Gomez-Manzano, C., & Fueyo, J. (2009). Chapter 13 Autophagy Pathways in Glioblastoma. In *Methods in Enzymology* (1st ed., Vol. 453, Issue C). Elsevier Inc. https://doi.org/10.1016/S0076-6879(08)04013-5

Jiang, H., Yu, K., Li, M., Cui, Y., Ren, X., Yang, C., Zhao, X., & Lin, S. (2020). Classification of Progression Patterns in Glioblastoma: Analysis of Predictive Factors and Clinical Implications. *Frontiers in Oncology*, *10*, 2408. https://doi.org/10.3389/FONC.2020.590648/BIBTEX

Johansen, M. D., Rochat, P., Law, I., Scheie, D., Poulsen, H. S., & Muhic, A. (2016). Presentation of Two Cases with Early Extracranial Metastases from Glioblastoma and Review of the Literature. *Case Reports in Oncological Medicine*, *2016*. https://doi.org/10.1155/2016/8190950

Jones, P. A., & Taylor, S. M. (1980). Cellular differentiation, cytidine analogs and DNA methylation. *Cell*, *20*(1), 85–93. https://doi.org/10.1016/0092-8674(80)90237-8

Jones, S., Wang, T. L., Shih, I. M., Mao, T. L., Nakayama, K., Roden, R., Glas, R., Slamon, D., Diaz, L. A., Vogelstein, B., Kinzler, K. W., Velculescu, V. E., &

Papadopoulos, N. (2010). Frequent mutations of chromatin remodeling gene ARID1A in ovarian clear cell carcinoma. *Science (New York, N.Y.)*, *330*(6001), 228–231. https://doi.org/10.1126/SCIENCE.1196333

Juergens, R. A., Wrangle, J., Vendetti, F. P., Murphy, S. C., Zhao, M., Coleman, B., Sebree, R., Rodgers, K., Hooker, C. M., Franco, N., Lee, B., Tsai, S., Delgado, I. E., Rudek, M. A., Belinsky, S. A., Herman, J. G., Baylin, S. B., Brock, M. v., & Rudin, C. M. (2011). Combination epigenetic therapy has efficacy in patients with refractory advanced non-small cell lung cancer. *Cancer Discovery*, *1*(7), 598–607. https://doi.org/10.1158/2159-8290.CD-11-0214

Jung, E., Osswald, M., Blaes, J., Wiestler, B., Sahm, F., Schmenger, T., Solecki, G., Deumelandt, K., Kurz, F. T., Xie, R., Weil, S., Heil, O., Thomé, C., Gömmel, M., Syed, M., Häring, P., Huber, P. E., Heiland, S., Platten, M., … Winkler, F. (2017). Tweety-Homolog 1 Drives Brain Colonization of Gliomas. *The Journal of Neuroscience : The Official Journal of the Society for Neuroscience*, *37*(29), 6837–6850. https://doi.org/10.1523/JNEUROSCI.3532-16.2017

Kaitin, K. I. (2010). Deconstructing the Drug Development Process: The New Face of Innovation. *Clinical Pharmacology and Therapeutics*, *87*(3), 356. https://doi.org/10.1038/CLPT.2009.293

Keep, R. F., Zhou, N., Xiang, J., Andjelkovic, A. v., Hua, Y., & Xi, G. (2014). Vascular disruption and blood-brain barrier dysfunction in intracerebral hemorrhage. *Fluids and Barriers of the CNS*, *11*(1), 1–13. https://doi.org/10.1186/2045-8118-11-18

Khakh, B. S., & Deneen, B. (2019). The Emerging Nature of Astrocyte Diversity. *Annual Review of Neuroscience*, *42*, 187–207. https://doi.org/10.1146/ANNUREV-NEURO-070918-050443

Kitajima, S., Sun, W., Lee, K. L., Ho, J. C., Oyadomari, S., Okamoto, T., Masai, H., Poellinger, L., & Kato, H. (2021). A KDM6 inhibitor potently induces ATF4 and its target gene expression through HRI activation and by UTX inhibition. *Scientific Reports 2021 11:1*, *11*(1), 1–14. https://doi.org/10.1038/s41598-021-83857-y

Kitange, G. J., Mladek, A. C., Carlson, B. L., Schroeder, M. A., Pokorny, J. L., Cen, L., Decker, P. A., Wu, W., Lomberk, G. A., Gupta, S. K., Urrutia, R. A., & Sarkaria, J. N. (2012). Inhibition of histone deacetylation potentiates the evolution of acquired temozolomide resistance linked to MGMT upregulation in glioblastoma xenografts. *Clinical Cancer Research*, *18*(15), 4070–4079. https://doi.org/10.1158/1078-

0432.CCR-12-0560/286351/AM/INHIBITION-OF-HISTONE-DEACETYLATION-POTENTIATES

Kooistra, S. M., & Helin, K. (2012). Molecular mechanisms and potential functions of histone demethylases. *Nature Reviews Molecular Cell Biology 2012 13:5*, *13*(5), 297–311. https://doi.org/10.1038/nrm3327

Kozono, D., Li, J., Nitta, M., Sampetrean, O., Gonda, D., Kushwaha, D. S., Merzon, D., Ramakrishnan, V., Zhu, S., Zhu, K., Matsui, H., Harismendy, O., Hua, W., Mao, Y., Kwon, C. H., Saya, H., Nakano, I., Pizzo, D. P., van den Berg, S. R., & Chen, C. C. (2015). Dynamic epigenetic regulation of glioblastoma tumorigenicity through LSD1 modulation of MYC expression. *Proceedings of the National Academy of Sciences of the United States of America*, *112*(30), E4055–E4064. https://doi.org/10.1073/PNAS.1501967112

Kuo, A. J., Cheung, P., Chen, K., Zee, B. M., Kioi, M., Lauring, J., Xi, Y., Park, B. H., Shi, X., Garcia, B. A., Li, W., & Gozani, O. (2011). NSD2 links dimethylation of histone H3 at lysine 36 to oncogenic programming. *Molecular Cell*, *44*(4), 609–620. https://doi.org/10.1016/J.MOLCEL.2011.08.042

Ladd-Acosta, C., Pevsner, J., Sabunciyan, S., Yolken, R. H., Webster, M. J., Dinkins, T., Callinan, P. A., Fan, J. B., Potash, J. B., & Feinberg, A. P. (2007). DNA Methylation Signatures within the Human Brain. *The American Journal of Human Genetics*, *81*(6), 1304–1315. https://doi.org/10.1086/524110

Lam, K. H. B., Valkanas, K., Djuric, U., & Diamandis, P. (2020). Unifying models of glioblastoma's intratumoral heterogeneity. *Neuro-Oncology Advances*, *2*(1), 1–3. https://doi.org/10.1093/NOAJNL/VDAA096

Lapointe, S., Perry, A., & Butowski, N. A. (2018). Primary brain tumours in adults. *The Lancet*, *392*(10145), 432–446. https://doi.org/10.1016/S0140-6736(18)30990-5

Lathia, J., Watson, D., Williford, S., Lauko, A., Zhou, Y., Seder, J., Mears, J., Cheng, F., & Hjelmeland, A. (2021). *Astrocytes donate mitochondria to increase glioblastoma tumorigenicity*. https://doi.org/10.21203/rs.3.rs-923533/v1

Lee, E. Q., Reardon, D. A., Schiff, D., Drappatz, J., Muzikansky, A., Grimm, S. A., Norden, A. D., Nayak, L., Beroukhim, R., Rinne, M. L., Chi, A. S., Batchelor, T. T., Hempfling, K., McCluskey, C., Smith, K. H., Gaffey, S. C., Wrigley, B., Ligon, K. L., Raizer, J. J., & Wen, P. Y. (2015). Phase II study of panobinostat in combination

with bevacizumab for recurrent glioblastoma and anaplastic glioma. *Neuro-Oncology*, *17*(6), 862–867. https://doi.org/10.1093/NEUONC/NOU350

Lee, J. H., Lee, J. E., Kahng, J. Y., Kim, S. H., Park, J. S., Yoon, S. J., Um, J. Y., Kim, W. K., Lee, J. K., Park, J., Kim, E. H., Lee, J. H., Lee, J. H., Chung, W. S., Ju, Y. S., Park, S. H., Chang, J. H., Kang, S. G., & Lee, J. H. (2018a). Human glioblastoma arises from subventricular zone cells with low-level driver mutations. *Nature*, *560*(7717), 243–247. https://doi.org/10.1038/s41586-018-0389-3

Lee, J. H., Lee, J. E., Kahng, J. Y., Kim, S. H., Park, J. S., Yoon, S. J., Um, J. Y., Kim, W. K., Lee, J. K., Park, J., Kim, E. H., Lee, J. H., Lee, J. H., Chung, W. S., Ju, Y. S., Park, S. H., Chang, J. H., Kang, S. G., & Lee, J. H. (2018b). Human glioblastoma arises from subventricular zone cells with low-level driver mutations. *Nature 2018 560:7717*, *560*(7717), 243–247. https://doi.org/10.1038/s41586-018-0389-3

Lee, S. Y. (2016). Temozolomide resistance in glioblastoma multiforme. *Genes & Diseases*, *3*(3), 198–210. https://doi.org/10.1016/j.gendis.2016.04.007

Lefranc, F., & Kiss, R. (2006). Autophagy, the Trojan horse to combat glioblastomas. *Neurosurgical Focus*, *20*(4), 1–6. https://doi.org/10.3171/foc.2006.20.4.4

Lein, E. S., Hawrylycz, M. J., Ao, N., Ayres, M., Bensinger, A., Bernard, A., Boe, A. F., Boguski, M. S., Brockway, K. S., Byrnes, E. J., Chen, L., Chen, L., Chen, T. M., Chin, M. C., Chong, J., Crook, B. E., Czaplinska, A., Dang, C. N., Datta, S., … Jones, A. R. (2006). Genome-wide atlas of gene expression in the adult mouse brain. *Nature 2006 445:7124*, *445*(7124), 168–176. https://doi.org/10.1038/nature05453

Leithe, E., Sirnes, S., Omori, Y., & Rivedal, E. (2006). Downregulation of Gap Junctions in Cancer Cells. *Critical Reviews™ in Oncogenesis*, *12*(3–4), 225–256. https://doi.org/10.1615/CRITREVONCOG.V12.I3-4.30

Lewis, C. A., Brault, C., Peck, B., Bensaad, K., Griffiths, B., Mitter, R., Chakravarty, P., East, P., Dankworth, B., Alibhai, D., Harris, A. L., & Schulze, A. (2015). SREBP maintains lipid biosynthesis and viability of cancer cells under lipid- and oxygen-deprived conditions and defines a gene signature associated with poor survival in glioblastoma multiforme. *Oncogene 2015 34:40*, *34*(40), 5128–5140. https://doi.org/10.1038/onc.2014.439

Li, G., Qin, Z., Chen, Z., Xie, L., Wang, R., & Zhao, H. (2017). Tumor microenvironment in treatment of glioma. *Open Medicine (Poland)*, *12*(1), 247–251. https://doi.org/10.1515/MED-2017-0035

Liberti, M. v, & Locasale, J. W. (2016). The Warburg Effect: How Does it Benefit Cancer Cells? (vol 41, pg 211, 2016). *Trends in Biochemical Sciences*, *41*(3, SI), 287. https://doi.org/10.1016/j.tibs.2016.01.004

Lochmann, T. L., Powell, K. M., Ham, J., Floros, K. v., Heisey, D. A. R., Kurupi, R. I. J., Calbert, M. L., Ghotra, M. S., Greninger, P., Dozmorov, M., Gowda, M., Souers, A. J., Patrick Reynolds, C., Benes, C. H., & Faber, A. C. (2018). Targeted inhibition of histone H3K27 demethylation is effective in high-risk neuroblastoma. *Science Translational Medicine*, *10*(441). https://doi.org/10.1126/SCITRANSLMED.AAO4680/SUPPL_FILE/AAO4680_TABLES_S1_TO_S9.ZIP

Louis, D. N., Ohgaki, H., Wiestler, O. D., Cavenee, W. K., Ellison, D. W., Figarella-Branger, D., Perry, A., Reifenberger, G., & Deimling, A. von. (2016). *WHO Classification of Tumours of the Central Nervous System, Revised. Fourth Edition* (D. N. Louis, Ed.; 4th rev, e). IARC. https://apps.who.int/bookorders/anglais/detart1.jsp?codlan=1&codcol=70&codcch=24001

Lucas, A. T., Price, L. S., Schorzman, A., & Zamboni, W. C. (2017). Complex effects of tumor microenvironment on the tumor disposition of carrier-mediated agents. *Nanomedicine*, *12*(16), 2021. https://doi.org/10.2217/NNM-2017-0101

Lv, D., Jia, F., Hou, Y., Sang, Y., Alvarez, A. A., Zhang, W., Gao, W. Q., Hu, B., Cheng, S. Y., Ge, J., Li, Y., & Feng, H. (2017). Histone acetyltransferase KAT6A upregulates PI3K/AKT signaling through TRIM24 binding. *Cancer Research*, *77*(22), 6190–6201. https://doi.org/10.1158/0008-5472.CAN-17-1388/652946/AM/HISTONE-ACETYLTRANSFERASE-KAT6A-UPREGULATES-PI3K

Mallick, S., Benson, R., Hakim, A., & Rath, G. K. (2016). Management of glioblastoma after recurrence: A changing paradigm. *Journal of the Egyptian National Cancer Institute*, *28*(4), 199–210. https://doi.org/10.1016/j.jnci.2016.07.001

Mariño-Ramírez, L., Kann, M. G., Shoemaker, B. A., & Landsman, D. (2005). Histone structure and nucleosome stability. *Expert Review of Proteomics*, *2*(5), 719. https://doi.org/10.1586/14789450.2.5.719

Marmorstein, R., & Zhou, M. M. (2014). Writers and Readers of Histone Acetylation: Structure, Mechanism, and Inhibition. *Cold Spring Harbor Perspectives in Biology*, *6*(7). https://doi.org/10.1101/CSHPERSPECT.A018762

Marti Gutierrez, N., Mikhalchenko, A., Ma, H., Koski, A., Li, Y., van Dyken, C., Tippner-Hedges, R., Yoon, D., Liang, D., Hayama, T., Battaglia, D., Kang, E., Lee, Y., Barnes, A. P., Amato, P., & Mitalipov, S. (2022). Horizontal mtDNA transfer between cells is common during mouse development. *IScience*, *25*(3), 103901. https://doi.org/10.1016/J.ISCI.2022.103901

Martínez-Jiménez, F., Muiños, F., Sentís, I., Deu-Pons, J., Reyes-Salazar, I., Arnedo-Pac, C., Mularoni, L., Pich, O., Bonet, J., Kranas, H., Gonzalez-Perez, A., & Lopez-Bigas, N. (2020). A compendium of mutational cancer driver genes. *Nature Reviews Cancer 2020 20:10*, *20*(10), 555–572. https://doi.org/10.1038/s41568-020-0290-x

Masui, K., Tanaka, K., Akhavan, D., Babic, I., Gini, B., Matsutani, T., Iwanami, A., Liu, F., Villa, G. R., Gu, Y., Campos, C., Zhu, S., Yang, H., Yong, W. H., Cloughesy, T. F., Mellinghoff, I. K., Cavenee, W. K., Shaw, R. J., & Mischel, P. S. (2013). mTOR Complex 2 Controls Glycolytic Metabolism in Glioblastoma through FoxO Acetylation and Upregulation of c-Myc. *Cell Metabolism*, *18*(5), 726–739. https://doi.org/10.1016/J.CMET.2013.09.013

McClelland, S. E., Burrell, R. A., & Swanton, C. (2009). Chromosomal instability: A composite phenotype that influences sensitivity to chemotherapy. *Https://Doi.Org/10.4161/Cc.8.20.9690*, *8*(20), 3262–3266. https://doi.org/10.4161/CC.8.20.9690

McLendon, R., Friedman, A., Bigner, D., van Meir, E. G., Brat, D. J., Mastrogianakis, G. M., Olson, J. J., Mikkelsen, T., Lehman, N., Aldape, K., Yung, W. K. A., Bogler, O., Weinstein, J. N., VandenBerg, S., Berger, M., Prados, M., Muzny, D., Morgan, M., Scherer, S., … Thomson, E. (2008). Comprehensive genomic characterization defines human glioblastoma genes and core pathways. *Nature*, *455*(7216), 1061–1068. https://doi.org/10.1038/nature07385

Messaoudi, K., Clavreul, A., & Lagarce, F. (2015). Toward an effective strategy in glioblastoma treatment. Part I: resistance mechanisms and strategies to overcome resistance of glioblastoma to temozolomide. In *Drug Discovery Today* (Vol. 20, Issue 7, pp. 899–905). Elsevier Ltd. https://doi.org/10.1016/j.drudis.2015.02.011

Miller, K. D., Ostrom, Q. T., Kruchko, C., Patil, N., Tihan, T., Cioffi, G., Fuchs, H. E., Waite, K. A., Jemal, A., Siegel, R. L., & Barnholtz-Sloan, J. S. (2021). Brain and other central nervous system tumor statistics, 2021. *CA: A Cancer Journal for Clinicians*, *71*(5), 381–406. https://doi.org/10.3322/CAAC.21693

Ming, J., Zhou, Y., Du, J., Fan, S., Pan, B., Wang, Y., Fan, L., & Jiang, J. (2015). miR-381 suppresses C/EBPα-dependent Cx43 expression in breast cancer cells. *Bioscience Reports*, *35*(6). https://doi.org/10.1042/BSR20150167

Mottamal, M., Zheng, S., Huang, T. L., & Wang, G. (2015). Histone deacetylase inhibitors in clinical studies as templates for new anticancer agents. *Molecules (Basel, Switzerland)*, *20*(3), 3898–3941. https://doi.org/10.3390/MOLECULES20033898

Neftel, C., Laffy, J., Filbin, M. G., Hara, T., Shore, M. E., Rahme, G. J., Richman, A. R., Silverbush, D., Shaw, M. L., Hebert, C. M., Dewitt, J., Gritsch, S., Perez, E. M., Gonzalez Castro, L. N., Lan, X., Druck, N., Rodman, C., Dionne, D., Kaplan, A., … Suvà, M. L. (2019). An Integrative Model of Cellular States, Plasticity, and Genetics for Glioblastoma. *Cell*, *178*(4), 835-849.e21. https://doi.org/10.1016/J.CELL.2019.06.024/ATTACHMENT/34FD6C93-F554-4A25-B967-E04B31F20647/MMC4.XLSX

Nelson, & Cox. (2011). Principles of Biochemistry Lehninger. *Chinese Journal of Integrative Medicine*, *17*(8), 631–634.

Nguyen, S., Meletis, K., Fu, D., Jhaveri, S., & Jaenisch, R. (2007). Ablation of de novo DNA methyltransferase Dnmt3a in the nervous system leads to neuromuscular defects and shortened lifespan. *Developmental Dynamics*, *236*(6), 1663–1676. https://doi.org/10.1002/DVDY.21176

Nikoloski, G., Langemeijer, S. M. C., Kuiper, R. P., Knops, R., Massop, M., Tönnissen, E. R. L. T. M., van der Heijden, A., Scheele, T. N., Vandenberghe, P., de Witte, T., van der Reijden, B. A., & Jansen, J. H. (2010). Somatic mutations of the histone methyltransferase gene EZH2 in myelodysplastic syndromes. *Nature Genetics*, *42*(8), 665–667. https://doi.org/10.1038/NG.620

Osswald, M., Jung, E., Sahm, F., Solecki, G., Venkataramani, V., Blaes, J., Weil, S., Horstmann, H., Wiestler, B., Syed, M., Huang, L., Ratliff, M., Karimian Jazi, K., Kurz, F. T., Schmenger, T., Lemke, D., Gömmel, M., Pauli, M., Liao, Y., …

Winkler, F. (2015). Brain tumour cells interconnect to a functional and resistant network. *Nature*, *528*(7580), 93–98. https://doi.org/10.1038/NATURE16071

Pang, B., Zheng, X.-R., Tian, J., Gao, T., Gu, G., Zhang, R., Fu, Y.-B., Pang, Q., Li, X.-G., Liu, Q., Pang, B., Zheng, X.-R., Tian, J., Gao, T., Gu, G., Zhang, R., Fu, Y.-B., Pang, Q., Li, X.-G., & Liu, Q. (2016). EZH2 promotes metabolic reprogramming in glioblastomas through epigenetic repression of EAF2-HIF1α signaling. *Oncotarget*, *7*(29), 45134–45143. https://doi.org/10.18632/ONCOTARGET.9761

Park, J., Shim, J. K., Kang, J. H., Choi, J., Chang, J. H., Kim, S. Y., & Kang, S. G. (2018). Regulation of bioenergetics through dual inhibition of aldehyde dehydrogenase and mitochondrial complex I suppresses glioblastoma tumorspheres. *Neuro-Oncology*, *20*(7), 954–965. https://doi.org/10.1093/NEUONC/NOX243

Perkins,A. Liu, G. (2016). Primary Brain Tumors in Adults: Diagnosis and Treatment - American Family Physician. *American Family Physician*, *93*(3), 211–218. www.aafp.org/afp

Perrin, S. L., Samuel, M. S., Koszyca, B., Brown, M. P., Ebert, L. M., Oksdath, M., & Gomez, G. A. (2019). Glioblastoma heterogeneity and the tumour microenvironment: Implications for preclinical research and development of new treatments. *Biochemical Society Transactions*, *47*(2), 625–638. https://doi.org/10.1042/BST20180444

Píškala, A., & Šorm, F. (1964). Nucleic acids components and their analogues. LI. Synthesis of 1-glycosyl derivatives of 5-azauracil and 5-azacytosine. *Collection of Czechoslovak Chemical Communications*, *29*(9), 2060–2076. https://doi.org/10.1135/CCCC19642060

Poteet, E., Choudhury, G. R., Winters, A., Li, W., Ryou, M. G., Liu, R., Tang, L., Ghorpade, A., Wen, Y., Yuan, F., Keir, S. T., Yan, H., Bigner, D. D., Simpkins, J. W., & Yang, S. H. (2013). Reversing the Warburg Effect as a Treatment for Glioblastoma. *Journal of Biological Chemistry*, *288*(13), 9153–9164. https://doi.org/10.1074/JBC.M112.440354

Pouget, J. P., & Mather, S. J. (2001). General aspects of the cellular response to low- and high-LET radiation. *European Journal of Nuclear Medicine*, *28*(4), 541–561. https://doi.org/10.1007/S002590100484

Puchalski, R. B., Shah, N., Miller, J., Dalley, R., Nomura, S. R., Yoon, J. G., Smith, K. A., Lankerovich, M., Bertagnolli, D., Bickley, K., Boe, A. F., Brouner, K., Butler,

S., Caldejon, S., Chapin, M., Datta, S., Dee, N., Desta, T., Dolbeare, T., … Foltz, G. D. (2018). An anatomic transcriptional atlas of human glioblastoma. *Science*, *360*(6389), 660–663. https://doi.org/10.1126/SCIENCE.AAF2666/SUPPL_FILE/AAF2666_TABLE-S9.XLSX

Pustchi, S. E., Avci, N. G., Akay, Y. M., & Akay, M. (2020). Astrocytes Decreased the Sensitivity of Glioblastoma Cells to Temozolomide and Bay 11-7082. *International Journal of Molecular Sciences*, *21*(19), 1–18. https://doi.org/10.3390/IJMS21197154

Qin, Y., Jiang, X., Yang, Q., Zhao, J., Zhou, Q., & Zhou, Y. (2021). The Functions, Methods, and Mobility of Mitochondrial Transfer Between Cells. *Frontiers in Oncology*, *11*, 1630. https://doi.org/10.3389/FONC.2021.672781/BIBTEX

Rice, J. C., Briggs, S. D., Ueberheide, B., Barber, C. M., Shabanowitz, J., Hunt, D. F., Shinkai, Y., & Allis, C. D. (2003). Histone Methyltransferases Direct Different Degrees of Methylation to Define Distinct Chromatin Domains. *Molecular Cell*, *12*(6), 1591–1598. https://doi.org/10.1016/S1097-2765(03)00479-9/ATTACHMENT/84E99CB8-9D8D-45F8-861F-BE8CFA557039/MMC10.JPG

Rodríguez-Paredes, M., & Esteller, M. (2011). Cancer epigenetics reaches mainstream oncology. In *Nature Medicine* (Vol. 17, Issue 3, pp. 330–339). Nature Publishing Group. https://doi.org/10.1038/nm.2305

Romani, M., Pistillo, M. P., & Banelli, B. (2018). Epigenetic targeting of glioblastoma. In *Frontiers in Oncology* (Vol. 8, Issue OCT). Frontiers Media S.A. https://doi.org/10.3389/fonc.2018.00448

Roth, S. Y., Denu, J. M., & Allis, C. D. (2003). Histone Acetyltransferases. *Http://Dx.Doi.Org/10.1146/Annurev.Biochem.70.1.81*, *70*, 81–120. https://doi.org/10.1146/ANNUREV.BIOCHEM.70.1.81

Russler-Germain, D. A., Spencer, D. H., Young, M. A., Lamprecht, T. L., Miller, C. A., Fulton, R., Meyer, M. R., Erdmann-Gilmore, P., Townsend, R. R., Wilson, R. K., & Ley, T. J. (2014). The R882H DNMT3A mutation associated with AML dominantly inhibits wild-type DNMT3A by blocking its ability to form active tetramers. *Cancer Cell*, *25*(4), 442–454. https://doi.org/10.1016/J.CCR.2014.02.010

Saha, T., Dash, C., Jayabalan, R., Khiste, S., Kulkarni, A., Kurmi, K., Mondal, J., Majumder, P. K., Bardia, A., Jang, H. L., & Sengupta, S. (2021). Intercellular

nanotubes mediate mitochondrial trafficking between cancer and immune cells. *Nature Nanotechnology 2021 17:1*, *17*(1), 98–106. https://doi.org/10.1038/s41565-021-01000-4

Salvadori, M., Cesari, N., Murgia, A., Puccini, P., Riccardi, B., & Dominici, M. (2019). Dissecting the Pharmacodynamics and Pharmacokinetics of MSCs to Overcome Limitations in Their Clinical Translation. *Molecular Therapy - Methods & Clinical Development*, *14*, 1–15. https://doi.org/10.1016/J.OMTM.2019.05.004

Sarkar, S., Horn, G., Moulton, K., Oza, A., Byler, S., Kokolus, S., & Longacre, M. (2013). Cancer Development, Progression, and Therapy: An Epigenetic Overview. *International Journal of Molecular Sciences*, *14*(10), 21087. https://doi.org/10.3390/IJMS141021087

Schiffer, D., Annovazzi, L., Casalone, C., Corona, C., & Mellai, M. (2019). Glioblastoma: Microenvironment and niche concept. In *Cancers* (Vol. 11, Issue 1). MDPI AG. https://doi.org/10.3390/cancers11010005

Semenza, G. L. (2003). Targeting HIF-1 for cancer therapy. *Nature Reviews Cancer 2003 3:10*, *3*(10), 721–732. https://doi.org/10.1038/nrc1187

Shalem, O., Sanjana, N. E., Hartenian, E., Shi, X., Scott, D. A., Mikkelsen, T. S., Heckl, D., Ebert, B. L., Root, D. E., Doench, J. G., & Zhang, F. (2014). Genome-Scale CRISPR-Cas9 Knockout Screening in Human Cells. *Science (New York, N.Y.)*, *343*(6166), 84. https://doi.org/10.1126/SCIENCE.1247005

Sharma, M., Astekar, M., Soi, S., Manjunatha, B., Shetty, D., & Radhakrishnan, R. (2015). pH Gradient Reversal: An Emerging Hallmark of Cancers. *Recent Patents on Anti-Cancer Drug Discovery*, *10*(3), 244–258. https://doi.org/10.2174/1574892810666150708110608

Shi, W., Palmer, J. D., Werner-Wasik, M., Andrews, D. W., Evans, J. J., Glass, J., Kim, L., Bar-Ad, V., Judy, K., Farrell, C., Simone, N., Liu, H., Dicker, A. P., & Lawrence, Y. R. (2016). Phase I trial of panobinostat and fractionated stereotactic re-irradiation therapy for recurrent high grade gliomas. *Journal of Neuro-Oncology 2016 127:3*, *127*(3), 535–539. https://doi.org/10.1007/S11060-016-2059-3

Sin, W. C., Crespin, S., & Mesnil, M. (2012). Opposing roles of connexin43 in glioma progression. *Biochimica et Biophysica Acta - Biomembranes*, *1818*(8), 2058–2067. https://doi.org/10.1016/j.bbamem.2011.10.022

Siracusa, R., Fusco, R., & Cuzzocrea, S. (2019). Astrocytes: Role and functions in brain pathologies. *Frontiers in Pharmacology*, *10*(SEP), 1114. https://doi.org/10.3389/FPHAR.2019.01114/BIBTEX

Šorm, F., Píškala, A., Čihák, A., & Veselý, J. (1964). 5-Azacytidine, a new, highly effective cancerostatic. *Experientia*, *20*(4), 202–203. https://doi.org/10.1007/BF02135399

Stegh, A. H., Brennan, C., Mahoney, J. A., Forloney, K. L., Jenq, H. T., Luciano, J. P., Protopopov, A., Chin, L., & DePinho, R. A. (2010). Glioma oncoprotein Bc12L12 inhibits the p53 tumor suppressor. *Genes and Development*, *24*(19), 2194–2204. https://doi.org/10.1101/gad.1924710

Strahl, B. D., & Allis, C. D. (2000). The language of covalent histone modifications. *Nature 2000 403:6765*, *403*(6765), 41–45. https://doi.org/10.1038/47412

Stupp, R., Hegi, M. E., Mason, W. P., van den Bent, M. J., Taphoorn, M. J., Janzer, R. C., Ludwin, S. K., Allgeier, A., Fisher, B., Belanger, K., Hau, P., Brandes, A. A., Gijtenbeek, J., Marosi, C., Vecht, C. J., Mokhtari, K., Wesseling, P., Villa, S., Eisenhauer, E., … Mirimanoff, R. O. (2009). Effects of radiotherapy with concomitant and adjuvant temozolomide versus radiotherapy alone on survival in glioblastoma in a randomised phase III study: 5-year analysis of the EORTC-NCIC trial. *The Lancet Oncology*, *10*(5), 459–466. https://doi.org/10.1016/S1470-2045(09)70025-7

Sui, A., Xu, Y., Li, Y., Hu, Q., Wang, Z., Zhang, H., Yang, J., Guo, X., Zhao, W., Sui, A., Xu, Y., Li, Y., Hu, Q., Wang, Z., Zhang, H., Yang, J., Guo, X., & Zhao, W. (2017). The pharmacological role of histone demethylase JMJD3 inhibitor GSK-J4 on glioma cells. *Oncotarget*, *8*(40), 68591–68598. https://doi.org/10.18632/ONCOTARGET.19793

Suvà, M. L., Rheinbay, E., Gillespie, S. M., Patel, A. P., Wakimoto, H., Rabkin, S. D., Riggi, N., Chi, A. S., Cahill, D. P., Nahed, B. v., Curry, W. T., Martuza, R. L., Rivera, M. N., Rossetti, N., Kasif, S., Beik, S., Kadri, S., Tirosh, I., Wortman, I., … Bernstein, B. E. (2014). Reconstructing and reprogramming the tumor-propagating potential of glioblastoma stem-like cells. *Cell*, *157*(3), 580–594. https://doi.org/10.1016/J.CELL.2014.02.030/ATTACHMENT/F0830830-7A37-48A2-8F56-E0941D0E157E/MMC4.XLSX

Tafani, M., di Vito, M., Frati, A., Pellegrini, L., de Santis, E., Sette, G., Eramo, A., Sale, P., Mari, E., Santoro, A., Raco, A., Salvati, M., de Maria, R., & Russo, M. A. (2011). Pro-inflammatory gene expression in solid glioblastoma microenvironment and in hypoxic stem cells from human glioblastoma. *Journal of Neuroinflammation*, *8*, 1–16. https://doi.org/10.1186/1742-2094-8-32

Takizawa, T., Nakashima, K., Namihira, M., Ochiai, W., Uemura, A., Yanagisawa, M., Fujita, N., Nakao, M., & Taga, T. (2001). DNA Methylation Is a Critical Cell-Intrinsic Determinant of Astrocyte Differentiation in the Fetal Brain. *Developmental Cell*, *1*(6), 749–758. https://doi.org/10.1016/S1534-5807(01)00101-0

Tang, J., He, D., Yang, P., He, J., & Zhang, Y. (2018). Genome-wide expression profiling of glioblastoma using a large combined cohort. *Scientific Reports*, *8*(1). https://doi.org/10.1038/s41598-018-33323-z

Tawa, R., Ono, T., Kurishita, A., Okada, S., & Hirose, S. (1990). Changes of DNA methylation level during pre-and postnatal periods in mice. *Differentiation*, *45*(1), 44–48. https://doi.org/10.1111/J.1432-0436.1990.TB00455.X

Taylor, S., Spugnini, E. P., Assaraf, Y. G., Azzarito, T., Rauch, C., & Fais, S. (2015). Microenvironment acidity as a major determinant of tumor chemoresistance: Proton pump inhibitors (PPIs) as a novel therapeutic approach. *Drug Resistance Updates : Reviews and Commentaries in Antimicrobial and Anticancer Chemotherapy*, *23*, 69–78. https://doi.org/10.1016/J.DRUP.2015.08.004

Thayanithy, V., Dickson, E. L., Steer, C., Subramanian, S., & Lou, E. (2014). Tumor-stromal cross talk: direct cell-to-cell transfer of oncogenic microRNAs via tunneling nanotubes. *Translational Research : The Journal of Laboratory and Clinical Medicine*, *164*(5), 359–365. https://doi.org/10.1016/J.TRSL.2014.05.011

The Development and Causes of Cancer - The Cell - NCBI Bookshelf. (n.d.). Retrieved May 16, 2022, from https://www.ncbi.nlm.nih.gov/books/NBK9963/

Tiedeken, S. D., & Chang, C. (2015). Principles of Epigenetic Treatment. *Epigenetics and Dermatology*, 443–465. https://doi.org/10.1016/B978-0-12-800957-4.00020-5

Tillib, S., Petruk, S., Sedkov, Y., Kuzin, A., Fujioka, M., Goto, T., & Mazo, A. (1999). Trithorax- and Polycomb-group response elements within an Ultrabithorax transcription maintenance unit consist of closely situated but separable sequences. *Molecular and Cellular Biology*, *19*(7), 5189–5202. https://doi.org/10.1128/MCB.19.7.5189

Torralba, D., Baixauli, F., & Sánchez-Madrid, F. (2016). Mitochondria know no boundaries: Mechanisms and functions of intercellular mitochondrial transfer. *Frontiers in Cell and Developmental Biology*, *4*(SEP), 107. https://doi.org/10.3389/FCELL.2016.00107/BIBTEX

Uddin, M. S., Mamun, A. al, Alghamdi, B. S., Tewari, D., Jeandet, P., Sarwar, M. S., & Ashraf, G. M. (2020). Epigenetics of glioblastoma multiforme: From molecular mechanisms to therapeutic approaches. *Seminars in Cancer Biology*. https://doi.org/10.1016/J.SEMCANCER.2020.12.015

van den Bent, M. J., Weller, M., Wen, P. Y., Kros, J. M., Aldape, K., & Chang, S. (2017). A clinical perspective on the 2016 WHO brain tumor classification and routine molecular diagnostics. *Neuro-Oncology*, *19*(5), 614–624. https://doi.org/10.1093/neuonc/now277

van Haaften, G., Dalgliesh, G. L., Davies, H., Chen, L., Bignell, G., Greenman, C., Edkins, S., Hardy, C., O'Meara, S., Teague, J., Butler, A., Hinton, J., Latimer, C., Andrews, J., Barthorpe, S., Beare, D., Buck, G., Campbell, P. J., Cole, J., … Futreal, P. A. (2009). Somatic mutations of the histone H3K27 demethylase gene UTX in human cancer. *Nature Genetics*, *41*(5), 521–523. https://doi.org/10.1038/NG.349

Venkataramani, V., Tanev, D. I., Strahle, C., Studier-Fischer, A., Fankhauser, L., Kessler, T., Körber, C., Kardorff, M., Ratliff, M., Xie, R., Horstmann, H., Messer, M., Paik, S. P., Knabbe, J., Sahm, F., Kurz, F. T., Acikgöz, A. A., Herrmannsdörfer, F., Agarwal, A., … Kuner, T. (2019). Glutamatergic synaptic input to glioma cells drives brain tumour progression. *Nature*, *573*(7775), 532–538. https://doi.org/10.1038/S41586-019-1564-X

Venteicher, A. S., Tirosh, I., Hebert, C., Yizhak, K., Neftel, C., Filbin, M. G., Hovestadt, V., Escalante, L. E., Shaw, M. L., Rodman, C., Gillespie, S. M., Dionne, D., Luo, C. C., Ravichandran, H., Mylvaganam, R., Mount, C., Onozato, M. L., Nahed, B. v., Wakimoto, H., … Suvà, M. L. (2017). Decoupling genetics, lineages, and microenvironment in IDH-mutant gliomas by single-cell RNA-seq. *Science*, *355*(6332). https://doi.org/10.1126/SCIENCE.AAI8478/SUPPL_FILE/VENTEICHER.SM.PDF

Ventelä, S., Toppari, J., & Parvinen, M. (2003a). Intercellular organelle traffic through cytoplasmic bridges in early spermatids of the rat: mechanisms of haploid gene

product sharing. *Molecular Biology of the Cell*, *14*(7), 2768–2780. https://doi.org/10.1091/MBC.E02-10-0647

Ventelä, S., Toppari, J., & Parvinen, M. (2003b). Intercellular Organelle Traffic through Cytoplasmic Bridges in Early Spermatids of the Rat: Mechanisms of Haploid Gene Product Sharing. *Molecular Biology of the Cell*, *14*(7), 2768. https://doi.org/10.1091/MBC.E02-10-0647

Verdone, L., Agricola, E., Caserta, M., & di Mauro, E. (2006). Histone acetylation in gene regulation. *Briefings in Functional Genomics*, *5*(3), 209–221. https://doi.org/10.1093/BFGP/ELL028

Veselý, J., & Čihák, A. (1978). 5-Azacytidine: Mechanism of action and biological effects in mammalian cells. *Pharmacology & Therapeutics. Part A: Chemotherapy, Toxicology and Metabolic Inhibitors*, *2*(4), 813–840. https://doi.org/10.1016/0362-5478(78)90016-5

Vidali, G., Boffa, L. C., Bradbury, E. M., & Allfrey, V. G. (1978). Butyrate suppression of histone deacetylation leads to accumulation of multiacetylated forms of histones H3 and H4 and increased DNase I sensitivity of the associated DNA sequences. *Proceedings of the National Academy of Sciences of the United States of America*, *75*(5), 2239–2243. https://doi.org/10.1073/PNAS.75.5.2239

Vidi, P. A., Bissell, M. J., & Lelièvre, S. A. (2013). Three-dimensional culture of human breast epithelial cells: the how and the why. *Methods in Molecular Biology (Clifton, N.J.)*, *945*, 193–219. https://doi.org/10.1007/978-1-62703-125-7_13

Vo, N., & Goodman, R. H. (2001). CREB-binding Protein and p300 in Transcriptional Regulation *. *Journal of Biological Chemistry*, *276*(17), 13505–13508. https://doi.org/10.1074/JBC.R000025200

Vorinostat, Temozolomide, and Radiation Therapy in Treating Patients With Newly Diagnosed Glioblastoma Multiforme - Full Text View - ClinicalTrials.gov. (n.d.). Retrieved May 17, 2022, from https://clinicaltrials.gov/ct2/show/NCT00731731

Vorinostat, Temozolomide, or Bevacizumab in Combination With Radiation Therapy Followed by Bevacizumab and Temozolomide in Young Patients With Newly Diagnosed High-Grade Glioma - Full Text View - ClinicalTrials.gov. (n.d.). Retrieved May 17, 2022, from https://clinicaltrials.gov/ct2/show/NCT01236560

Wang, J., Liu, X., Qiu, Y., Shi, Y., Cai, J., Wang, B., Wei, X., Ke, Q., Sui, X., Wang, Y., Huang, Y., Li, H., Wang, T., Lin, R., Liu, Q., & Xiang, A. P. (2018). Cell adhesion-

mediated mitochondria transfer contributes to mesenchymal stem cell-induced chemoresistance on T cell acute lymphoblastic leukemia cells. *Journal of Hematology & Oncology*, *11*(1). https://doi.org/10.1186/S13045-018-0554-Z

Wardlaw, J. M., Benveniste, H., Nedergaard, M., Zlokovic, B. v., Mestre, H., Lee, H., Doubal, F. N., Brown, R., Ramirez, J., MacIntosh, B. J., Tannenbaum, A., Ballerini, L., Rungta, R. L., Boido, D., Sweeney, M., Montagne, A., Charpak, S., Joutel, A., Smith, K. J., & Black, S. E. (2020). Perivascular spaces in the brain: anatomy, physiology and pathology. *Nature Reviews Neurology 2020 16:3*, *16*(3), 137–153. https://doi.org/10.1038/s41582-020-0312-z

Watson, D. C., Bayik, D., Williford, S. E., Lauko, A., Zhou, Y., Deshpande, G., Seder, J., Mears, J. A., Cheng, F., Hjelmeland, A. B., & Lathia, J. D. (2021). Horizontal mitochondrial transfer from the microenvironment increases glioblastoma tumorigenicity. *BioRxiv*, 2021.09.01.458565. https://doi.org/10.1101/2021.09.01.458565

Weil, S., Osswald, M., Solecki, G., Grosch, J., Jung, E., Lemke, D., Ratliff, M., Hänggi, D., Wick, W., & Winkler, F. (2017). Tumor microtubes convey resistance to surgical lesions and chemotherapy in gliomas. *Neuro-Oncology*, *19*(10), 1316–1326. https://doi.org/10.1093/NEUONC/NOX070

Weisse, A. B. (1991). *Medical odysseys : the different and sometimes unexpected pathways to twentieth-century medical discoveries*. 250.

Whittaker, S. J., Demierre, M. F., Kim, E. J., Rook, A. H., Lerner, A., Duvic, M., Scarisbrick, J., Reddy, S., Robak, T., Becker, J. C., Samtsov, A., McCulloch, W., & Kim, Y. H. (2010). Final results from a multicenter, international, pivotal study of romidepsin in refractory cutaneous T-cell lymphoma. *Journal of Clinical Oncology : Official Journal of the American Society of Clinical Oncology*, *28*(29), 4485–4491. https://doi.org/10.1200/JCO.2010.28.9066

Wijewardhane, N., Dressler, L., & Ciccarelli, F. D. (2021). Normal Somatic Mutations in Cancer Transformation. *Cancer Cell*, *39*(2), 125–129. https://doi.org/10.1016/J.CCELL.2020.11.002

Wilson, N. S., Dixit, V., & Ashkenazi, A. (2009). Death receptor signal transducers: nodes of coordination in immune signaling networks. *Nature Immunology 2009 10:4*, *10*(4), 348–355. https://doi.org/10.1038/ni.1714

Wodarz, D., Newell, A. C., & Komarova, N. L. (2018). Passenger mutations can accelerate tumour suppressor gene inactivation in cancer evolution. *Journal of The Royal Society Interface*, *15*(143). https://doi.org/10.1098/RSIF.2017.0967

Wojtkowiak, J. W., Verduzco, D., Schramm, K. J., & Gillies, R. J. (2011). Drug resistance and cellular adaptation to tumor acidic pH microenvironment. *Molecular Pharmaceutics*, *8*(6), 2032–2038. https://doi.org/10.1021/MP200292C

Wolf, A., Agnihotri, S., Munoz, D., & Guha, A. (2011). Developmental profile and regulation of the glycolytic enzyme hexokinase 2 in normal brain and glioblastoma multiforme. *Neurobiology of Disease*, *44*(1), 84–91. https://doi.org/10.1016/J.NBD.2011.06.007

Wolf, K. W., Mentzel, M., & Mendoza, A. S. (1996). DNA-containing cytoplasmic bridges in a human breast cancer cell line, MX-1: morphological markers of a highly mobile cell type? *Journal of Submicroscopic Cytology and Pathology*, *28*(3), 369–373. https://pubmed.ncbi.nlm.nih.gov/8765579/

Wood, A., & Shilatifard, A. (2004). Posttranslational Modifications of Histones by Methylation. *Advances in Protein Chemistry*, *67*, 201–222. https://doi.org/10.1016/S0065-3233(04)67008-2

Wu, H., Liu, Q., Cai, T., Chen, Y. dan, Liao, F., & Wang, Z. fei. (2014). MiR-136 modulates glioma cell sensitivity to temozolomide by targeting astrocyte elevated gene-1. *Diagnostic Pathology*, *9*(1), 1–6. https://doi.org/10.1186/S13000-014-0173-0/FIGURES/3

Yan, H., Parsons, D. W., Jin, G., McLendon, R., Rasheed, B. A., Yuan, W., Kos, I., Batinic-Haberle, I., Jones, S., Riggins, G. J., Friedman, H., Friedman, A., Reardon, D., Herndon, J., Kinzler, K. W., Velculescu, V. E., Vogelstein, B., & Bigner, D. D. (2009). IDH1 and IDH2 Mutations in Gliomas. *New England Journal of Medicine*, *360*(8), 765–773. https://doi.org/10.1056/NEJMoa0808710

Yang, C., Rahimpour, S., Yu, A. C. H., Lonser, R. R., & Zhuang, Z. (2013). Regulation and dysregulation of astrocyte activation and implications in tumor formation. *Cellular and Molecular Life Sciences*, *70*(22), 4201–4211. https://doi.org/10.1007/s00018-013-1274-8

Yang, N., Yan, T., Zhu, H., Liang, X., Leiss, L., Sakariassen, P. Ø., Skaftnesmo, K. O., Huang, B., Costea, D. E., Enger, P. Ø., Li, X., & Wang, J. (2014). A co-culture model with brain tumor-specific bioluminescence demonstrates astrocyte-induced

drug resistance in glioblastoma. *Journal of Translational Medicine*, *12*(1). https://doi.org/10.1186/s12967-014-0278-y

Yi, L., Cui, Y., Xu, Q., & Jiang, Y. (2016). Stabilization of LSD1 by deubiquitinating enzyme USP7 promotes glioblastoma cell tumorigenesis and metastasis through suppression of the p53 signaling pathway. *Oncology Reports*, *36*(5), 2935–2945. https://doi.org/10.3892/OR.2016.5099/HTML

Yin, X., Yang, S., Zhang, M., & Yue, Y. (2019). The role and prospect of JMJD3 in stem cells and cancer. *Biomedicine & Pharmacotherapy*, *118*, 109384. https://doi.org/10.1016/J.BIOPHA.2019.109384

Zampieri, L. X., Silva-Almeida, C., Rondeau, J. D., & Sonveaux, P. (2021). Mitochondrial Transfer in Cancer: A Comprehensive Review. *Int. J. Mol. Sci*, *22*, 3245. https://doi.org/10.3390/ijms22063245

Zandi, R., Larsen, A. B., Andersen, P., Stockhausen, M. T., & Poulsen, H. S. (2007). Mechanisms for oncogenic activation of the epidermal growth factor receptor. *Cellular Signalling*, *19*(10), 2013–2023. https://doi.org/10.1016/j.cellsig.2007.06.023

Zhang, X., Ding, K., Wang, J., Li, X., & Zhao, P. (2019). Chemoresistance caused by the microenvironment of glioblastoma and the corresponding solutions. In *Biomedicine and Pharmacotherapy* (Vol. 109, pp. 39–46). Elsevier Masson SAS. https://doi.org/10.1016/j.biopha.2018.10.063

Zhang, Y. A., Nemunaitis, J., Scanlon, K. J., & Tong, A. W. (2000). Anti-tumorigenic effect of a K-ras ribozyme against human lung cancer cell line heterotransplants in nude mice. *Gene Therapy*, *7*(23), 2041–2050. https://doi.org/10.1038/sj.gt.3301331

Zhao, L. Y., Song, J., Liu, Y., Song, C. X., & Yi, C. (2020). Mapping the epigenetic modifications of DNA and RNA. *Protein and Cell*, *11*(11), 792–808. https://doi.org/10.1007/S13238-020-00733-7/FIGURES/2

Ziemys, A., Klemm, S., Milosevic, M., Yokoi, K., Ferrari, M., & Kojic, M. (2016). Computational analysis of drug transport in tumor microenvironment as a critical compartment for nanotherapeutic pharmacokinetics. *Drug Delivery*, *23*(7), 2524–2531. https://doi.org/10.3109/10717544.2015.1022837/SUPPL_FILE/IDRD_A_1022837_SM1265.PDF